UNIVERSITY OF CALIFORNIA
RIVERSIDE

On Robust and Energy-Limited Joint Source-Channel Coding

A Dissertation submitted in partial satisfaction
of the requirements for the degree of

Doctor of Philosophy

in

Electrical Engineering

by

Erman Koken

September 2017

Dissertation Committee:

Dr. Ertem Tuncel, Chairperson
Dr. Ilya Dumer
Dr. Yingbo Hua

The Dissertation of Erman Koken is approved:

Committee Chairperson

University of California, Riverside

Acknowledgments

Firstly, I would like to express my sincere gratitude to my advisor Prof. Ertem Tuncel for the continuous support of my Ph.D. study and related research, for his patience, motivation, and immense knowledge. His guidance helped me in all the time of research and writing of this thesis. I could not have imagined having a better advisor and mentor for my Ph.D. study.

I am also grateful to my dissertation committee members Prof. Ilya Dumer and Prof. Yingbo Hua for their insightful comments and encouragement.

My sincere thanks go to my friends Tuğcan Aktaş and Pınar Şen Aktaş whose friendship and support was always with me.

Last but not the least, I would like to thank my parents and my brother for supporting me throughout writing this thesis and my life in general. Without their help, I would not have been here.

The materials published in this thesis were partly presented in IEEE Transaction on Information Theory and IEEE Transaction on Communications.

To my parents and my brother for all the support.

ABSTRACT OF THE DISSERTATION

On Robust and Energy-Limited Joint Source-Channel Coding

by

Erman Koken

Doctor of Philosophy, Graduate Program in Electrical Engineering
University of California, Riverside, September 2017
Dr. Ertem Tuncel, Chairperson

In this thesis we investigate the lossy transmission of single and bivariate Gaussian sources over bandwidth-mismatched additive Gaussian white noise and broadcast channels. For these scenarios we proposed novel hybrid digital/analog based joint source-channel coding schemes which generalize or outperform existing schemes. In the first scenario we assume that side information is available at the receiver, channel state information of additive interference is available at the transmitter, and power is limited. For this scenario we proposed hybrid digital/analog schemes, for both bandwidth expansion and bandwidth compression cases, which can attain the optimum reconstruction levels. For bandwidth expansion we showed that the scheme can attain optimum distortion levels for a set of receivers with different side information and channel qualities simultaneously with a single set of scheme parameters. In the second scenario, where no side information or interference are present, we consider the robustness of scheme where it must attain the optimal distortion at a target signal-to-noise-ratio and we would like to attain the best distortion pair for two possible receivers one with better and the other with worse channel quality. We extended

Tian *et al.*'s result to a set of non-integer bandwidth expansion ratios. Then we investigate the transmission of bivariate sources over broadcast channels. For this scenario we proposed a scheme which outperforms the known schemes which are either purely digital or hybrid schemes. Finally we analyzed energy-distortion tradeoff for lossy transmission of a Gaussian source over bandwidth-unlimited channel. We performed asymptotical analyses as signal-to-noise-ratio goes to infinity. We also considered zero-delay transmission of the source.

Contents

List of Figures

List of Tables

Chapter 1

Introduction

In lossy transmission of a source over a noisy point-to-point bandwidth-mismatched channel, it is shown in Shannon's landmark paper [37] that the minimum distortion can be achieved asymptotically, i.e., as both source and channel codewords goes to infinity, by using separate source and channel codes. However separable schemes suffer from the threshold effect, i.e., when the channel quality is lower than expected the codewords cannot be decoded reliably and the performance degrades drastically. They cannot benefit from an occasional increase in the channel quality either, which is called the leveling-off effect. Naturally a direct mapping from the source sequence to the channel input, which is called *joint source-channel coding*, is expected to perform at least as good as separate coding.

One of the prominent class of joint source-channel coding schemes is *hybrid digital/analog* (HDA) coding. HDA schemes are robust in the sense that they mitigate the detrimental effects of the ambiguity in the channel signal-to-noise-ratio (SNR).

HDA schemes prove useful not only in point-to-point communication systems. It

is known that separation of source and channel codes cannot offer optimal distortion in most of the multiple user scenarios such as broadcast channels, multiple access channels, interference channels, etc., where many sources are transmitted to many receivers. HDA coding increases the reconstruction quality of the source at the receivers in such scenarios.

In this thesis we propose novel HDA based joint source channel coding schemes for different scenarios. Our schemes essentially rely on typicality arguments.

Another scenario we address in the thesis is the case where the energy per source symbol is limited but the channel uses per source symbol is unlimited, which corresponds to unlimited bandwidth. We use aforementioned schemes to characterize the achievable distortion exponents. Our analyses are also extended to zero-delay transmission.

In Chapter 2 lossy transmission of a Gaussian source over an additive white Gaussian (AWGN) channel with a noncausal side information (SI) at the decoder and channel state information (CSI) at the encoder is tackled under bandwidth mismatch. A previously known scheme, hybrid digital/analog Wyner-Ziv (HDA-WZ) coding is shown to remain optimal when extended from the bandwidth matched case to the bandwidth mismatched case. The extended scheme also exhibits similar robustness properties under mismatched side information and/or channel quality under the regime of bandwidth expansion. Finally, under the criterion of min-max distortion loss, the extended HDA-WZ scheme is shown to outperform a purely-digital scheme known as the common description scheme (CDS).

Chapter 3 is devoted to the robustness analysis of the proposed scheme with respect to the variations in SNR. For transmission of memoryless Gaussian sources over channels with AWGN, the tradeoff between the distortion levels when the channel quality is good

and bad is investigated under the constraint that the distortion is optimal when the channel has the targeted median quality. The problem was proposed by Tian and Shamai who subsequently proved remarkable achievability results for bandwidth expansion ratios κ which are integers or unit fractions, i.e., $\kappa = 2, 3, 4, ...$ or $\kappa = 1/2, 1/3, 1/4, ...$ Their result is extended here to all $\kappa \geq 2$ and $\kappa \leq 1/2$ by generalizing the HDA scheme of Wilson *et al.* to the case of bandwidth mismatch. Finally, novel schemes are proposed for $1/2 \leq \kappa < 1$ and $1 < \kappa \leq 2$ achieving nontrivial tradeoffs outperforming all known schemes. These latter schemes rely on another extension of the HDA scheme by Wilson *et al.*, namely, relaxation of the independence of source and channel input sequences.

In Chapter 4 we consider the problem of transmitting a pair of Gaussian sources over a Gaussian broadcast channel, where each receiver is interested in reconstructing only one source component. This scenario is relevant in sensor network settings where sensors are taking measurements of multiple environmental phenomena, such as temperature, humidity, pressure, that are typically correlated with each other. On the other hand, each receiving agent may be interested in just one of these measurements.

In Chapter 5 we deviate from HDA schemes and we particularly focus on high-ENR zero-delay schemes. An achievable scheme for zero-delay transmission of an i.i.d. Gaussian source over an AWGN channel with no bandwidth limitation is introduced, and its energy-distortion performance is analyzed. By the nature of the problem, one must transmit each source sample separately but can use the channel infinitely many times. We introduce an outage concept, and analyze the expected distortion conditioned on no outage. We show that the proposed scheme can approach to the asymptotical decay for large enough energy

for arbitrary outage probability. The proposed scheme builds on separation of source and channel coding, whereby the source is quantized with a high-resolution optimal quantizer. In the high energy-to-noise ratio (ENR) regime, the minimum energy required to obtain a given distortion level in the proposed scheme can approach arbitrarily close the Shannon bound, which can only be achieved using infinite delay.

Some of the proofs are deferred to Appendix A.

Chapter 2

Hybrid Digital/Analog Coding with Side Information and Channel State Information

2.1 Introduction and Problem Definition

In this chapter, we consider the lossy transmission of a unit-variance i.i.d. Gaussian source X^{nN} over an AWGN channel with bandwidth mismatch, where the receiver has access to noncausal side information Y^{nN} correlated with the source. More specifically, $X^{nN} = Y^{nN} + Z^{nN}$ with $Z^{nN} \sim \mathcal{N}\left(0, \sigma_Z^2 \mathbf{I}\right)$ and $Y^{nN} \sim \mathcal{N}\left(0, \left(1-\sigma_Z^2\right)\mathbf{I}\right)$ being independent. There is also an additive interference $S^{mN} \sim \mathcal{N}\left(0^{mN}, \sigma_S^2 \mathbf{I}_{mN}\right)$ which is noncausally and perfectly known by the encoder. The interference is independent of the source. The output of the channel is modeled by $V^{mN} = U^{mN} + S^{mN} + W^{mN}$ where the i.i.d. channel noise variance

σ_W^2 is γ^{-1}. This scenario is illustrated in Fig. 2.1.

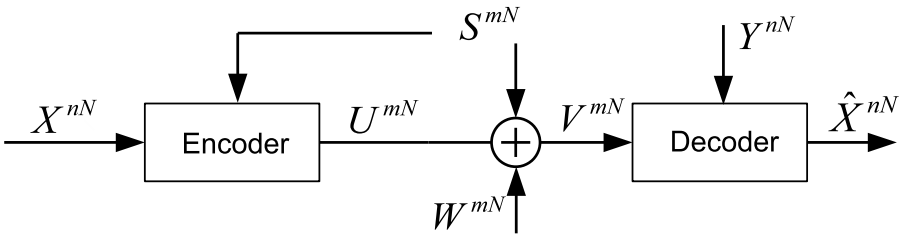

Figure 2.1: The bandwidth mismatched case where the SI is available only at the decoder and the interference in perfectly available at the encoder.

As usual, the channel input is power constrained, i.e.,

$$\frac{1}{mN}\sum_{i=1}^{mN}\mathbb{E}\left[U_i^2\right] \leq P \tag{2.1}$$

where $P = 1$ without loss of generality and the quality of reconstruction is measured by the average expected square-error distortion

$$D = \frac{1}{nN}\sum_{i=1}^{nN}\mathbb{E}\left[\left(X_i - \hat{X}_i\right)^2\right]. \tag{2.2}$$

We take m, n, and N as integers, where N is the length of blocks consisting of super-symbols X^n, Y^n , X^n, U^m, V^m, and W^m , while m and n determine the bandwidth expansion ratio as $\kappa = \frac{m}{n}$. We will call the system bandwidth expansion (BE) if $\kappa \geq 1$ and bandwidth compression (BC) if $\kappa \leq 1$. In the subsequent asymptotic analysis, N will approach infinity while m and n will be finite and fixed.

While this problem is known to be separable [25], i.e., a combination of digital source and channel codes can achieve the optimal tradeoff, i.e., $D = \sigma_Z^2 2^{-2\kappa C}$, or

$$D = \frac{\sigma_Z^2}{(1+\gamma)^{\kappa}},$$

digital codes are vulnerable to changes in channel and/or side information quality: After the system is built for a target $\left(\sigma_Z^2, \sigma_W^2\right)$, if σ_Z^2 and/or σ_W^2 increases, the decoding of the digital information breaks down (also known as the thresholding effect). On the other hand, decreasing σ_Z^2 and σ_W^2 does not translate to any reduction in distortion (also known as the leveling-off effect). It is well-known both thresholding and leveling-off can be mitigated by HDA coding (for example, see [7], [13], [35], [45] and references therein).

In [45], the authors introduced the HDA-WZ-Costa scheme that can achieve the same minimum distortion for the bandwidth-matched case, i.e., $m = n = 1$, which operates as follows. A codebook of size 2^{NR} is generated according to an auxiliary random variable defined by

$$T = U + kX + aS$$

where $U \sim \mathcal{N}(0, 1)$ is independent of X and S. The encoder finds a codeword $T^N(j)$ jointly typical with X^N and S^N, and transmits $U^N = T^N(j) - kX^N - aS^N$. Given the channel output $V^N = U^N + S^N + W^N$, the receiver finds the unique $T^N(j)$ typical with V^N and Y^N. This is possible if

$$I(T; X, S) \leq R \leq I(T; V, Y).$$

The receiver then computes the minimum mean square error (MMSE) estimate

$$\hat{X}^N = c_1 T^N + c_2 V^N + c_3 Y^N.$$

By carefully choosing

$$k^2 = \frac{\gamma}{\sigma_Z^2 (1 + \gamma)}$$

and

$$a = \frac{\gamma}{1+\gamma},$$

together with the optimal choice of c_1, c_2, and c_3, it was shown in [45] that one can achieve the optimum distortion

$$D = \frac{\sigma_Z^2}{1+\gamma}.$$

Throughout this section we will follow the same approach of finding an appropriate auxiliary random variable to generate codewords then make use of these codewords at both the transmitter and the receiver end. We end this section by providing a lemma which will be instrumental in simplifying the calculation of the MMSE error and mutual information expressions in various cases.

Lemma 1 *For jointly Gaussian random variables (X, Y, Z) where $Y - X - Z$ forms a Markov chain, i.e., $Y = k_1 X + W_1$, $Z = k_2 X + W_2$, with $W_i \sim \mathcal{N}(0, N_i)$, $X \sim \mathcal{N}(0,1)$, and $X \perp W_1 \perp W_2$, we have*

$$I(X;Y,Z) = \frac{1}{2}\log\left(1 + \frac{k_1^2}{N_1} + \frac{k_2^2}{N_2}\right)$$

and

$$\begin{aligned}\sigma_{Z|Y,Z}^2 &= \frac{1}{\frac{1}{\sigma_{X|Y}^2} + \frac{1}{\sigma_{X|Z}^2} - 1} \\ &= \frac{1}{1 + \frac{k_1^2}{N_1} + \frac{k_2^2}{N_2}}.\end{aligned}$$

Proof. Follows from standard MMSE analysis and noting that

$$I(X;Y,Z) = h(X) - h(X \mid Y,Z) = \frac{1}{2}\log\left(\frac{1}{\sigma_{X|Y,Z}^2}\right).$$

■

2.2 The Coding Schemes

2.2.1 HDA-WZ-Costa-BE ($\kappa \geq 1$)

The main approach we take here for extending the original coding scheme [45], and throughout Chapter 2 and 3, is to treat the source X^{nN} and the channel input U^{mN} (also SI Y^{nN} and additional interference S^{nN} if applicable) as bandwidth-matched (length-N) superblocks consisting of supersymbols X^n and U^m. Since the superblock lengths match, we can employ the usual typicality arguments. However, since the lengths n and m do not match, we still recourse to breaking either X^n into subsources, or U^m into subchannels, or both, to relate the two.

As in the original approach in [45], the codeworks are generated independently and randomly according to the auxiliary random variable

$$T^m = \begin{bmatrix} kX^n \\ \\ 0^{m-n} \end{bmatrix} + U^m + aS^m$$

where $U^m \sim \mathcal{N}(0^m, \mathbf{I})$ and $X^n \perp U^m \perp S^m$. After finding an auxiliary codeword $T^{mN}(j)$ which is typical with the source and the interference as depicted in Fig.2.2, the channel input U^{mN} is calculated supersymbol-by-supersymbol using

$$U^m = \begin{bmatrix} U_1^n \\ \\ U_2^{m-n} \end{bmatrix} = T^m - \begin{bmatrix} kX^n \\ \\ 0^{m-n} \end{bmatrix} - a \begin{bmatrix} S_1^n \\ \\ S_2^{m-n} \end{bmatrix}.$$

At the receiver, after finding the unique auxiliary codeword, the estimate can be computed again supersymbol-by-supersymbol as

$$\hat{X}^n = c_T T_1^n + c_V V_1^n + c_Y Y^n. \tag{2.3}$$

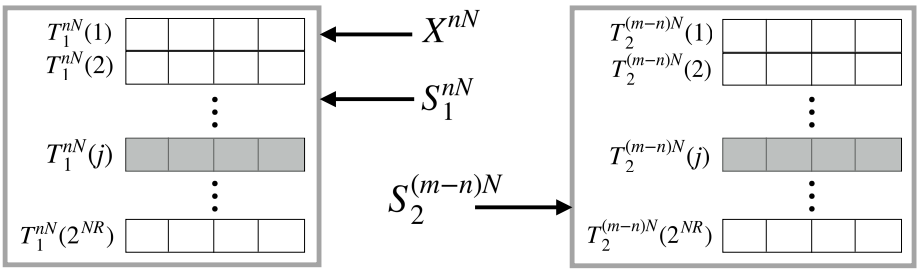

Figure 2.2: The encoder for the HDA-WZ-Costa-BE coding, which looks for an index j such that $T_1^{nN}(j)$ is jointly typical with $\left(X^{nN}, S_1^{nN}\right)$ and $T_2^{(m-n)N}(j)$ is jointly typical with $S_2^{(m-n)N}$.

Theorem 2 *The HDA-WZ-Costa-BE scheme can attain the optimum distortion with proper coefficients* (k, a).

Proof. In order for a reliable communication the mutual informations should satisfy

$$I\left(T^m; X^n, S^m\right) \leq I\left(T^m; V^m, Y^n\right) \tag{2.4}$$

where

$$\begin{aligned} I\left(T^m; X^n, S^m\right) &= I\left(T_1^n; X^n, S_1^n\right) + I\left(T_2^{m-n}; S_2^{m-n}\right)\left(1+k^2+a^2\sigma_S^2\right)^n\left(1+a^2\sigma_S^2\right)^{m-n} \\ &= \frac{n}{2}\log\left(1+k^2+a^2\sigma_S^2\right) + \frac{m-n}{2}\log\left(1+a^2\sigma_S^2\right) \end{aligned}$$

and

$$\begin{aligned} I\left(T^m; V^m, Y^n\right) &= I\left(T_1^n; V_1^n, Y^n\right) + I\left(T_2^{m-n}; V_2^{m-n}\right) \\ &= \frac{n}{2}\log\left(\frac{1+k^2+a^2\sigma_S^2}{1+\sigma_Z^2k^2+a^2\sigma_S^2}\right) + \frac{n}{2}\log\left(\frac{1+\sigma_Z^2k^2+a^2\sigma_S^2}{M+\sigma_Z^2k^2}\right) \\ &\quad + \frac{m-n}{2}\log\left(\frac{1+a^2\sigma_S^2}{M}\right) \end{aligned}$$

with

$$M = 1 + a^2\sigma_S^2 - \frac{\left(1 + a\sigma_S^2\right)^2}{\left(1 + \frac{1}{\gamma} + \sigma_S^2\right)}. \tag{2.5}$$

It is easy to see that inequality (2.4) boils down to

$$\left(M + \sigma_Z^2 k^2\right) M^{\kappa - 1} \leq 1. \tag{2.6}$$

Now define

$$\begin{aligned}
\tilde{T}_i &= T_{1,i} - \frac{\mathbb{E}\left[T_{1,1} V_i\right]}{\mathbb{E}\left[V_{1,i}^2\right]} V_{1,i} \\
&= kX_i + \left(1 - \frac{1 + a\sigma_S^2}{1 + \gamma^{-1} + \sigma_S^2}\right) U_{1,i} + \left(a - \frac{1 + a\sigma_S^2}{1 + \gamma^{-1} + \sigma_S^2}\right) S_{1,i} - \frac{1 + a\sigma_S^2}{1 + \gamma^{-1} + \sigma_S^2} W_{1,i} \\
&\doteq kX_i + \tilde{W}_i
\end{aligned}$$

with $\tilde{W}_i = \mathcal{N}\left(0, \sigma_{\tilde{W}_i}^2\right)$ and $\tilde{W}_i \perp X_i$, where after some algebra, it can be shown that $\sigma_{\tilde{W}_i}^2 = M$. The MMSE estimate in (2.3) can be simplified to

$$\hat{X}_i = \mathbb{E}\left[X_i \mid \tilde{T}_i, Y_i\right]$$

because $V_{1,i}$ is independent of $\tilde{T}_i$,Y_i, and X_i. Now let D_Y and $D_{\tilde{T}}$ denote

$$\begin{aligned}
D_Y &\doteq \mathbb{E}\left[\left(X_i - \mathbb{E}\left[X_i \mid Y_i\right]\right)^2\right] \\
&= \sigma_Z^2
\end{aligned}$$

and

$$\begin{aligned}
D_{\tilde{T}} &\doteq \mathbb{E}\left[\left(X_i - \mathbb{E}\left[X_i \mid \tilde{T}_i\right]\right)^2\right] \\
&= \frac{M}{k^2 + M}.
\end{aligned}$$

Since the Gaussian random variables form a Markov chain the distortion can be calculated using Lemma 1 as

$$\begin{aligned} D &= \frac{1}{D_{\tilde{T}}^{-1} + D_Y^{-1} - 1} \\ &= \frac{\sigma_Z^2 M}{M + \sigma_Z^2 k^2}. \end{aligned} \tag{2.7}$$

Clearly, the distortion will be minimized by choosing k^2 to satisfy equality in (2.6) as

$$k^2 = \frac{M\left(M^{-\kappa} - 1\right)}{\sigma_Z^2}$$

resulting in

$$D = \sigma_Z^2 M^{\kappa}. \tag{2.8}$$

Note that M is a convex quadratic function of a, and is minimized by setting

$$a = \frac{\gamma}{1+\gamma} \tag{2.9}$$

yielding the minimum value of M as

$$M = \frac{\gamma}{1+\gamma} \tag{2.10}$$

for which the corresponding value of k^2 becomes

$$k^2 = \frac{(1+\gamma)^{\kappa} - 1}{\sigma_Z^2\,(1+\gamma)}. \tag{2.11}$$

Finally, it follows from (2.8) and (2.10) that with this choice of (k, a), we obtain the desired optimum distortion $D = \frac{\sigma_Z^2}{(1+\gamma)^{\kappa}}$. ■

Corollary 3 *If SNR γ_+ and/or SI quality $\sigma^2_{Z_+}$ is better than expected, i.e., $\gamma_+ > \gamma$ and/or $\sigma^2_{Z_+} < \sigma^2_Z$, then the resultant distortion D_+ can be expressed as*

$$D_+ = \left(\frac{\left((1+\gamma)^{\kappa+1} - 1 - \gamma\right)\left(1 + \left(1+\sigma_S^2\right)\gamma_+\right)}{\sigma_Z^2\left((1+\gamma)^2 + \sigma_S^2\left(\gamma^2 + \gamma_+\right)\right)} + \frac{1}{\sigma^2_{Z_+}} \right)^{-1} \tag{2.12}$$

If, on the other hand, $T^{mN}(j)$ cannot be decoded due to lower SI or channel quality, i.e., $\gamma_- < \gamma$ and/or $\sigma^2_{Z_+} < \sigma^2_Z$, no decoding available, due to lower side information or channel quality, then the distortion becomes

$$D_- = \sigma^2_{Z_-}. \tag{2.13}$$

Proof. Keeping (k, a) as in (2.9) and (2.11) and defining

$$M_+ = 1 + a^2\sigma_S^2 - \frac{\left(1 + a\sigma_S^2\right)^2}{\left(1 + \gamma_+^{-1} + \sigma_S^2\right)}$$

we can use the same analysis to derive (2.7) and obtain

$$\begin{aligned} D_+ &= \frac{\sigma^2_{Z_+} M_+}{M_+ + \sigma^2_{Z_+} k^2} \\ &= \left(\frac{(1+\gamma)^\kappa - 1}{\sigma_Z^2(1+\gamma)\left[1 + a^2\sigma_S^2 - \frac{\left(1+a\sigma_S^2\right)^2}{\left(1+\gamma_+^{-1}+\sigma_S^2\right)}\right]} + \frac{1}{\sigma^2_{Z_+}} \right)^{-1} \\ &= \left(\frac{(1+\gamma)^{\kappa+1} - 1 - \gamma}{\sigma_Z^2\left[(1+\gamma)^2 + \gamma^2\sigma_S^2 - \frac{\left(1+\gamma+\gamma\sigma_S^2\right)^2}{\left(1+\gamma_+^{-1}+\sigma_S^2\right)}\right]} + \frac{1}{\sigma^2_{Z_+}} \right)^{-1} \end{aligned}$$

which can be further simplified to (2.12).

As for (2.13), it suffices to observe that since X^n is independent of U^m, and thus of V^m, its reconstruction must solely rely on Y^n if $T^{mN}(j)$ is not decoded.

■ If there is no SI or no interference, the scheme will be termed HDA-Costa-BE or HDA-WZ-BE, respectively. HDA-WZ-BE will be compared to a previously known robust coding scheme, i.e., Common Description Scheme, in terms of maximum distortion loss metric in Section 2.3.

2.2.2 HDA-WZ-Costa-BC ($\kappa \leq 1$)

We use the same approach as we did for BE case. The codeworks are generated independently and randomly according to the auxiliary random variable

$$T^n = \begin{bmatrix} T_1^m \\ \\ T_2^{n-m} \end{bmatrix} = \begin{bmatrix} k_1 X_1^m \\ \\ k_2 X_2^{n-m} \end{bmatrix} + \begin{bmatrix} U^m \\ \\ Q^{n-m} \end{bmatrix} + \begin{bmatrix} aS^m \\ \\ 0^{n-m} \end{bmatrix} \tag{2.14}$$

where the source supersymbol X^n is decomposed into X_1^m and X_2^{n-m} with $Q^{n-m} \sim \mathcal{N}(0^{n-m}, \mathbf{I}_{n-m})$, and $X^n \perp U^m \perp S^m \perp Q^{n-m}$. After finding a suitable codeword $T^{nN}(j)$ typical with the source and the interference, the channel input supersymbol is calculated as

$$U^m = T_1^m - k_1 X_1^m - aS^m.$$

After uniquely decoding $T^{nN}(j)$ at the receiver, the MMSE estimate is found as

$$\hat{X_1}^m = c_{T,1} T_1^m + c_V V^m + c_{Y,1} Y_1^m$$

and

$$\hat{X_2}^{n-m} = c_{T,2} T_2^{n-m} + c_{Y,2} Y_2^{n-m}$$

where the estimate and SI supersymbols $\hat{X}^n$ and Y^n are decomposed similarly as X^n does. We denote by D_1 and D_2 the corresponding estimation errors.

Remark 4 *Similar to the HDA-WZ-Costa-BE scheme proposed in Section 2.2.1, this can be thought of as two coding modules working together: the encoder searches for* $T^{nN}(j)$ *with typical* $\left(T_1^{mN}(j), X_1^{mN}\right)$ *and* $\left(T_2^{(n-m)N}(j), X_2^{(n-m)N}\right)$ *simultaneously, and the decoder searches for* $T^{nN}(j)$ *with typical* $\left(T_1^{mN}(j), V^{mN}, Y_1^{mN}\right)$ *and* $\left(T_2^{(n-m)N}(j), Y_2^{(n-m)N}\right)$ *simultaneously.*

Theorem 5 *The optimum distortion can be attained by the HDA-WZ-Costa-BC scheme with proper coefficients* (k_1, k_2, a).

Proof. For reliable communication, we need

$$I\left(T^m; X^n, S^m\right) \leq I\left(T^m; V^m, Y^n\right),$$

which, after some algebra similar to that used in simplifying (2.4), can be written as

$$\left(M + \sigma_Z^2 k_1^2\right)^{\kappa} \leq \left(1 + \sigma_Z^2 k_2^2\right)^{\kappa - 1} \tag{2.15}$$

where M is as in (2.5). Noting that

$$\begin{aligned} D_{2,T_2} &\doteq \mathbb{E}\left[\left(X_{2,i} - \mathbb{E}\left[X_{2,i} \mid T_{2,i}\right]\right)^2\right] \\ &= \left(1 + k_2^2\right)^{-1} \\ D_{2,Y_2} &\doteq \mathbb{E}\left[\left(X_{2,i} - \mathbb{E}\left[X_{2,i} \mid Y_{2,i}\right]\right)^2\right] \\ &= \sigma_Z^2 \end{aligned}$$

and that $T_{2,i} - X_{2,i} - Y_{2,i}$ forms a Markov chain, it follows from Lemma 1 that

$$\begin{aligned} D_2 &= \frac{1}{D_{2,T_2}^{-1} + D_{2,Y_2}^{-1} - 1} \\ &= \frac{\sigma_Z^2}{\sigma_Z^2 k_2^2 + 1} \end{aligned}$$

and also setting

$$k_2^2 = \frac{(1+\gamma)^{\kappa} - 1}{\sigma_Z^2}$$

one can obtain $D_2 = \sigma_Z^2 (1+\gamma)^{-\kappa}$. This also reduces (2.15) to

$$\left(M + \sigma_Z^2 k_1^2\right) \leq (1+\gamma)^{\kappa - 1}$$

which is the same as (2.6) with the choice the source components corresponding to X_1^m as we did in BE case, it is seen that, the choice of $a = \frac{\gamma}{(1+\gamma)}$. Repeating the same analysis as in the BE case (cf. (2.7) and (2.11)), one can then show that if

$$k_1^2 = \frac{(1+\gamma)^{\kappa} - 1}{\sigma_Z^2 (1+\gamma)},$$

D_1 also becomes $\sigma_Z^2 (1+\gamma)^{-\kappa}$, which makes the overall average distortion $D = \kappa D_1 + (1-\kappa) D_2 = \sigma_Z^2 (1+\gamma)^{-\kappa}$. ■

Corollary 6 *If SNR and/or side information quality is better than expected, i.e., $\gamma_+ > \gamma$ and/or $\sigma_{Z_+}^2 < \sigma_Z^2$, then the distortion will be*

$$\begin{aligned} D_+ &= \kappa \left(\frac{\left((1+\gamma)^{\kappa+1} - 1 - \gamma\right)\left(1 + \gamma_+ \left(1 + \sigma_S^2\right)\right)}{\sigma_Z^2 \left((1+\gamma)^2 + \sigma_S^2 (\gamma^2 + \gamma_+)\right)} + \frac{1}{\sigma_{Z_+}^2} \right)^{-1} \\ &\quad + (1-\kappa) \left(\frac{(1+\gamma)^{\kappa} - 1}{\sigma_Z^2} + \frac{1}{\sigma_{Z_+}^2} \right)^{-1}. \end{aligned}$$

If, on the other hand, $T^{nN}(j)$ cannot be decoded, the distortion takes the catastrophic value $D_- = \sigma_{Z_-}^2$ as in the BE case.

2.3 Performance of HDA-WZ-BE under mismatched SNR and/or SI quality

In [20] we made a performance comparison between HDA-WZ-BE, a previously known robust scheme, namely *common description scheme* (CDS) [30], and the uncoded transmission when $\sigma_S^2 = 0$, i.e., no additional interference, and $\kappa \geq 1$, i.e., BE case. The comparison was based on a performance metric we introduced: the *distortion loss*

$$L\left(\sigma_{Z_*}^2, \gamma_*\right) = \frac{D\left(\sigma_{Z_*}^2, \gamma_*\right)}{\sigma_{Z_*}^2 \left(1+\gamma_*\right)^{-\kappa}}$$

where the system parameters are adjusted as to attain the optimal distortion at a target $\left(\sigma_Z^2, \gamma\right)$ pair. By using HDA-WZ-BE in this scenario, it follows from (2.6) and (2.11) that the auxiliary codeword can be detected and benefitted from as long as

$$\frac{(1+\gamma)^{\kappa} - 1}{\sigma_Z^2 (1+\gamma)} \leq \frac{(1+\gamma_*)^{\kappa} - 1}{\sigma_{Z_*}^2 (1+\gamma_*)} \tag{2.16}$$

holds and the scheme attains the optimal distortion $\sigma_{Z_*}^2 \left(1+\gamma_*\right)^{-\kappa}$ at $\left(\sigma_{Z_*}^2, \gamma_*\right)$ if (2.16) holds with equality. CDS is shown in [30] to exhibit similar robustness performance, i.e., the auxiliary codeword is uniquely decoded as long as

$$\frac{(1+\gamma)^{\kappa} - 1}{\sigma_Z^2} \leq \frac{(1+\gamma_*)^{\kappa} - 1}{\sigma_{Z_*}^2} \tag{2.17}$$

and if it holds with equality then the optimal distortion is attained at $\left(\sigma_{Z_*}^2, \gamma_*\right)$. Both of these schemes suffer from the threshold effect if the corresponding inequalities do not hold.

We now compare the performances of CDS, HDA-WZ, and uncoded transmission methods in terms of the distortion loss that they incur. We likewise define the *distortion*

	If (2.16) or (2.17) satisfied	Otherwise
L_{HDA}	$\left(\frac{(1+\gamma)^{\kappa}-1}{\sigma_Z^2}\cdot\frac{1+\gamma_*}{1+\gamma}+\frac{1}{\sigma_{Z_*}^2}\right)^{-1}\frac{(1+\gamma_*)}{\sigma_{Z_*}^2}$	$(1+\gamma_*)^{\kappa}$
L_{CDS}	$\left(\frac{(1+\gamma)^{\kappa}-1}{\sigma_Z^2}\cdot\frac{1+\gamma_*}{1+\gamma}+\frac{1}{\sigma_{Z_*}^2}\right)^{-1}\frac{(1+\gamma_*)}{\sigma_{Z_*}^2}$	$(1+\gamma_*)^{\kappa}$
L_{UNC}	$\frac{(1+\gamma_*)^{\kappa}}{\left(1+\gamma\kappa\sigma_{Z_*}^2\right)}$	

Table 2.1: The distortion loss expressions for the three schemes

gain as

$$G\left(\sigma_{Z_*}^2,\gamma_*\right)=\frac{1}{L\left(\sigma_{Z_*}^2,\gamma_*\right)}.$$

Note that $L\left(\sigma_{Z_*}^2,\gamma_*\right)$ larger than or equal to 1 while $L\left(\sigma_{Z_*}^2,\gamma_*\right)$ is between 0 and 1 for any $\left(\sigma_{Z_*}^2,\gamma_*\right)$ pair with any scheme. The distortion loss expressions for HDA-WZ, CDS, and uncoded transmission are given in Table 2.1.

In Fig. 2.3, the distortion gains are depicted in an RGB-coded diagram, where "red", "green", and "blue" colors account for G_{HDA}, G_{CDS}, and G_{UNC}, respectively. In this sense a true "yellow" color at any point means $G_{\text{HDA}}=G_{\text{CDS}}=1$ and G_{UNC} at that $\left(\sigma_{Z_*}^2,\gamma_*\right)$ pair. Likewise, a true "white" color corresponds to all the schemes being optimal whereas a true "black" color means distortion loss for all of the schemes are very high. In the figure, $\kappa=1.2$ and the target is set to $\rho=\sqrt{\left(1-\sigma_Z^2\right)}\approx 0.7071$ and $\gamma=5$.

Table 2.2 shows numerical values for G_{HDA}, G_{CDS}, and G_{UNC} at several points indicated on Fig. 2.3. On the curve indicated by points **f-a-g**, $G_{\text{HDA}}=1$ since (2.16) is satisfied with equality. For all points to the upper right of that curve, the HDA-WZ scheme successfully decodes T^{mN}. Likewise, on the curve **b-a-c**, $G_{\text{CDS}}=1$ since (2.17) is satisfied with equality and to the upper-right of that curve, CDS decodes the auxiliary codeword

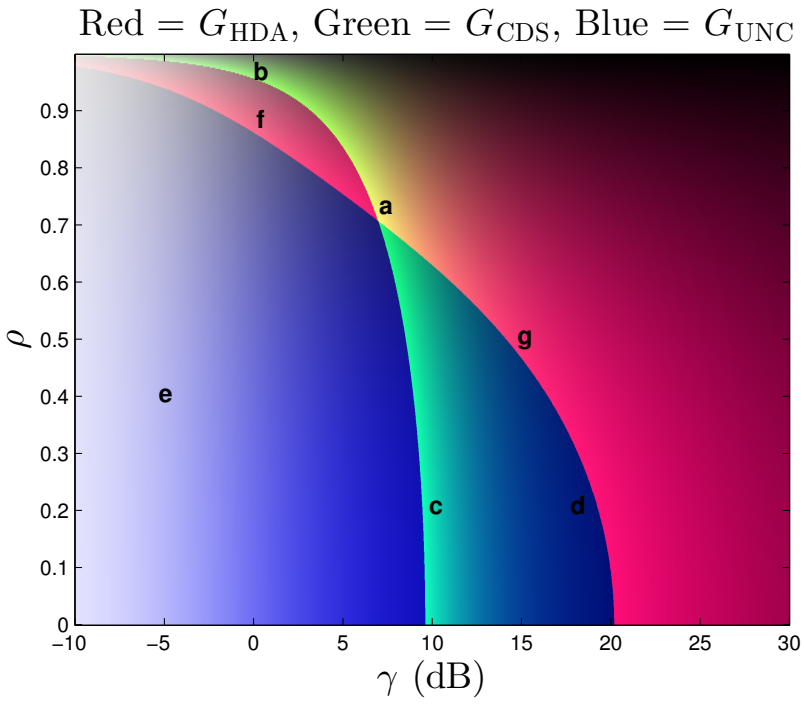

Figure 2.3: An RGB-coded representation of G_{HDA}, G_{CDS}, and G_{UNC}

Point	R(G_{HDA})	G(G_{CDS})	B(G_{UNC})	γ (dB)	ρ
a	1.000	1.000	0.465	6.99	0.707
b	0.627	1.000	0.487	-0.16	0.958
c	0.064	1.000	0.721	9.48	0.194
d	0.005	0.080	0.478	19.00	0.200
e	0.719	0.719	0.948	-5.00	0.400
f	1.000	0.428	0.566	0.12	0.860
g	1.000	0.217	0.467	14.54	0.486

Table 2.2: The points on Fig. 2.3 and corresponding values.

successfully. On the point **a**, which corresponds to the target, both CDS and HDA-WZ achieves a gain of 1, as expected. On points **d** and **e**, the uncoded transmission scheme outperforms the other two.

In [20] we extended our comparison under the criterion that

$$\mathcal{L}(\mathcal{R}) = \min \max_{(\sigma^2_{Z_*}, \gamma_*) \in \mathcal{R}} L\left(\sigma^2_{Z_*}, \gamma_*\right)$$

and we showed that $\mathcal{L}_{\text{HDA}}(\mathcal{R}) \leq \mathcal{L}_{\text{CDS}}(\mathcal{R})$ for every rectangular region

$$\mathcal{R} = \left\{ \left(\sigma^2_{Z_*}, \gamma_*\right) \middle| \sigma^2_{Z1} \leq \sigma^2_{Z_*} \leq \sigma^2_{Z2}, \sigma^2_{Z1}\gamma_1 \leq \gamma_* \leq \gamma_2 \right\}.$$

Chapter 3

On Robustness of HDA Schemes Against Channel Quality Mismatch

3.1 Problem Definition and Motivation

In this chapter we consider a similar scenario as in the previous one where it differs in 1) that there is no SI and/or additional interference and 2) there are two additional receivers. We aim at achieving the best tradeoff between the distortion levels when the channel quality is *good* and *bad* under the constraint that the distortion is optimal when the channel has the targeted *median* quality.

Explicitly, we consider lossy transmission of an i.i.d. unit-variance Gaussian source X^{nN} over an AWGN bandwidth mismatched broadcast channel with three receivers having different SNR values, i.e., γ, γ_+, and γ_- where the subscript ' ', '+', and '−' indicate entities realting to the *median*, the *good*, and the *bad* receiver, respectively. We also use the

subscript '*' to make a general statement about all three channels or receivers.

The transmitter maps X^{nN} into the channel input U^{mN} which is power constrained by (2.1) where again $P = 1$ for convenience. Each receiver observes the corrupted version of U^{mN} which is $V_*^{mN} = U^{mN} + W_*^{mN}$ with $W_*^{mN} \sim \mathcal{N}\left(\mathbf{0}, \gamma_*^{-1}\mathbf{I}_{mN}\right)$. The receivers then estimate the source as $\hat{X}_*^{nN}$ using their observations V_*^{mN}. The scenario is illustrated in Fig.3.1.

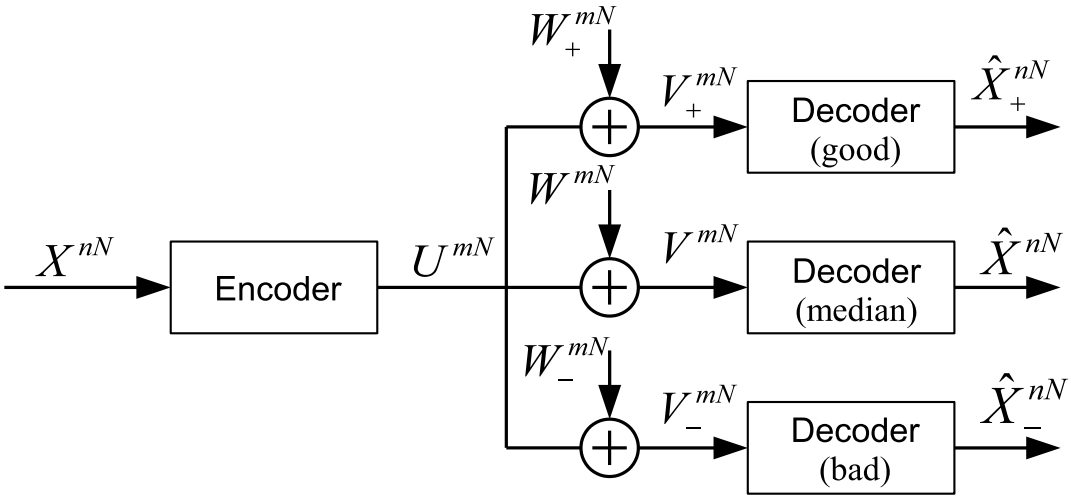

Figure 3.1: The scenario with three receivers with a common source and common encoder.

The quality of reconstruction at each receiver is again measured by the average expected square-error distortion

$$D_* = \lim_{N\to\infty} \frac{1}{nN} \sum_{i=1}^{nN} \mathbb{E}\left[\left(X_i - \hat{X}_{*i}\right)^2\right].$$

For the BE case $\kappa > 1$, when the distortion D at the median receiver is fixed at its minimum possible value, i.e.,

$$D = \frac{1}{(1+\gamma)^{\kappa}}, \tag{3.1}$$

the minimum value of D_+ that can be achieved is due to the coding schemes by Reznic *et al.* [35], Prabhakaran *et al.* [32] and also by Mittal and Phamdo [26], and is given by

$$D_+ = \frac{1}{(1+\gamma)^{\kappa-1}(1+\gamma_+)}. \tag{3.2}$$

To achieve this, the schemes mentioned above all reduce to sending the quantization error from the first nN channel uses and dedicating the remaining $(m-n)N$ uses for digital communication of the source codewords.

If we seek to minimize D_- instead, while keeping D optimal as in (3.1), the best known coding schemes, by Reznic *et al.* [35], Prabhakaran et al. [32], and also by Shamai *et al.* [36], all of which in this case reduce to sending the source uncoded from the first nN uses and dedicating the remaining uses for the Wyner-Ziv coding by treating the received signal of uncoded transmission as SI, achieve

$$D_- = \frac{1}{1+\gamma_-}. \tag{3.3}$$

However, none of the aforementioned schemes can achieve (3.1), (3.2), and (3.3) simultaneously.

For the BC case, on the other hand, the best known scheme, by Prabharakaran *et al.* [33], can either achieve (3.1) and

$$D_+ = (1-\kappa)D + \kappa\frac{\gamma}{(1+\gamma)^{\kappa}\gamma_+ + \gamma - \gamma_+} \tag{3.4}$$

or (3.1) and

$$D_- = 1 - \kappa\gamma_- \frac{1+\gamma-(1+\gamma)^{1-\kappa}}{\gamma\,(1+\gamma_-)}. \tag{3.5}$$

In the first case, the scheme reduces to sending the superposition of uncoded transmission of the first mN source symbols and digital data pertaining to the remaining source symbols, whereas in the second case it is equivalent to uncoded transmission of the first mN source symbols together with the Costa coding for the remaining source symbols with the remaining power. These special cases were also described in [28], where a duality between the schemes was demonstrated. Similar to the BE case, however, the scheme cannot achieve (3.1), (3.4), and (3.5) simultaneously.

In [40], Tian and Shamai posed the problem of finding the tradeoff between D_+ and D_-, while keeping D optimum as in (3.1). They subsequently showed in [42] that (3.1), (3.2), and (3.3), or (3.1), (3.4), and (3.5) can be achieved simultaneously for bandwidth expansion factors that are integers or unit fractions, respectively. Their scheme was based on successive utilization of bandwidth-matched HDA-WZ or HDA-Costa coding both of which are introduced in [45]. For an integer $\kappa > 1$, the source is transmitted uncoded from the first subband, and HDA-WZ is utilized at the second subband, treating the observation received from the first subband as decoder SI. At each subsequent subband, HDA-WZ is employed similarly, except it is the estimate of the source from the previous stage which serves as SI. For κ with $1/\kappa \in \mathbb{Z}^+$, the source is divided into $1/\kappa$ subsources. First subsource is transmitted uncoded, and the rest of subsources are transmitted using a hierarchy of HDA-Costa codes, each level of which treats the channel inputs above it as interference and

below it as noise.

In this chapter we propose coding schemes which extend the result in [42] to noninteger $\kappa \geq 2$ and non-unit fraction $\kappa \leq 1/2$. That is for any rational $\kappa \geq 2$, (3.1), (3.2), and (3.3) can be achieved simultaneously, and similarly for any rational $\kappa \leq 1/2$, (3.1), (3.4), and (3.5) can be achieved simultaneously. These coding schemes, described in detail in Sections 3.3 and 3.4, rely on uncoded transmission together with extensions of the HDA-WZ-Costa scheme of Wilson *et al.* [45] to bandwidth mismatch, that are introduced in Chapter 2. For $1 < \kappa < 2$ and $1/2 < \kappa < 1$, on the other hand, although we cannot simultaneously achieve (3.1), (3.2), and (3.3), or (3.1), (3.4), and (3.5) , we devise competitive schemes in Sections 3.5 and 3.6, respectively, that can achieve nontrivial tradeoffs between D_+ and D_- when D is kept optimal. These schemes are competitive in the sense that even at the extreme ends of minimized D_+ or D_-, the achieved (D_+, D_-) pairs significantly outperform those appeared in the literature. They rely on a modification of the coding combination by introducing correlation between the source and the channel input supersymbols. This approach is explained in detail in the following section.

3.2 HDA with Correlated Source and Channel Input

Note that in the HDA coding schemes given in Chapter 2 the channel output V^{mN} provides us with no information unless the auxiliary codeword is decoded because X^{nN} and U^{mN} are independent. We now relax this constraint and send a channel input that gives information about the source on its own. In Sections 3.5 and 3.6, we will employ the technique developed here in conjunction with those developed in Sections 3.3 and 3.4

to achieve the best known (D_+, D_-) tradeoff for $1/2 < \kappa < 2$.

3.2.1 BE case

Similar to before, let the auxiliary codewords be generated according to the random variable

$$T^m = \begin{bmatrix} T_1^n \\ T_2^{m-n} \end{bmatrix} = \begin{bmatrix} k_1 X^n \\ 0^{m-n} \end{bmatrix} + \begin{bmatrix} Q^n \\ G^{m-n} \end{bmatrix}$$

where $Q^n \sim \mathcal{N}\left(0^n, \sigma_Q^2 \mathbf{I}_n\right)$, $G^{m-n} \sim \mathcal{N}\left(0^n, \mathbf{I}_{m-n}\right)$, and $X^n \perp Q^n \perp G^{m-n}$. However, after a typical codeword $T^{mn}(j)$ is found, let the channel input be calculated supersymbol-by-supersymbol as

$$U^m = \begin{bmatrix} U_1^n \\ U_2^{m-n} \end{bmatrix} = \begin{bmatrix} \alpha\left(T_1^n - X^n\right) \\ T_2^{m-n} \end{bmatrix}$$

with attenuation constant

$$\alpha = \frac{1}{\sqrt{\left(1 - k_1\right)^2 + \sigma_Q^2}} \tag{3.6}$$

to ensure that $U^m \sim \mathcal{N}\left(0^{mN}, \mathbf{I}_{mN}\right)$. Observe that unlike before, U^m and X^n are correlated unless $k_1 = 1$. At the receiver the supersymbol-wise MMSE estimation of X^n will be based on T_1^n, if $T^{mN}(j)$ is uniquely decoded, and $V_1^n = U_1^n + W_1^n$, as before.

For reliable communication we need

$$I\left(T^m; X^n\right) \leq I\left(T^m; V^m\right) \tag{3.7}$$

where

$$I\left(T^m; X^n\right) = \frac{n}{2} \log\left(1 + \frac{k_1^2}{\sigma_Q^2}\right), \tag{3.8}$$

and

$$I\left(T^m;V^m\right)=\frac{n}{2}\log\left(\frac{\left(1+\frac{k_1^2}{\sigma_Q^2}\right)(1+\gamma)}{1+\frac{k_1^2}{\sigma_Q^2}+\alpha^2\gamma}\right)+\frac{m-n}{2}\log\left(1+\gamma\right). \tag{3.9}$$

Equations (3.7)-(3.9) together yield

$$1+\frac{k_1^2}{\sigma_Q^2}+\alpha^2\gamma\leq\left(1+\gamma\right)^{\kappa}. \tag{3.10}$$

Theorem 7 *For every* $\left(k_1,\sigma_Q^2\right)$ *pair that satisfies (3.10) with equality, the above scheme attains optimal distortion.*

Proof. Using the same arguments for the MMSE estimation before and noting that

$$\begin{aligned}\hat{X}_i &= \mathbb{E}\left[X_i\mid T_{1,i},V_{1,i}\right]\\ &= \mathbb{E}\left[X_i\mid T_{1,i},V_{1,i}-\alpha T_{1,i}\right]\\ &= \mathbb{E}\left[X_i\mid k_1X_i+Q_i-\alpha X_i+W_{1,i}\right],\end{aligned}$$

the distortion, provided that the auxiliary codeword is decoded, can be found invoking Lemma 1 as

$$D=\left(1+\frac{k_1^2}{\sigma_Q^2}+\alpha^2\gamma\right)^{-1}.$$

Since the $\left(k_1,\sigma_Q^2\right)$ pair is chosen so that (3.10) is satisfied with equality, $D=(1+\gamma)^{-\kappa}$, which is optimal. ■

Corollary 8 *If the SNR is better than expected, i.e.,* $\gamma_+>\gamma$*, the distortion can be similarly found as*

$$D_+=\left(1+\frac{k_1^2}{\sigma_Q^2}+\alpha^2\gamma_+\right)^{-1}.$$

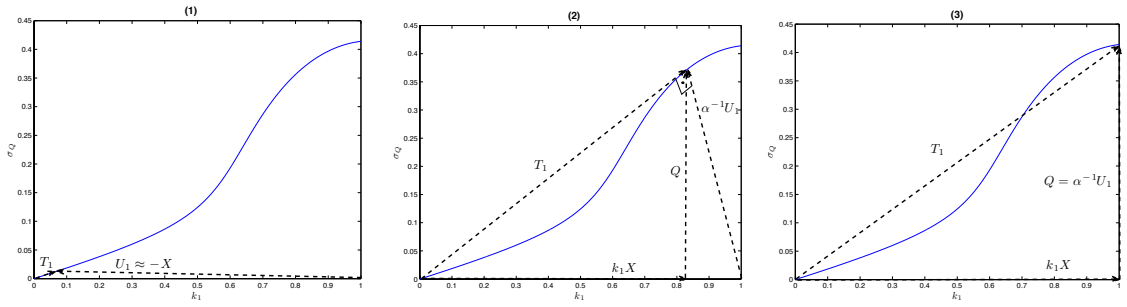

Figure 3.2: The (k_1, σ_Q) pairs satisfying (3.10) with equality and the relation between random variables T_1, X, Q, and U_1. The three figures correspond to the three special cases of **(1)** $k_1 \to 0$, **(2)** $k_1 = 1 - (1+\gamma)^{1-\kappa}$, and **(3)** $k_1 = 1$ discussed in the text.

On the other hand, unlike in Chapter 2, the distortion is not catastrophic when the SNR drops to $\gamma_- < \gamma$, because V_1^n is correlated with X^n. The MMSE estimate $\hat{X}^n = c_V V_1^n$ will yield the distortion

$$\begin{aligned} D_- &= 1 - \frac{\alpha^2 (1-k_1)^2}{1+\gamma_-^{-1}} \\ &= \frac{(1-k_1)^2 + \sigma_Q^2 (1+\gamma_-)}{(1+\gamma_- \alpha^{-2})}. \end{aligned}$$

Therefore, by using the freedom in choosing any $\left(k_1, \sigma_Q^2\right)$ satisfying (3.10) with equality, one can obtain a tradeoff of (D_+, D_-) pairs (instead of a single (D_+, D_-) pair as in Section 2.2). Note that for every k_1, the value of σ_Q^2 to satisfy (3.10) with equality can be found by solving a quadratic equation. The resultant (k_1, σ_Q) pairs for the parameters, $\gamma = 5$ and $\kappa = 2$ are depicted in Fig. 3.2. As can be seen in the figure, as $k_1 \to 0$, σ_Q^2 approaches 0 as well. In fact, it can be shown using some algebra that in this extreme,

$$\frac{k_1}{\sigma_Q} \to \sqrt{(1+\gamma)^\kappa - 1 - \gamma}.$$

The relation between random variables T_1, X, Q, and U_1 is also illustrated in Fig. 3.2. Since k_1 and σ_Q^2 are actually the magnitudes (i.e., standard deviations) of $k_1 X$ and Q,

respectively, and $X \perp Q$, the tip of the vector $T_1 = k_1 X + Q$ traverses the curve of $\left(k_1, \sigma_Q^2\right)$ pairs satisfying (3.10) with equality. Three important choices of (k_1, σ_Q) shown in Fig. 3.2 correspond to

- **(1)** $k_1 \to 0$ and $\sigma_Q \to 0$, which implies that $U_1^n \to -X^n$. Moreover, from Fig. 3.2, it is also clear that this choice minimizes the angle between T_1 and X (thereby maximizing $\frac{k_1}{\sigma_Q}$), and as a result, it follows from (3.8), (3.9), and equality in (3.10) that both $I\left(T_1^n; X^n\right)$ and $I\left(T_1^n; V_1^n\right)$ are maximized. With this choice, the scheme is also equivalent to sending the source uncoded from the first nN channel uses and using Wyner-Ziv coding for the rest of the bandwidth while treating the received signal V_1^n as SI (cf. [35], [36]). It thus achieves the best known D_- given in (3.3).

- **(2)** $k_1 = 1 - (1+\gamma)^{1-\kappa}$ and $\sigma_Q^2 = k_1\left(1 - k_1\right)$, resulting in $T_1^n \perp U_1^n$ (and therefore $T_1^n \perp V_1^n$) and minimum $I\left(T_1^n; X^n\right)$ by the same angle argument. This makes the scheme equivalent to sending the quantization noise $T_1^n - X_1^n$ (which is orthogonal to the quantized vector T_1^n) from the first nN channel uses and dedicating the rest of the bandwidth to the transmission of digital data, using which the reciever can decode T_1^n (cf. [26, 35]). Hence, it achieves the best known D_+ given in (3.2).

- **(3)** $k_1 = 1$, yielding $X^n \perp U_1^n$, reducing the scheme exactly to HDA-BE, i.e., without any SI or interference (cf. [20]).

Even though we will use this scheme only as a component of a more complex scheme, looking at its (D_+, D_-) depicted in Fig. 3.3 sheds some insight on the benefit of correlating X_n and U_m. For example, not only can we recover the best known D_- and best known

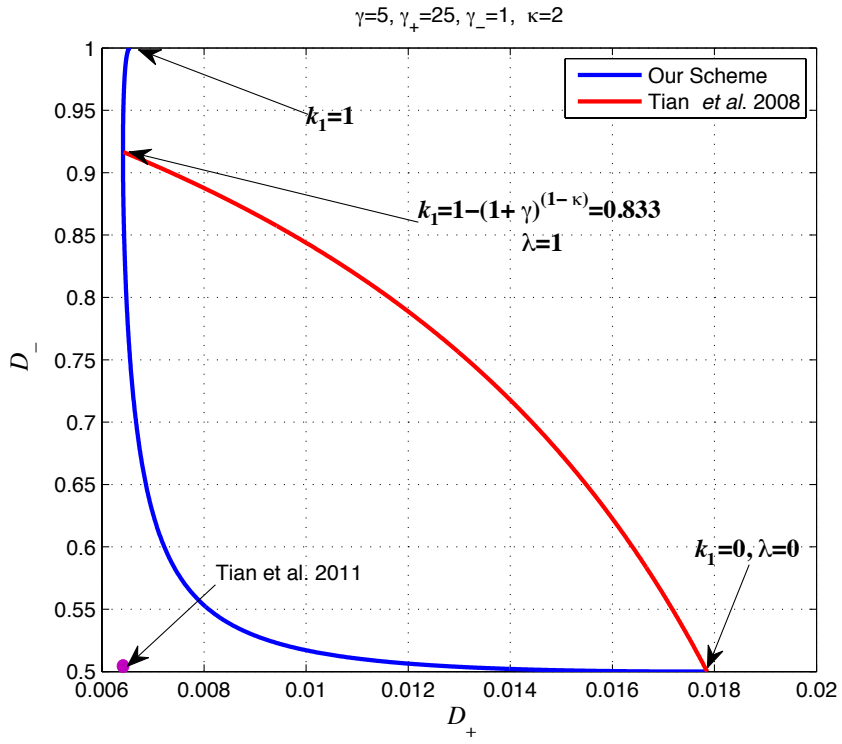

Figure 3.3: The distortion tradeoff between the good and bad receivers while the median receiver achieves the optimum distortion, for $\gamma_- = 1$, $\gamma = 5$, $\gamma = 25$, and $\kappa = 2$. The red dashed curve depicts the tradeoff attained by [40] while the blue solid curve is the tradeoff achieved by the HDA scheme with correlated source and channel input. The numbering of the special cases on the curve matches those in Fig. 3.2.

D_+ as special cases **(1)** and **(2)**, respectively, but we also observe that unlike Tian et al's scheme in [40], intermediate values of k_1 between the two cases yield (D_+, D_-) points that are not achievable simply by time sharing.

3.2.2 BC Case

The source X^{nN}, in this case, is divided into two subsources X_1^{mN} and $X_2^{(n-m)N}$ both of which will be regarded as collections of supersymbols X_1^m and X_2^{n-m}, respectively. The codewords are generated according to

$$T^n = \begin{bmatrix} T_1^m \\ T_2^{n-m} \end{bmatrix} = \begin{bmatrix} k_1 X_1^m \\ k_2 X_2^{n-m} \end{bmatrix} + \begin{bmatrix} Q^m \\ G^{m-n} \end{bmatrix}$$

where $Q^m \sim \mathcal{N}\left(0^m, \sigma_Q^2 \mathbf{I}_m\right)$, $G^{n-m} \sim \mathcal{N}\left(0^{n-m}, \mathbf{I}_{n-m}\right)$, and $X^n \perp Q^m \perp G^{n-m}$. After a codeword $T^{nN}(j)$ which is jointly typical with the source is found, the channel input U^{mN} is computed supersymbol-wise as

$$U^m = \alpha\left(T_1^m - X_1^m\right)$$

where α is as in (3.6). At the receiver the supersymbol-wise MMSE estimation of the subsource X_1^m will be based on T_1^m, if $T^{mN}(j)$ is uniquely decoded, and $V^m = U^m + W^m$ as before. On the other hand, X_2^{n-m} will be reconstructed based only on T_2^{n-m}, again if $T^{mN}(j)$ is uniquely decoded.

The rate inequality

$$I\left(T^n; X^n\right) \leq I\left(T^n; V^m\right)$$

where

$$I\left(T^n; X^n\right) = \frac{m}{2}\log\left(1 + \frac{k_1^2}{\sigma_Q^2}\right) + \frac{n-m}{2}\log\left(1 + k_2^2\right)$$

and

$$I\left(T^n;V^m\right)=\frac{m}{2}\log\left(1+\frac{k_1^2}{\sigma_Q^2}\right)-\frac{m}{2}\log\left(\frac{1+\frac{k_1^2}{\sigma_Q^2}+\alpha^2\gamma}{1+\gamma}\right)$$

leads to

$$\left(\frac{1+\frac{k_1^2}{\sigma_Q^2}+\alpha^2\gamma}{1+\gamma}\right)\leq\left(1+k_2^2\right)^{\kappa-1} \tag{3.11}$$

which is very similar to (3.10). In fact, since the estimation of the subsource X_2^{n-m} relies only on the digital information T_2^{n-m}, we have

$$D_2=\frac{1}{1+k_2^2}.$$

To achieve the minimum possible distortion $D_2=(1+\gamma)^{-\kappa}$, we set $k_2^2=(1+\gamma)^{\kappa}-1$, thereby making (3.11) exactly the same as (3.10). This action therefore makes $D_1=(1+\gamma)^{-\kappa}$ for all $\left(k_1,\sigma_Q^2\right)$ pairs satisfying (3.11) with equality, as in the BE case. Hence, we have the following theorem immediately:

Theorem 9 *When $k_2^2=(1+\gamma)^{\kappa}-1$, for every $\left(k_1,\sigma_Q^2\right)$ pair that satisfies (3.11) with equality, the above scheme attains optimal distortion.*

Corollary 10 *If the SNR increases to $\gamma_+>\gamma$ or drops to $\gamma_-<\gamma$, the resultant distortion expressions can be found as in Corollary 8 as*

$$\begin{aligned}D_+ &= \kappa D_{1,+}+(1-\kappa)D_{2,+}\\ &= \kappa\left(1+\frac{k_1^2}{\sigma_Q^2}+\alpha^2\gamma_+\right)^{-1}+\frac{(1-\kappa)}{(1+\gamma)^{\kappa}}\end{aligned}$$

and

$$\begin{aligned}D_- &= \kappa D_{1,-}+(1-\kappa)D_{2,-}\\ &= \kappa\frac{(1-k_1)^2+\sigma_Q^2(1+\gamma_-)}{\alpha^{-2}(1+\gamma_-)}+(1-\kappa),\end{aligned}$$

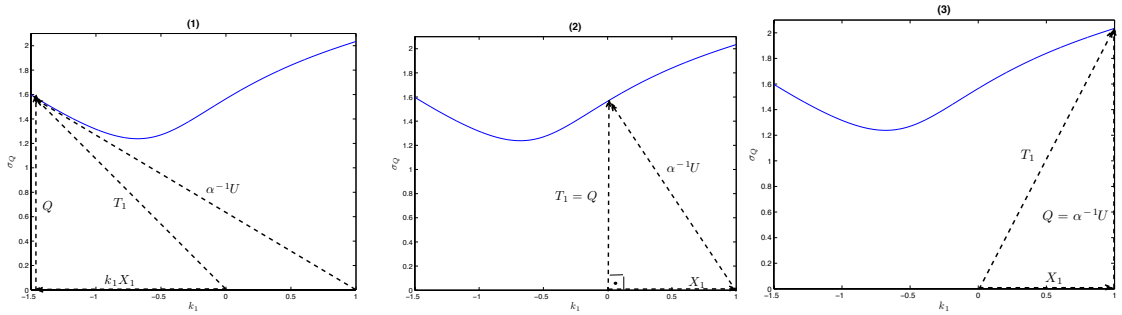

Figure 3.4: The (k_1, σ_Q) pairs satisfying (3.11) with equality and the relation between random variables T_1, X_1, Q, and U. The three figures correspond to the three special cases of **(1)** $k_1 = 1 - (1+\gamma)^{1-\kappa}$, **(2)** $k_1 = 0$, and **(3)** $k_1 = 1$, as discussed in the text.

where $D_{2,+} = (1+\gamma)^{-\kappa}$ *and* $D_{2,-} = 1$*, because the transmission of* $X_2^{(n-m)N}$ *suffers from both leveling-off and thresholding effects.*

Similar to the BE case, one can obtain a (D_+, D_-) tradeoff by choosing any $\left(k_1, \sigma_Q^2\right)$ satisfying (3.11) with equality when $k_2^2 = (1+\gamma)^{\kappa} - 1$. The resultant (k_1, σ_Q) pairs for the parameters $\gamma = 5$ and $\kappa = 1$ are depicted in Fig. 3.4, together with the relation between T_1, X_1, Q, and U, and the corresponding (D_+, D_-) tradeoff is shown in Fig. 3.5.

Three special choices of $\left(k_1, \sigma_Q^2\right)$ shown in Fig. 3.4 correspond to

- **(1)** $k_1 = 1 - (1+\gamma)^{1-\kappa}$ and $\sigma_Q^2 = \frac{k_1(1-k_1)}{1-(1+\gamma)^{-\kappa}}$, with which $I\left(X^m; U^m\right)$ is maximized (because the angle between X_1 and U is minimized). With the choice of this $\left(k_1, \sigma_Q^2\right)$ pair, the scheme is equivalent to sending $-X^{mN}$ uncoded, and treating a scaled version of $-X^{mN}$ as interference, using Costa coding to send the digital data pertaining to $X_2^{(n-m)N}$. This equivalent scheme was termed *Hybrid Costa Coding* in [28, Sec.III-B-d], and was shown to be a special case of the coding scheme in [33, 32]. Therefore, it achieves the same best known D_- in (3.5), as emphasized in Fig. 3.5.

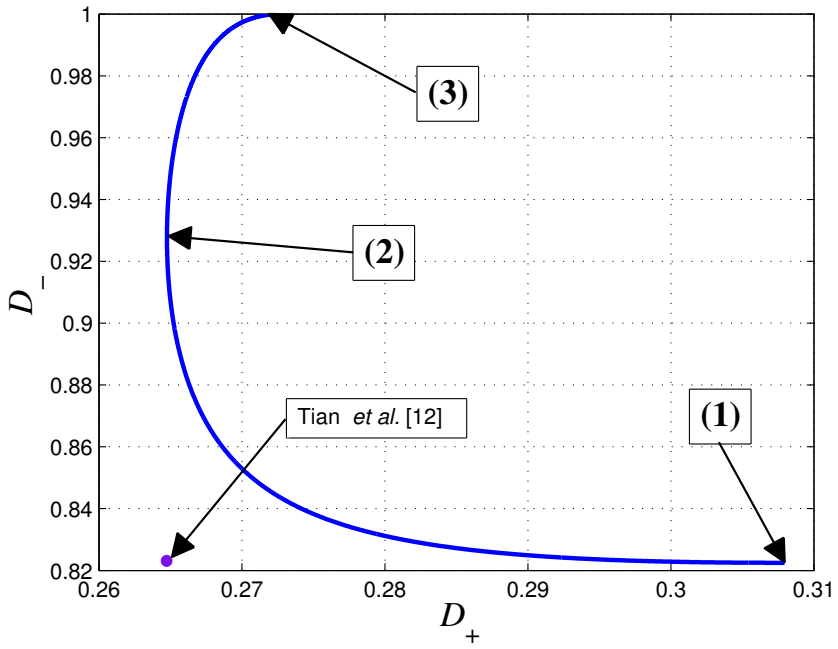

Figure 3.5: The distortion tradeoff between the good and bad receiver (BC). The blue curve gives the tradeoff for different k_1 values while $\gamma = 5$, $\gamma_- = 1$, $\gamma_+ = 25$, and $\kappa = 1/2$. The numbering of the special cases on the curve matches those in Fig. 3.4.

- **(2)** $k_1 = 0$ and $\sigma_Q^2 = \frac{1+\gamma-(1+\gamma)^\kappa}{(1+\gamma)^\kappa-1}$, resulting in $T_1 \perp X_1$. In this case that the scheme is equivalent to sending the superposition of the analog information about the first part of the source, i.e., a scaled version of $-X^{mN}$, and purely digital information about the second part of the source $X_2^{(n-m)N}$. This equivalent scheme was discussed in [28, Sec.III.B-b] and was shown to be a special case of the coding scheme in [33, 32]. Therefore, the resultant D_+ coincides with the best known D_+ in (3.4), as observed in Fig. 3.5.

- **(3)** $k_1 = 1$, yielding $X_1^m \perp U^m$, reducing the scheme to HDA-BC, i.e., without any SI or interference.

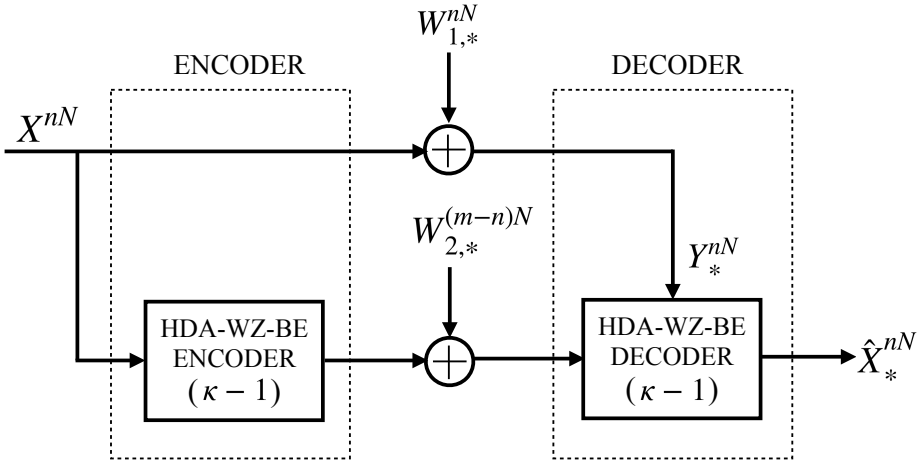

Figure 3.6: The corrupted version of the source $Y_*^{nN} = X^{nN} + W_{1,*}^{nN}$ serves as SI. Note that the bandwidth expansion factor for HDA-WZ-BE encoder and decoder is $\kappa - 1 \geq 1$. The encoder and the decoder for the overall coding scheme is enclosed in dashed rectangles.

3.3 When $\kappa \geq 2$

Out of mN channel uses nN are dedicated to uncoded transmission with unit power. In the remaining $(m-n)\,N$ uses, we send the source again using HDA-WZ-BE (with bandwidth expansion factor $\frac{m-n}{n} = \kappa - 1$) by treating the received signal at the first nN channel uses as SI. The coding scheme is illustrated in Fig.3.6.

Theorem 11 *The scheme described above achieves (3.1), (3.2), and (3.3) simultaneously for any $\kappa \geq 2$.*

Proof. Follows from Theorem 2 and Corollary 3 after substituting $\kappa - 1$ for the effective bandwidth expansion factor together with $\sigma_{Z_*}^2 = (1+\gamma_*)^{-1}$ and $\sigma_S^2 = 0$. This substitution yields

$$D = \frac{(1+\gamma)^{-1}}{(1+\gamma)^{\kappa-1}} = (1+\gamma)^{\kappa}$$

which agrees with (3.1), and (2.12) and (2.13) yields (3.2) and (3.3), respectively. ■

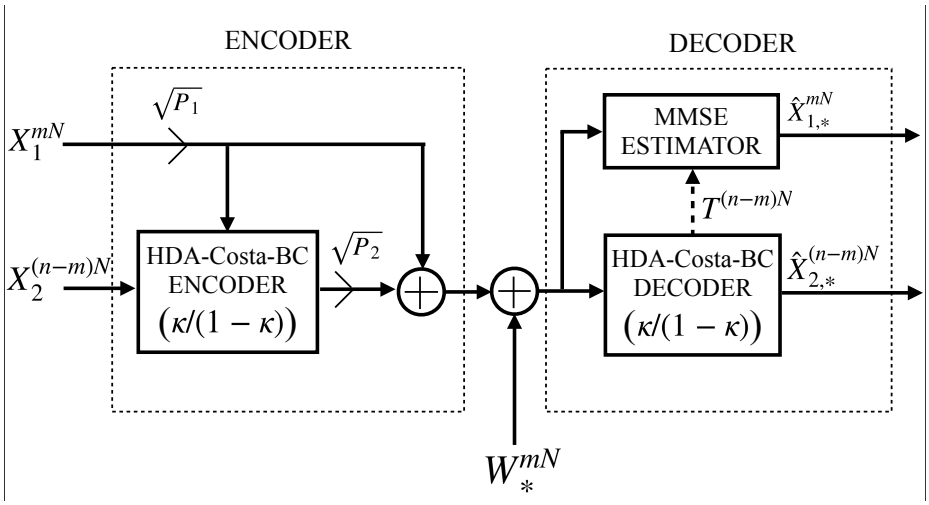

Figure 3.7: The first part of the input, X_1^{mN}, serves as interference for the transmission of the second part, $X_2^{(n-m)N}$. The encoder and the decoder for the overall coding scheme is enclosed in dashed rectangles.

3.4 When $\kappa \leq 1/2$

The source X^{nN} is divided into subsequences X_1^{mN} and X_2^{mN}. While X_1^{mN} is transmitted uncoded with power P_1, $X_2^{(n-m)N}$ is transmitted using HDA-Costa-BC with power $P_2 = 1 - P_1$ over the channel, treating $\sqrt{P_1}X_1^{mN}$ as an interference signal. The effective bandwidth compression factor is therefore $\frac{m}{n-m} = \frac{\kappa}{1-\kappa} \leq 1$. The overall scheme is represented in Fig.3.7.

Theorem 12 *The scheme described above achieves (3.1), (3.4), and (3.5) simultaneously for any $\kappa \leq 1/2$.*

Proof. We are going to invoke Theorem 5 and Corollary 6. However, we need the output of the HDA-Costa-BC encoder to have power 1 (as opposed to P_2). Towards that end, observe that the performance would not change if we multiply the channel output by $1/\sqrt{P_2}$ before using it for decoding or estimation. But if we "push" this multiplier toward the channel

input, that would make the HDA-Costa-BC encoder output power 1, the SNR $P_2\gamma_*$, and the interference variance $\sigma_S^2 = P_1/P_2$. Since no SI is available, $\sigma_{Z_*}^2 = 0$.

Adapting (2.14) to the proposed coding scheme, the relation between X_1^m, X_2^{n-m}, U^m, and auxiliary random variable T^{n-m} can be re-written as

$$T^{n-m} = \begin{bmatrix} T_1^m \\ T_2^{n-2m} \end{bmatrix} = \begin{bmatrix} k_1 X_{2,1}^m \\ k_2 X_{2,2}^{n-2m} \end{bmatrix} + \begin{bmatrix} T_1^m \\ T_2^{n-2m} \end{bmatrix} + \begin{bmatrix} U^m \\ Q^{n-2m} \end{bmatrix} + \begin{bmatrix} a\sqrt{\frac{P_1}{P_2}} X_1^m \\ 0^{n-2m} \end{bmatrix}$$

where X_2^{n-m} is broken into two more pieces $X_{2,1}^m$ and $X_{2,2}^{n-2m}$.

Because of the fact that (i) $T_1^m - V^m - X_1^m$ forms a Markov chain when (k_1, a) is chosen optimally as in the proof of Theorem 5, i.e., as

$$a = \frac{P_2\gamma}{1 + P_2\gamma}$$

and

$$k_1^2 = \frac{(1 + P_2\gamma)^{\frac{\kappa}{1-\kappa}} - 1}{1 + P_2\gamma},$$

and (ii) $T_2^{n-2m} \perp X_1^m$, the auxiliary codeword $T^{(n-m)N}$ cannot give any further information about X_1^{mN} at the median receiver, given the channel output V^{mN}. Therefore the distortion for X_1^{mN} at the median receiver is simply

$$D_1 = \frac{1 + P_2\gamma}{1 + \gamma}. \tag{3.12}$$

By choosing

$$1 + P_2\gamma = (1 + \gamma)^{1-\kappa} \tag{3.13}$$

one immediately obtains (3.1) and since $T^{(n-m)N}$ is not available at the bad receiver, we have

$$D_{1,-} = \frac{\gamma_- \left((1 + \gamma)^{1-\kappa} - 1\right) + \gamma}{\gamma\,(1 + \gamma_-)}. \tag{3.14}$$

When SNR is $\gamma_+ > \gamma$, the above Markov chain breaks down, and the MMSE estimation for X_1^{mN} is performed using not only V^{mN} but also the auxiliary codeword T_1^{mN}, and using (3.13)

$$D_{1,+} = (1+\gamma)^{-\kappa} - \frac{\frac{\gamma_+ - \gamma}{1+\gamma}\left((1+\gamma)^{\kappa} - 1\right)}{\gamma - \gamma_+ + \gamma_+ (1+\gamma)^{\kappa}}. \tag{3.15}$$

For $X_2^{(n-m)N}$, the expressions for D_2, $D_{2,-}$ and $D_{2,+}$ can be borrowed from D, D_-, and D_+ in Theorem 5 and Corollary 6 after substituting $\kappa/(1-\kappa)$ for the effective bandwidth, together with $\sigma^2_{Z_*} = 1$, SNR$= P_2\gamma_*$, and $\sigma_S^2 = P_1/P_2$ as discussed above. Together with (3.12), (3.14), and(3.15), this yields (3.1), (3.4), and 3.5). ■

3.5 When $1 \leq \kappa < 2$

In this case we could not find a coding scheme achieving (3.1), (3.2), and (3.3) simultaneously. We instead propose a new scheme achieving a nontrivial tradeoff between D_+ and D_- while keeping D optimal as before. First the source X^{nN} is decomposed into two subsources $X_1^{(2n-m)N}$ and $X_2^{(m-n)}$ and the auxiliary codebook of T^{nN} vectors is generated according to

$$T^n = \begin{bmatrix} T_1^{2n-m} \\ \\ T_2^{m-n} \end{bmatrix} = \begin{bmatrix} k_1 X_1^{2n-m} \\ \\ k_2 X_2^{m-n} \end{bmatrix} + \begin{bmatrix} Q^{2n-m} \\ \\ G^{m-n} \end{bmatrix}$$

where $Q^{2n-m} \sim \mathcal{N}\left(0^{2n-m}, \sigma_Q^2 \mathbf{I}_{2n-m}\right)$, $G^{m-n} \sim \mathcal{N}\left(0^{m-n}, \mathbf{I}_{m-n}\right)$, and $Q^{2n-m} \perp G^{m-n} \perp X^n$. After a typical $T^{nN}(j)$ if found, the channel input is calculated supersymbol-by-

supersymbol as

$$U^m = \begin{bmatrix} U_1^{2n-m} \\ U_2^{m-n} \\ U_3^{m-n} \end{bmatrix} = \begin{bmatrix} \alpha\left(T_1^{2n-m} - X_1^{2n-m}\right) \\ X_2^{m-n} \\ T_2^{m-n} - k_2 X_2^{m-n} \end{bmatrix}$$

with attenuation constant α is chosen as in (3.6).

Note that the relation between the subsource X_1^{2n-m} and channel input U_1^{2n-m} is exactly as that between X^n and U_1^n in Section 3.2.1. In particular, X_1^{2n-m} is not orthogonal to U_1^{2n-m} unless $k_1 = 1$. Similarly, the relation between X_2 and $\left(U_2^{m-n}, U_3^{m-n}\right)$ is exactly as in Section 3.3 with a bandwidth expansion factor of 2. We can use these relations in deriving the distortion expressions $D_{1,*}$ and $D_{2,*}$, and hence $D_* = (2-\kappa)\, D_{1,*} + (\kappa - 1)\, D_{2,*}$. However, as before, the overall scheme must not be understood as a mere combination of two independent schemes, as the encoding and decoding are both performed jointly. In particular, for reliable communication of $T^{nN}(j)$, we need

$$I\left(X^n; T^n\right) \leq I\left(T^n; V^m\right)$$

which yields

$$\left(\frac{1 + \frac{k_1^2}{\sigma_Q^2} + \alpha^2\gamma}{1+\gamma}\right)^{2-\kappa} \leq \left(\frac{1+k_2^2}{1+\gamma}\right)^{1-\kappa}. \tag{3.16}$$

With the choice of

$$k_2^2 = (1+\gamma)^{\kappa-1} - 1,$$

for $D_{2,*}$, we have $D_2 = (1+\gamma)^{-\kappa}$, and $(D_{2,+}, D_{2,-})$ can be shown to achieve (3.2) and (3.3) simultaneously, just as in Theorem 2 and Corollary 3. With this choice of k_2, (3.16) reduces to (3.10). That in turn means that we can borrow distortion expressions D_1, $D_{1,+}$, and

$D_{1,-}$ for X_1^{2n-m} from Theorem 7 and Corollary 8 as

$$\begin{aligned} D_1 &= \left(1+\frac{k_1^2}{\sigma_Q^2}+\alpha^2\gamma\right)^{-1} \\ D_{1,+} &= \left(1+\frac{k_1^2}{\sigma_Q^2}+\alpha^2\gamma_+\right)^{-1} \\ D_{1,-} &= \frac{(1-k_1)^2+\sigma_Q^2\,(1+\gamma_-)}{(1+\gamma_-)\,\alpha^{-2}}. \end{aligned}$$

Provided $\left(k_1, \sigma_Q^2\right)$ satisfies (3.10) with equality, we have $D_1 = (1+\gamma)^{-\kappa}$, thereby making $D = D_{\text{opt}}$ as required. Therefore, as in Section 3.2, by using the freedom in choosing any $\left(k_1, \sigma_Q^2\right)$ satisfying (3.10) with equality, one can obtain a tradeoff of (D_+, D_-) pairs. The resultant tradeoff is depicted in Fig. 3.8 for $\kappa = 1.5$.

3.6 When $1/2 < \kappa \leq 1$

Once again, we do not have a coding scheme achieving (3.1), (3.4), and (3.5) simultaneously. Instead, we strive for a nontrivial (D_+, D_-) tradeoff as in the previous section.

This time, it is the source which is decomposed into three subsources $X_1^{(2m-n)N}$, $X_2^{(n-m)N}$, and $X_3^{(n-m)N}$. The codewords T^{mN} are created according to

$$\begin{bmatrix} T_1^{2m-n} \\ T_2^{n-m} \end{bmatrix} = \begin{bmatrix} k_1 X_1^{2m-n} \\ k_2 X_2^{n-m} \end{bmatrix} + \begin{bmatrix} Q^{2m-n} \\ G^{n-m} \end{bmatrix} + \begin{bmatrix} 0^{2m-n} \\ a\sqrt{P_1} X_3^{n-m} \end{bmatrix}$$

where $G^{n-m} \sim \mathcal{N}\left(0^{n-m}, \mathbf{I}_{n-m}\right)$ and $Q^{2m-n} \sim \mathcal{N}\left(0^{2m-n}, \sigma_Q^2 \mathbf{I}_{2m-n}\right)$ are independent to the source and each other.

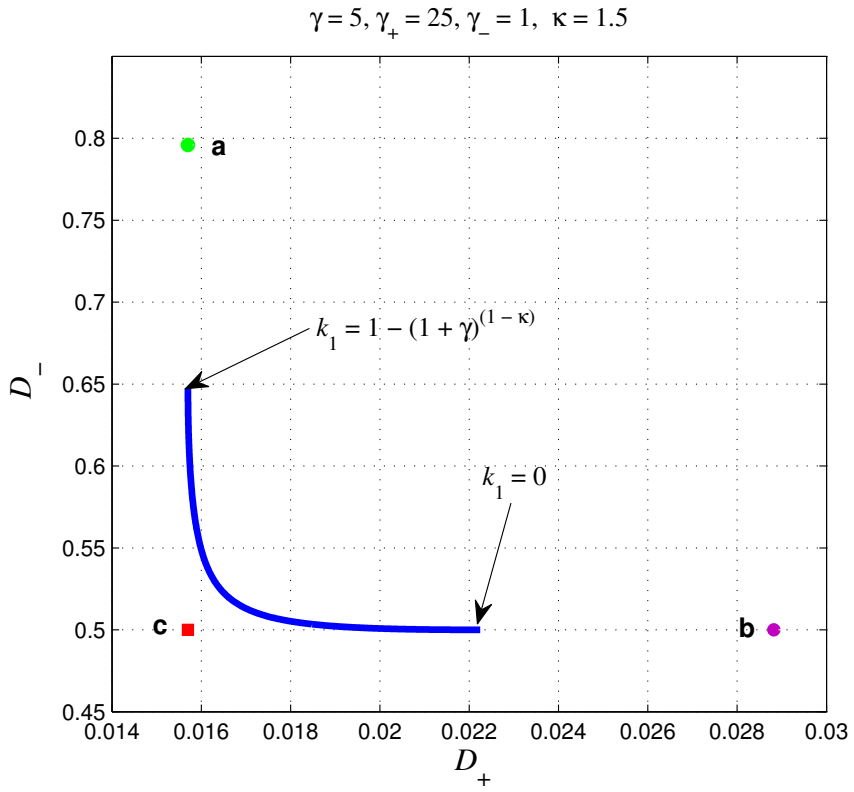

Figure 3.8: Tradeoff between D_+ and D_- when $\gamma = 5$, $\gamma_+ = 25$, $\gamma_- = 1$, and $\kappa = 1.5$. Only $0 < k_1 < 1 - (1+\gamma)^{1-\kappa}$ is considered because the scheme performs worse than the blue curve for other k_1. Point **a** can be obtained by schemes in [26], [32], and [35], and point **b** by those in [32], [35], and [36]. No known scheme can obtain point **c**, which satisfies (3.1), (3.2), and (3.3) simultaneously.

After a typical $T^{mN}(j)$ is found, the channel input U^m is calculated according to

$$\begin{bmatrix} U_1^{2m-n} \\ U_2^{n-m} \end{bmatrix} = \begin{bmatrix} \alpha\left(T_1^{2m-n} - X_1^{2m-n}\right) \\ \sqrt{P_2}\left(T_2^{n-m} - k_2 X_2^{n-m} - a\sqrt{P_1}X_3^{n-m}\right) + \sqrt{P_1}X_3^{n-m} \end{bmatrix}$$

where $P_1 + P_2 = 1$ and $\alpha = \left((1-k_1)^2 + \sigma_Q^2\right)^{-1/2}$ to ensure unit power at the channel input. The rate inequality $I(T^m; X^n) \leq I\left(T^m; V^m\right)$ leads to

$$\frac{1 + \frac{k_1^2}{\sigma_Q^2} + \alpha^2\gamma}{1+\gamma} \leq \left(1 + k_2^2 + a^2\frac{P_1}{P_2} - \frac{P_2\gamma}{1+\gamma}\left(1 + a\frac{P_1}{P_2}\right)^2\right)^{\frac{\kappa-1}{2\kappa-1}}. \tag{3.17}$$

If the parameters are chosen as

$$\begin{aligned} a &= \frac{P_2\gamma}{1+P_2\gamma} \\ k_2^2 &= \frac{(1+P_2\gamma)^{\frac{\kappa}{1-\kappa}} - 1}{1+P_2\gamma} \\ 1 + P_2\gamma &= (1+\gamma)^{1-\kappa}, \end{aligned}$$

it follows from Section 3.4 that we have

$$\begin{aligned} D_2 &= (1+\gamma)^{-\kappa} \\ D_{2,+} &= \frac{\gamma + \frac{\gamma_+ - \gamma}{1+\gamma}\left((1+\gamma)^\kappa - 1\right)}{\gamma - \gamma_+ + \gamma_+(1+\gamma)^\kappa} \\ D_{2,-} &= 1 \\ D_3 &= (1+\gamma)^{-\kappa} \\ D_{3,+} &= (1+\gamma)^{-\kappa} - \frac{\gamma + \frac{\gamma_+ - \gamma}{1+\gamma}\left((1+\gamma)^\kappa - 1\right)}{\gamma - \gamma_+ + \gamma_+(1+\gamma)^\kappa} \\ D_{3,-} &= \frac{\gamma_-\left((1+\gamma)^{1-\kappa} - 1\right) + \gamma}{\gamma(1+\gamma_-)}. \end{aligned}$$

Furthermore, with these choices (3.17) becomes the same as (3.10). Thus, using

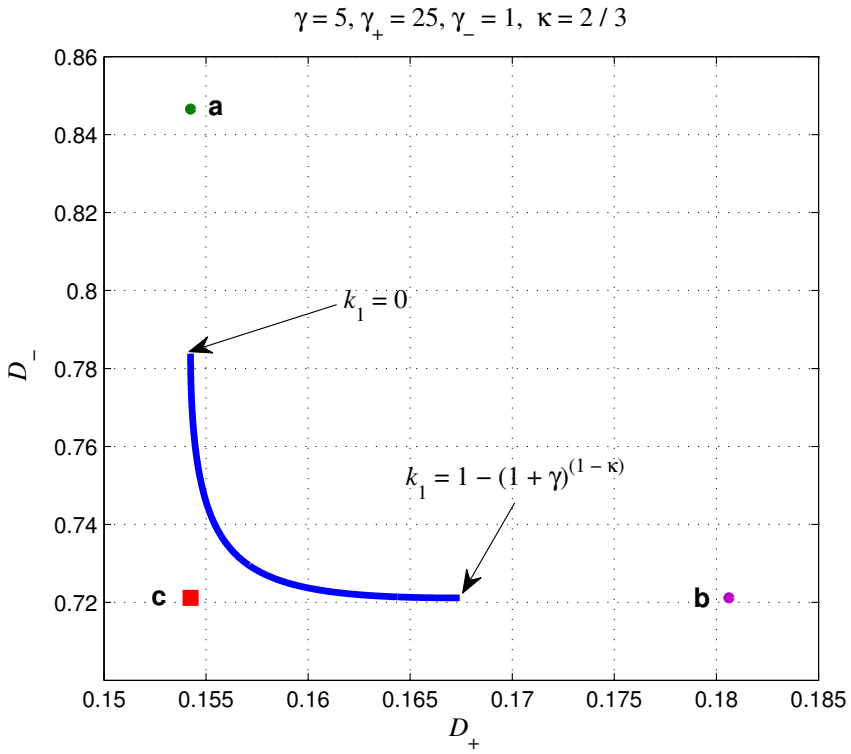

Figure 3.9: Tradeoff when $\kappa = \frac{2}{3}$. Points **a** and **b** can be obtained by schemes in [32]. Only $1-(1+\gamma)^{1-\kappa} < k_1 < 0$ is considered because the scheme performs worse than the blue curve for other k_1. No known scheme can obtain point **c**, which satisfies (3.1), (3.4), and (3.5) simultaneously.

Theorem 9 and Corollary 10, for every $\left(k_1, \sigma_Q^2\right)$ satisfying (3.10), we obtain

$$\begin{aligned} D_1 &= (1+\gamma)^{-\kappa} \\ D_{1,+} &= \left(1 + \frac{k_1^2}{\sigma_Q^2} + \alpha^2 \gamma_+\right)^{-1} \\ D_{1,-} &= \frac{(1-k_1)^2 + \sigma_Q^2 (1+\gamma_-)}{(1+\gamma_-)\,\alpha^{-2}}. \end{aligned}$$

Finally, the (D_+, D_-) tradeoff can be characterized by $D_* = (2\kappa - 1)\, D_{1,*} + (1-\kappa)\, D_{2,*} + (1-\kappa)\, D_{3,*}$. The tradeoff obtained for $\kappa = \frac{2}{3}$ is displayed in Fig.3.9.

Chapter 4

Broadcasting Correlated Sources Over Gaussian Broadcast Channels

4.1 Introduction

We consider the problem of transmitting a pair of Gaussian sources over a Gaussian broadcast channel, where each receiver is interested in reconstructing only one source component. This scenario is relevant in sensor network settings where sensors are taking measurements of multiple environmental phenomena, such as temperature, humidity, pressure, that are typically correlated with each other. On the other hand, each receiving agent may be interested in just one of these measurements.

This problem has attracted considerable attention in the past decade. Bross *et al.* showed in [8] that sending a linear combination of the two sources, which is purely analog, is optimal in the bandwidth-matched (BM) regime provided that parameters of

the problem satisfy a certain inequality. Later, Tian *et al.* showed in [41] that a hybrid code achieves the optimum distortion tradeoff using the outer bound given in [8] yielding a complete characterization of the distortion tradeoff in the BM regime.

For the bandwidth mismatch scenarios, Behroozi *et al.* [4, 5, 6] proposed HDA coding schemes that are inspired by [35] and [45] which focused on sending a single Gaussian source. They introduced schemes both for BE and BC regimes, but especially for the BC case, they demonstrated that the gap between the performances of their scheme and a genie-aided outer bound was fairly small [6]. In [14], Gao and Tuncel showed that optimal *separate* source-channel coding, based on successive coding of correlated sources introduced in [29], can outperform the joint source-channel coding schemes in [6] for some source/channel parameters. In [38], the lossy transmission of correlated Gaussian vectors over bandwidth-matched Gaussian broadcast channels is investigated and achievable distortion region is found for the vector-scalar case. Recently, Abou Saleh *et al.* considered the joint recovery of correlated sources together with the interference in bandwidth-matched case [1].

In this paper, we propose new hybrid digital/analog coding schemes for both BE and BC regimes. The schemes make use of similar layered coding structures and coding techniques as those proposed in the aforementioned work. We demonstrate that, to our best knowledge, the proposed schemes offer the best distortion tradeoffs reported in the literature so far. In particular, for both bandwidth expansion and compression, distortion regions of the proposed schemes reduce to those characterized in [6, 14] for special choices of parameters. We also show that both of our schemes for the bandwidth expansion and compression cases specialize to the same coding scheme when the bandwidth expansion

ratio approaches 1 from either side. Although this specialized scheme is not the same as the one given in [41], we show analytically that it achieves the same (optimal) performance.

The rest of the paper is organized as follows. After formulating the problem in Section 4.2, in Section 4.3 we briefly explain the previously known schemes along with introducing a separate source-channel coding alternative to the scheme in [14]. Sections 4.4 and 4.5 are devoted to the proposed schemes for bandwidth expansion and compression, respectively.

4.2 Problem Formulation

Let (X_1^n, X_2^n) be an i.i.d. Gaussian source generated according to the probability distribution $p_{X_1X_2} = \mathcal{N}(0, \mathbf{C})$ with

$$\mathbf{C} = \begin{bmatrix} 1 & \rho \\ \rho & 1 \end{bmatrix}$$

where the correlation coefficient satisfies $0 \leq \rho < 1$.[1] At the transmitter the encoder

$$\psi^{m,n} : \mathbb{R}^n \times \mathbb{R}^n \to \mathbb{R}^m$$

maps the source into the channel input $U^m = \psi^{m,n}(X_1^n, X_2^n)$ which is power-limited by

$$\frac{1}{m}\sum_{t=1}^{m} \mathbb{E}\left[U^2(t)\right] \leq P.$$

The ith receiver, $i = 1, 2$, observes $V_i^m = U^m + W_i^m$ with $W_i^m \sim \mathcal{N}\left(\mathbf{0}_m, \sigma_{W_i}^2 \mathbf{I}_m\right)$, and uses the decoding function

$$\phi_i^{m,n} : \mathbb{R}^m \to \mathbb{R}^n$$

[1] As explained in [8, Remark 2.2] there is no loss of generality when assuming that the variances of the sources are 1 and ρ is non-negative. When $\rho = 1$ the scenario becomes identical to that in [35].

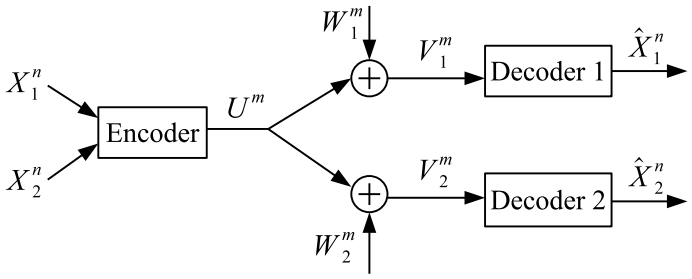

Figure 4.1: The block diagram for broadcast scenario with correlated sources.

to estimate the ith source as $\hat{X}_i^n = \phi_i^{m,n}(V_i^m)$. We will assume that the SNR at the second receiver is greater than that at the first receiver, i.e., $\gamma_2 > \gamma_1$ where

$$\gamma_i = \frac{P}{\sigma_{W_i}^2} \ .$$

The ratio $\frac{m}{n}$ is referred to as the bandwidth expansion factor.

The scenario is illustrated in Fig.4.1.

Definition 13 *A quadruple* (P, D_1, D_2, κ) *is* achievable *if for any* $\epsilon > 0$ *there exists a triple of* $(\psi^{m,n}, \phi_1^{m,n}, \phi_2^{m,n})$ *with some* m, n *such that*

$$\begin{aligned} \frac{1}{n}\mathbb{E}\Big[||X_1^n - \hat{X}_1^n||^2\Big] &\leq D_1 + \epsilon \\ \frac{1}{n}\mathbb{E}\Big[||X_2^n - \hat{X}_2^n||^2\Big] &\leq D_2 + \epsilon \\ \frac{m}{n} &\leq \kappa + \epsilon \ . \end{aligned}$$

Definition 14 *The achievability region* $\mathcal{D}_\kappa(P)$ *is defined as*

$$\mathcal{D}_\kappa(P) = \{(D_1, D_2) : (P, D_1, D_2, \kappa) \ \textit{is achievable}\} \ .$$

4.3 Previous Work

4.3.1 Reznic-Feder-Zamir (RFZ)

The scheme in [35] was designed to transmit a single Gaussian source to two receivers over Gaussian broadcast channel with BE, i.e., $\rho = 1$, $X^n = X_1^n = X_2^n$, and $\kappa > 1$. The source is first optimally quantized into $\tilde{X}_1^n$ using the backward test channel $X = \tilde{X}_1 + Z$. The quantization error Z^n is scaled and sent using the first n channel uses in an uncoded fashion, and the remaining bandwidth of $m - n$ channel uses is dedicated to the transmission of digital data with two superposed layers, expending power levels ηP and $\overline{\eta} P$, respectively, where here and in the sequel, we use $\overline{s} = 1 - s$ for any s. The first layer of digital information consists of the quantization index of $\tilde{X}_1^n$. For the second layer, the quantization error Z^n is quantized again into $\tilde{X}_2^n$. The quantization index is Wyner-Ziv coded and only the resultant binning index is transmitted, for the noisy version of Z^n serves as side information available at the receiver for $\tilde{X}_2^n$. Combining all the analog and digital information available, the receivers output $\hat{X}_1^n$ and $\hat{X}_2^n$. This scheme attains

$$D_1 = \frac{1}{1+\gamma_1}\left(\frac{1+\overline{\eta}\gamma_1}{1+\gamma_1}\right)^{\kappa-1} \tag{4.1}$$

$$D_2 = \frac{1}{1+\gamma_2}\left(\frac{1}{1+\overline{\eta}\gamma_2}\right)^{\kappa-1}\left(\frac{1+\overline{\eta}\gamma_1}{1+\gamma_1}\right)^{\kappa-1} \tag{4.2}$$

for any $0 \le \eta \le 1$.

In [32, Section V], this inner bound was further improved by simply adjusting the power distribution between the bandwidth matching the source, i.e., the analog part, and

the remaining bandwidth, i.e., the digital part, as

$$\begin{aligned} D_1 &= \frac{1}{1+\omega\gamma_1}\left(\frac{1+\overline{\eta}\hat{\omega}\gamma_1}{1+\hat{\omega}\gamma_1}\right)^{\kappa-1} \\ D_2 &= \frac{1}{1+\omega\gamma_2}\left(\frac{1}{1+\overline{\eta}\hat{\omega}\gamma_2}\right)^{\kappa-1}\left(\frac{1+\overline{\eta}\hat{\omega}\gamma_1}{1+\hat{\omega}\gamma_1}\right)^{\kappa-1} \end{aligned}$$

where $0 \leq \eta \leq 1$, $0 \leq \omega \leq \kappa$ and $\hat{\omega} = \frac{\kappa-\omega}{\kappa-1}$.

Also for transmission of single Gaussian source over broadcast channel with bandwidth compression, a scheme, which is dual of the RFZ scheme as pointed out in [28], was given in [32]. That scheme yields

$$D_1 = \kappa\frac{1+\overline{\eta}\gamma_1}{1+\gamma_1\left(\overline{\eta}+\eta\,\lambda\right)} + (1-\kappa)\left(\frac{1+\gamma_1\left(\overline{\eta}+\eta\,\lambda\right)}{1+\gamma_1}\right)^{\frac{\kappa}{1-\kappa}} \tag{4.3}$$

$$D_2 = \kappa\frac{1+\overline{\eta}\gamma_2}{1+\gamma_2\left(\eta\lambda+\overline{\eta}\right)} + (1-\kappa)\left(\frac{1+\gamma_1\left(\overline{\eta}+\eta\lambda\right)}{\left(1+\gamma_1\right)\left(1+\overline{\eta}\gamma_2\right)}\right)^{\frac{\kappa}{1-\kappa}} \tag{4.4}$$

for any $0 \leq \lambda, \eta \leq 1$.

4.3.2 Behroozi-Alajaji-Linder (BAL)

One of the HDA coding schemes of Behroozi, Alajaji, and Linder in [6] for bandwidth expansion is very similar to the RFZ scheme [35], except the two layers of information transmitted using superposition are not the indices of a two-stage quantizer. Instead, they are the quantization indices for the two components of the source, X_1^n and X_2^n. More specifically, X_1^n is quantized into $\tilde{X}_1^n$, and the quantization error Z^n is transmitted uncoded in the first n uses of the channel. In the remaining $m-n$ channel uses, the quantization index M_1 of $\tilde{X}_1^n$ is superposed onto the Wyner-Ziv coded quantization index M_2 of $\tilde{X}_2^n$. In this case, Wyner-Ziv coding utilizes as side information the MMSE estimate of the first source, $\hat{X}_1^n$. It is also worth noting that the scheme does not benefit from power adjustment as in

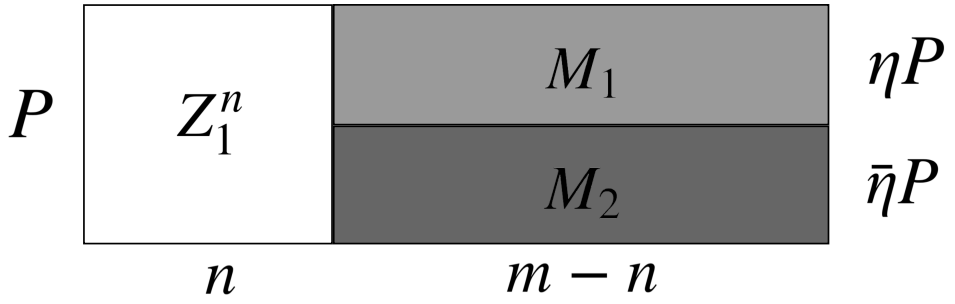

Figure 4.2: The diagram of power/bandwidth splitting in the BAL scheme for bandwidth expansion. While the first subband is dedicated to transmission of the analog layer, the messages M_1 and M_2, which are the quantization index of $\tilde{X}_1^n$ and the Wyner-Ziv coded quantization index of $\tilde{X}_2^n$, respectively, are transmitted from the second subband.

[32].

The distribution of power and bandwidth is illustrated in Fig. 4.2. Here, and in any illustration of superposed information in the sequel, we adopt the convention that upper items "treat" lower items as noise, and once decoded, upper items can be eliminated either through subtraction or dirty-paper decoding.

The resultant (D_1, D_2) pair is expressed as

$$D_1 = \frac{1}{1+\gamma_1}\left(\frac{1+\overline{\eta}\gamma_1}{1+\gamma_1}\right)^{\kappa-1} \tag{4.5}$$

$$D_2 = \left(\frac{1}{1+\overline{\eta}\gamma_2}\right)^{\kappa-1}\left(1-\rho^2+\frac{\rho^2}{1+\gamma_2}\left(\frac{1+\overline{\eta}\gamma_1}{1+\gamma_1}\right)^{\kappa-1}\right) \tag{4.6}$$

for any $0 \leq \eta \leq 1$. Comparing (4.5)-(4.6) to (4.1)-(4.2), it is clear that the former reduces to the latter as $\rho \to 1$.

In their work [6], the authors presented another coding scheme (referred to as the HWZ scheme) for the same scenario, and observed identical numerical results. The two schemes were analytically shown to have identical performance later in [14].

Note that with this scheme the distortion at the second, *i.e., better*, receiver cannot be minimized to the value $D_2 = D_{2,\min} = (1+\gamma_2)^{-\kappa}$ unless $\rho = 1$ because the first subband and a fraction $(1/\kappa)$ of power is dedicated to the uncoded transmission of the first component of the source X_1^n. We will address this shortcoming in our proposed scheme in Section 4.4 by introducing a digital layer in the first subband.

Behroozi, Alajaji, and Linder [6] also considered the BC regime. Although they only analyzed the special case $\kappa = 1/2$, their scheme can easily be generalized to any $\kappa \leq 1$. Each component of the source is divided into two parts, i.e., $X_i^n = \left(X_{i,h}^m, X_{i,d}^{n-m}\right)$. There are one analog and three digital superposed layers in this scheme. In the analog layer, a linear combination of the first parts of the source components, $Z_a^m = \theta X_{1,h}^m + \overline{\theta} X_{2,h}^m$ is sent uncoded. In the first digital layer, which is meant for both receivers, the second part of the first component $X_{1,d}^{n-m}$ is quantized to $\tilde{X}_{1,d}^{n-m}$ and the quantization index M_1 is sent. The second digital layer consists of the quantization index M_2 of the residual signal $X_{1,d}^{n-m} - \tilde{X}_{1,d}^{n-m}$, intended to be decoded only at the second receiver. The third and last digital layer is dirty-paper coded, where the previous layers are treated as channel state information available at the encoder. This layer is used for sending the message M_3 (i.e., the bin index) obtained by Wyner-Ziv coding of $X_{2,d}^{n-m}$ where the estimation from the previous layers are used as side information.

The distribution of power and the source is illustrated in Fig. 4.3. As can be seen from the diagram, the analog layer is placed between the second and third digital layers. That is because Z_a^m is treated as noise in the decoding of M_1 and M_2, but its effect can be circumvented through the dirty-paper coding process of M_3, since using Costa coding [10],

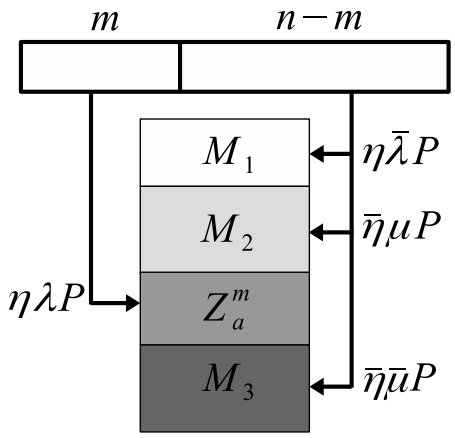

Figure 4.3: The diagram of power/source splitting in the BAL scheme for bandwidth compression. The first m symbols of the source is represented only through the linearly combined analog information Z_a^m, whereas the remaining $n-m$ symbols are encoded in three digital layers.

the same communication rate can be achieved as if there is no interference (i.e., channel state information) in AWGN channels.

For all $\kappa < 1$ the scheme attains

$$D_1 = \kappa\left(1 - \frac{(\theta+\rho\bar{\theta})^2}{\alpha^2}\cdot\frac{\gamma_1\eta\lambda}{1+\gamma_1(\bar{\eta}+\eta\lambda)}\right) + (1-\kappa)\left(\frac{1+\gamma_1(\bar{\eta}+\eta\lambda)}{1+\gamma_1}\right)^{\frac{\kappa}{1-\kappa}} \tag{4.7}$$

$$D_2 = \kappa\left(1 - \frac{(\rho\theta+\bar{\theta})^2}{\alpha^2}\frac{\gamma_2\eta\lambda}{1+\gamma_2(\eta\lambda+\bar{\eta}\bar{\mu})}\right) + (1-\kappa)\left(\frac{1}{1+\bar{\mu}\bar{\eta}\gamma_2}\right)^{\frac{\kappa}{1-\kappa}}\left(1-\rho^2(1-D_{12}^{\star})\right) \tag{4.8}$$

for some $0 \le \eta, \mu, \lambda, \theta \le 1$, where

$$\alpha = \sqrt{1 - 2\theta\bar{\theta}(1-\rho)} \tag{4.9}$$

and

$$D_{12}^{\star} = \left(\frac{1+\gamma_1(\bar{\eta}+\eta\lambda)}{1+\gamma_1}\right)^{\frac{\kappa}{1-\kappa}} \cdot \left(\frac{1+\gamma_2(\eta\lambda+\bar{\mu}\bar{\eta})}{1+\gamma_2(\bar{\eta}+\eta\lambda)}\right)^{\frac{\kappa}{1-\kappa}}.$$

Once again, it is not difficult to see that as $\rho \to 1$, (4.7)-(4.8) reduce to (4.3)-(4.4) with $\mu = 0$.

The scheme seems to have the handicap that while M_2 is decoded only at the second receiver, which is interested in the second source, it encodes information that is about the first source, i.e., $X_{1,d}^{n-m} - \tilde{X}_{1,d}^{n-m}$. This is, at least intuitively, not an efficient way of communicating X_2^n. Indeed, when we removed M_2 and ran extensive set of simulations with different parameters, we observed that the resultant distortion regions did not change. This phenomenon is illustrated for a few sample cases in Fig. 4.4. Using this numerical observation, we will set $\mu = 0$, and represent the achievable distortion region equivalently as

$$D_1 = \kappa\left(1 - \frac{(\theta + \rho\bar{\theta})^2}{\alpha^2} \cdot \frac{\gamma_1\eta\lambda}{1 + \gamma_1\left(\bar{\eta} + \eta\lambda\right)}\right) + (1-\kappa)\left(\frac{1 + \gamma_1\left(\bar{\eta} + \eta\lambda\right)}{1 + \gamma_1}\right)^{\frac{\kappa}{1-\kappa}} \tag{4.10}$$

$$D_2 = \kappa\left(1 - \frac{(\rho\theta + \bar{\theta})^2}{\alpha^2} \frac{\gamma_2\eta\lambda}{1 + \gamma_2\left(\eta\lambda + \bar{\eta}\right)}\right) + (1-\kappa)\left(\frac{1}{1 + \bar{\eta}\gamma_2}\right)^{\frac{\kappa}{1-\kappa}} \left(1 - \rho^2\left(1 - D_{12}^{\star}\right)\right) \tag{4.11}$$

where

$$D_{12}^{\star} = \left(\frac{1 + \gamma_1\left(\bar{\eta} + \eta\lambda\right)}{1 + \gamma_1}\right)^{\frac{\kappa}{1-\kappa}} \cdot \left(\frac{1 + \gamma_2\left(\eta\lambda + \bar{\eta}\right)}{1 + \gamma_2\left(\bar{\eta} + \eta\lambda\right)}\right)^{\frac{\kappa}{1-\kappa}}.$$

Another possible handicap is that the analog signal Z_a^m is the only information conveyed about the first subband of the source pair (X_1^m, X_2^m).

We will address these shortcomings in our proposed scheme in Section 4.5.

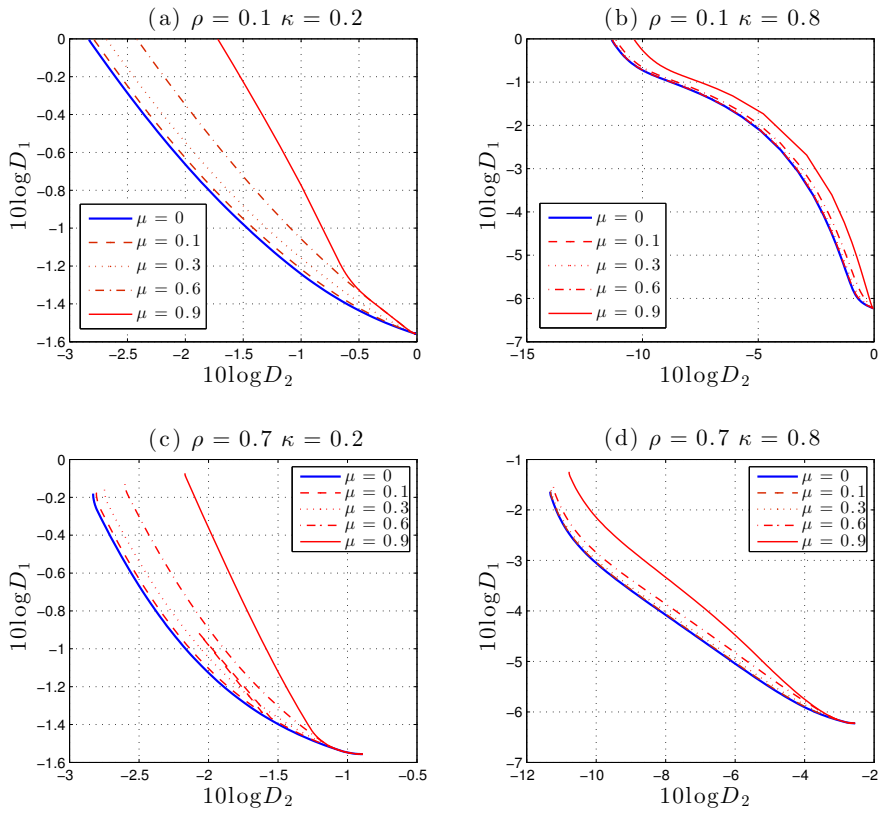

Figure 4.4: For different ρ, κ, and μ values the (D_1, D_2) tradeoffs are depicted in log domain where μ ranges from 0 to 0.9. In all figures we set $P = 2$, $N_1 = 1$, and $N_2 = 0.3$. The figures demonstrate how $\mu = 0$ always leads to the best distortion region. This numerical observation suggests that the second layer in the BAL scheme is completely redundant.

4.3.3 Genie-Aided Outer Bound

In [6], the authors also obtained a genie-aided outer bound. It is based on the scenario that the noisy version of the first component of the source

$$X_1' = \beta X_1 + Z$$

with $Z \sim \mathcal{N}(0, 1-\beta^2)$ is provided at the second receiver for free. In this new scenario, the resultant outer bound given as

$$\begin{aligned} D_1 &\geq \left(\frac{1+\eta\gamma_1}{1+\gamma_1}\right)^{\kappa} \\ D_2 &\geq \max_{0\leq\beta\leq 1}\left\{\left(1-\beta^2\rho^2\right)\left(\frac{1}{1+\gamma_2\left(1-\beta^2\overline{\eta}\right)}\right)^{\kappa}\right\} \end{aligned}$$

for some $0 \leq \eta \leq 1$, must clearly also be an outer bound for the original scenario. This outer bound is the best known to date.

4.3.4 Gao-Tuncel (GT)

Nayak and Tuncel introduced in [29] a layered joint source coding of correlated Gaussian sources, referred to as *successive coding of correlated sources*, where the encoder

$$\phi_{\text{src}} : \mathbb{R}^n \times \mathbb{R}^n \to \mathcal{M}_1 \times \mathcal{M}_2$$

maps the source (X_1^n, X_2^n) into two messages $\mathrm{m}_1 \in [1 : 2^{nR_1}]$ and $\mathrm{m}_2 \in [1 : 2^{nR_2}]$, the first decoder

$$\phi_{\text{src},1} : \mathcal{M}_1 \to \mathbb{R}^n$$

maps the first message M_1 into the estimation of the first source $\hat{X}_1(M_1)$, and the second decoder maps the message pair (M_1, M_2) into the estimation of the second source $\hat{X}_2^n(M_1, M_2)$. In [14], Gao and Tuncel showed that the optimal *separate source-channel coding* scheme, comprising of successive coding of [29] followed by superposition coding over the broadcast channel can somewhat surprisingly outperform the BAL schemes in [6] for some source/channel parameters.

Although it is not immediately clear, the successive-coding-based scheme of [14] is equivalent in performance to the alternative described below, as will be shown in Lemma 16.

Alternative Separate Coding Scheme: The encoder quantizes a linear combination

$$X_a^n = \theta X_1^n + \overline{\theta} X_2^n$$

to $\tilde{X}_a^n$ and sends the quantization index with power ηP in the first layer, to be decoded by both receivers. In the second layer with power $\overline{\eta} P$, X_2^n is quantized and Wyner-Ziv coded, utilizing $\tilde{X}_a^n$ as side information available at the second receiver.

The theorem below states the resultant achievable region.

Theorem 15 *For all $\kappa > 0$, the alternative separate coding scheme described above achieves the distortion levels*

$$D_1 = 1 - \frac{(\theta + \rho\overline{\theta})^2}{\alpha^2} \left\{ 1 - \left(\frac{1 + \overline{\eta}\gamma_1}{1 + \gamma_1} \right)^{\kappa} \right\} \tag{4.12}$$

$$D_2 = \frac{D_2^*}{(1 + \overline{\eta}\gamma_2)^{\kappa}} \tag{4.13}$$

for any $0 \leq \theta, \eta \leq 1$, where α is as in (4.9) and

$$D_2^* = 1 - \frac{(\rho\theta + \overline{\theta})^2}{\alpha^2} \left\{ 1 - \left(\frac{1 + \overline{\eta}\gamma_1}{1 + \gamma_1} \right)^{\kappa} \right\} . \tag{4.14}$$

Now we are ready to state the equivalence of the two separate source-channel coding schemes. The equivalence is crucial, as the joint source-channel coding schemes we propose can easily be specialized to achieve the (D_1, D_2)-region in Theorem 15, thereby showing their superiority against separate coding.

Lemma 16 *The achievable region in Theorem 15 is the same as that of the GT scheme.*

The proofs of Theorem 15 and Lemma 16 are deferred to Appendix A.1 and Appendix A.2, respectively.

4.4 Proposed Scheme for Bandwidth Expansion

As mentioned in of Section 4.3.2, the main drawback of the BAL scheme for BE is that the first subband is dedicated to the transmission of X_1^n, in which only the first receiver is interested. As proposed originally by the authors, it does not benefit from a power adjustment either. As shown in [32], such an adjustment proves useful in the lossy transmission of a single i.i.d. Gaussian source over a bandwidth mismatched broadcast channel (i.e., when $\rho = 1$). Moreover, albeit being an HDA scheme, it can be outperformed at some achievable distortion points by a purely digital scheme, i.e., the GT scheme, which is described in Section 4.3.4. This fact suggests the existence of an HDA scheme with more layers which could not only subsume both schemes but also outperform them with respect to the achievable distortion region.

We propose an HDA coding scheme with three digital layers and one analog layer. The bandwidth is divided as the previous schemes into two subbands, the bandwidth matching the source, i.e., n channel uses, and the remaining bandwidth, i.e., $m - n$ channel uses. The analog layer and the third digital layer are transmitted from the first subband with power ωP for some $0 \leq \omega \leq \kappa$, while the first and the second layers are from the second subband with power $\hat{\omega} P$ with

$$\hat{\omega} = \frac{\kappa - \omega}{\kappa - 1} \, .$$

Note that the average power constraint over the entire bandwidth is still satisfied, as

$$\frac{\omega P + (\kappa - 1)\hat{\omega} P}{\kappa} = P \, .$$

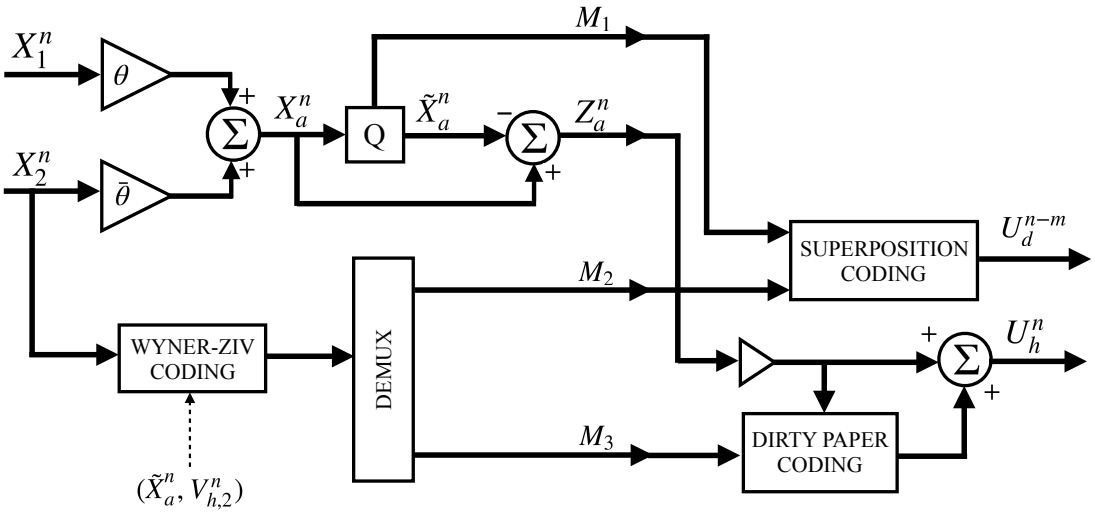

Figure 4.5: The proposed joint source-channel encoder in the bandwidth expansion case. Q stands for the quantizer and Σ is for superposition or addition of vectors. While the hybrid signal U_h^n is transmitted from the first n channel uses, U_d^{m-n}, conveying purely digital data, is transmitted from the remaining $m-n$ channel uses. The Wyner-Ziv coder exploits the fact that in addition to $\tilde{X}_a^n$, the (second) receiver has access to $V_{h,2}^n = U_h^n + W_2^n$.

The first step is to optimally quantize a linear combination of the sources

$$X_a^n = \theta X_1^n + \overline{\theta} X_2^n$$

to a source codeword $\tilde{X}_a^n$ with rate R_1. The quantization error $Z_a^n = X_a^n - \tilde{X}_a^n$, is normalized to have a power of $\omega\lambda P$ and sent through the analog layer (in n channel uses). Note that $Z_a^n \sim \mathcal{N}\left(\mathbf{0}_n, \alpha^2 2^{-2R_1}\mathbf{I}_n\right)$.

In the first digital layer, M_1, the message for the quantization index of $\tilde{X}_a$ is channel encoded into $S_1^{m-n}(M_1)$ in a standard manner and transmitted from the second subband (in $m-n$ channel uses) with power $\hat{\omega}\eta P$. This "common" message is intended to be decoded at both receivers.

Treating the decoded $\tilde{X}_a^n$ and $V_{h,2}^n$, the observed signal at the second receiver from the first n channels uses, as the side information at the receiver, the second component of

the source, X_2^n, is then Wyner-Ziv coded with rate $R_{WZ} = R_2 + R_3$ where the binning index is demultiplexed into the messages M_2 and M_3 with cardinalities 2^{nR_2} and 2^{nR_3}, respectively. M_2 is mapped into a digital channel word $S_2^{m-n}(M_2)$ which has power $\hat{\omega}\bar{\eta}P$ and superimposed on the first digital layer, and sent through the second subband (in $m-n$ channel uses). The message M_3, on the other hand, is sent from the first subband using dirty paper coding with power $\omega\bar{\lambda}P$ regarding the analog layer as channel state information. Both "private" messages M_2 and M_3 are to be decoded only by the second receiver.

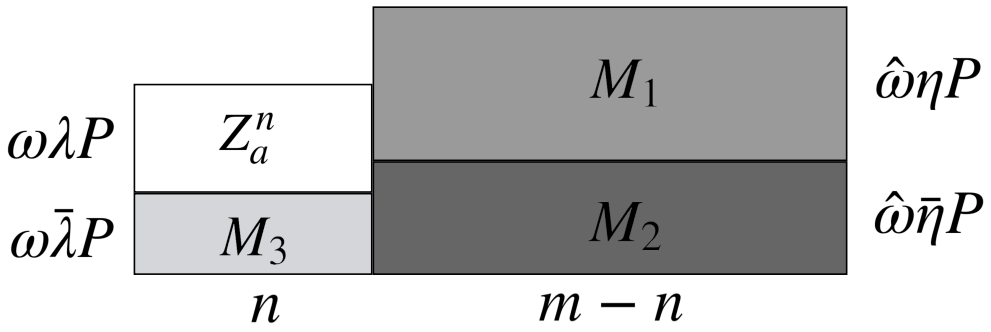

Figure 4.6: The diagram of power/bandwidth splitting for bandwidth expansion. The upper layers "see" the lower layers as noise, while the lower layers cancel the effect of the upper ones by either subtraction or via dirty paper coding. The lower layers are intended for the second receiver only.

The encoding procedure is illustrated in Fig. 4.5 and the power/bandwidth splitting between the layers is illustrated in Fig. 4.6.

We are ready to state the main result of this section.

Theorem 17 *For bandwidth expansion factor $\kappa > 1$, the distortion pair*

$$D_1 = 1 - \frac{\left(\theta + \rho\bar{\theta}\right)^2}{\alpha^2}\left(1 - \frac{1+\omega\bar{\lambda}\gamma_1}{1+\omega\gamma_1}\left(\frac{1+\hat{\omega}\bar{\eta}\gamma_1}{1+\hat{\omega}\gamma_1}\right)^{\kappa-1}\right) \tag{4.15}$$

$$D_2 = \frac{D_2^\star}{\left(1+\omega\bar{\lambda}\gamma_2\right)\left(1+\hat{\omega}\bar{\eta}\gamma_2\right)^{\kappa-1}} \tag{4.16}$$

is achievable for any $0 \le \eta, \theta, \lambda \le 1$ and $0 \le \omega \le \kappa$, where α is as in (4.9), and

$$D_2^\star = 1 - \frac{\left(\rho\theta + \bar{\theta}\right)^2}{\alpha^2}\left(1 - \frac{1+\omega\bar{\lambda}\gamma_2}{1+\omega\gamma_2}\left(\frac{1+\hat{\omega}\bar{\eta}\gamma_1}{1+\hat{\omega}\gamma_1}\right)^{\kappa-1}\right) . \tag{4.17}$$

Proof. It follows from the behavior of the capacity region of degraded Gaussian channels [11] and the fact that interference can be completely circumvented in Gaussian dirty paper coding [10] that the message M_1 is correctly decoded at both receivers, and M_2 and M_3 are correctly decoded at the second receiver if

$$R_1 = \frac{\kappa-1}{2}\log\left(\frac{1+\hat{\omega}\gamma_1}{1+\hat{\omega}\bar{\eta}\gamma_1}\right) - \delta \tag{4.18}$$

$$R_2 = \frac{\kappa-1}{2}\log\left(1+\hat{\omega}\bar{\eta}\gamma_2\right) - \delta \tag{4.19}$$

$$R_3 = \frac{1}{2}\log\left(1+\omega\bar{\lambda}\gamma_2\right) - \delta \tag{4.20}$$

for any arbitrarily small $\delta > 0$. Defining $V_{h,i}^n = U_h^n + W_i^n$ at receiver $i = 1, 2$, it follows that

$$\begin{aligned}\mathbb{E}\{X_1\tilde{X}_a\} &= \left(1 - 2^{-2R_1}\right)\mathbb{E}\{X_1 X_a\} \\ &= \left(1 - 2^{-2R_1}\right)\left(\theta + \rho\bar{\theta}\right)\end{aligned}$$

and

$$\begin{aligned}\mathbb{E}\{X_1 V_{h,1}\} &= \frac{\omega\lambda P}{2^{-R_1}\alpha}\mathbb{E}\{X_1 Z_a\} \\ &= \frac{2^{-R_1}}{\alpha}\left(\theta + \rho\bar{\theta}\right)\sqrt{\omega\lambda P}\end{aligned}$$

where the single letter representations are used for calculations since the sources are i.i.d. and the codewords are created in i.i.d. fashion. Since $V_{h,1}$ and $\tilde{X}_a$ are orthogonal to each other together with $\mathbb{E}\{V_{h,1}^2\} = \omega P + \sigma_{W_1}^2$ and $\mathbb{E}\{\tilde{X}_a^2\} = \left(1 - 2^{-2R_1}\right)\alpha^2$, we have

$$\begin{aligned} D_1 &= 1 - \frac{\mathbb{E}\{X_1 V_{h,1}\}^2}{\mathbb{E}\{V_{h,1}^2\}} - \frac{\mathbb{E}\{X_1 \tilde{X}_a\}^2}{\mathbb{E}\{\tilde{X}_a^2\}} \\ &= 1 - \frac{\left(\theta + \rho\bar{\theta}\right)^2}{\alpha^2}\left(1 - 2^{-2R_1}\frac{\omega\bar{\lambda}P + \sigma_{W_1}^2}{\omega P + \sigma_{W_1}^2}\right). \end{aligned} \tag{4.21}$$

At the second receiver we first make use of only M_1 and the observation from the first subband $V_{h,2}^n$ to have an initial estimation. Following the same calculations as we did above, the distortion with the initial estimation is

$$D_2^\star = 1 - \frac{\left(\rho\theta + \bar{\theta}\right)^2}{\alpha^2}\left(1 - 2^{-2R_1}\frac{\omega\bar{\lambda}P + \sigma_{W_2}^2}{\omega P + \sigma_{W_2}^2}\right). \tag{4.22}$$

Since M_2 and M_3 are used for the Wyner-Ziv coding we have

$$D_2 = D_2^\star 2^{-2(R_2+R_3)}. \tag{4.23}$$

Substituting the rates (4.18)-(4.20) into (4.21)-(4.23) finishes the proof. ■

Corollary 18 *The proposed scheme outperforms both the GT and BAL schemes.*

Proof. We immediately observe that, as expected, setting $\omega = \hat{\omega} = 1$ and $\lambda = \eta$, (4.15)-(4.17) reduce to (4.12)-(4.14). Similarly, setting $\omega = \hat{\omega} = 1$, $\theta = 1$, and $\lambda = 1$ reduces (4.15)-(4.17) to (4.5)-(4.6). Therefore, the proposed scheme can only perform better than both the BAL and GT schemes. ■

It turns out that in some cases, there are in fact considerable performance gains in adopting the proposed scheme as demonstrated in Fig. 4.7. The gains are especially

pronounced when κ is small, where the proposed schemes comes significantly closer to the genie-aided lower bound.

4.5 Proposed Scheme for Bandwidth Compression

In light of the shortcomings of the BAL scheme for BC mentioned in Section 4.3.2, we propose the following scheme. Each component of the source, X_i^n, is grouped into two subsources $X_{i,h}^m$ and $X_{i,d}^{n-m}$ where the first one is transmitted using hybrid codingwhile the second subsource utilizes only digital coding. The transmission consists of one analog and three digital layers as in the proposed coding scheme for bandwidth expansion. However, since there is no bandwidth splitting in the channel, all four layers are superimposed.

Let α_d and α_h are defined as in (4.9) where θ is replaced with θ_d and θ_h, respectively, and $0 \leq \theta_h, \theta_d \leq 1$. The first step is to take the linear combination

$$X_{ah}^m = \theta_h X_{1,h}^m + \overline{\theta_h} X_{2,h}^m$$

and send the scaled version cX_{ah}^m through as the analog layer with power $\eta\lambda P$, i.e., $c = \sqrt{\frac{\eta\lambda P}{\alpha_h^2}}$. Next, the linear combination

$$X_{ad}^{n-m} = \theta_d X_{1,d}^{n-m} + \overline{\theta_d} X_{2,d}^{n-m}$$

is optimally quantized to a source codeword $\tilde{X}_{ad}^{n-m}$ with rate R_1, mapped to the message M_1, and sent through the first digital layer after being channel coded into $S_1^m(M_1)$ in a standard manner with power $\eta\overline{\lambda}P$. This message is intended for both receivers.

The next step is to quantize $X_{2,h}^m$ to $\tilde{X}_{2,h}^m$, and Wyner-Ziv code the quantization index, treating the noisy version of X_{ah}^m, i.e., $V_2^m - S_1^m(M_1)$, as side information available at

the receiver, with a rate R_2. The resultant bin index M_2 is intended to be decoded only at the second receiver, and transmitted using dirty paper coding as $S_2^m(M_2)$ with power $\mu\overline{\eta}P$, treating the sum of the analog and the first digital layers as channel state information.

Finally, $X_{2,d}^{n-m}$ is quantized to $\tilde{X}_{2,d}^{n-m}$ in a conditional manner, i.e., treating the information from the first layer, $\tilde{X}_{ad}^{n-m}$, as side information available both at the transmitter and the receiver, expending rate R_3. The coding index M_3 is then mapped into the signal $S_3^m(M_3)$ and transmitted with power $\overline{\mu}\,\overline{\eta}P$ using dirty paper coding, treating all other layers as channel state information. This is at the highest rank in the decoding hierarchy and intended for the second receiver only. The encoding procedure is illustrated in Fig. 4.8 and the power splitting with the coding hierarchy is illustrated in Fig. 4.9.

We are now ready for the main result.

Theorem 19 *For a bandwidth compression factor $\kappa < 1$, the distortion pair*

$$\begin{aligned} D_1 &= \kappa\left[1-\frac{\left(\theta_h+\rho\overline{\theta_h}\right)^2}{\alpha_h^2}\left\{1-\left(\frac{1+\gamma_1\overline{\eta}}{1+\gamma_1\left(\eta\lambda+\overline{\eta}\right)}\right)\right\}\right] \\ &\quad +\overline{\kappa}\left[1-\frac{\left(\theta_d+\rho\overline{\theta_d}\right)^2}{\alpha_d^2}\left\{1-\left(\frac{1+\gamma_1\left(\eta\lambda+\bar{\eta}\right)}{1+\gamma_1}\right)^{\frac{\kappa}{1-\kappa}}\right\}\right] \end{aligned} \tag{4.24}$$

and

$$\begin{aligned} D_2 &= \kappa\left[1-\frac{\left(\rho\theta_h+\overline{\theta_h}\right)^2}{\alpha_h^2}\left\{1-\left(\frac{1+\gamma_2\bar{\eta}}{1+\gamma_2\left(\eta\lambda+\bar{\eta}\right)}\right)\right\}\right]\cdot\left(\frac{1+\gamma_2\bar{\mu}\bar{\eta}}{1+\gamma_2\bar{\eta}}\right) \\ &\quad +\overline{\kappa}\left[1-\frac{\left(\rho\theta_d+\overline{\theta_d}\right)^2}{\alpha_d^2}\left\{1-\left(\frac{1+\gamma_1\left(\eta\lambda+\bar{\eta}\right)}{1+\gamma_1}\right)^{\frac{\kappa}{1-\kappa}}\right\}\right]\cdot\left(1+\gamma_2\bar{\mu}\bar{\eta}\right)^{-\frac{\kappa}{1-\kappa}} \end{aligned} \tag{4.25}$$

is achievable for any $0 \le \theta_h, \theta_d, \mu, \eta, \lambda \le 1$, where

$$\begin{aligned} \alpha_d &= \sqrt{1-2\theta_d\overline{\theta_d}\left(1-\rho\right)} \\ \alpha_h &= \sqrt{1-2\theta_h\overline{\theta_h}\left(1-\rho\right)}\,. \end{aligned}$$

Proof. As in the proof of Theorem 17, it follows from standard channel coding results provided that the rates are

$$R_1 = \frac{\kappa}{2\overline{\kappa}} \log\left(\frac{1+\gamma_1}{1+\gamma_1\left(\eta\lambda+\bar{\eta}\right)}\right) - \delta \tag{4.26}$$

$$R_2 = \frac{\kappa}{2\overline{\kappa}} \log\left(\frac{1+\gamma_2\bar{\eta}}{1+\gamma_2\overline{\mu}\,\overline{\eta}}\right) - \delta \tag{4.27}$$

$$R_3 = \frac{\kappa}{2\overline{\kappa}} \log\left(1+\gamma_2\overline{\mu}\,\overline{\eta}\right) - \delta\,, \tag{4.28}$$

for arbitrarily small $\delta > 0$, the messages are correctly decoded at the intended receivers.

Note that the first receiver makes use of the first two layers to estimate the first component of the source. After M_1 is decoded the estimation of $X_{1,d}^{m-n}$ is performed by using only $\tilde{X}_{ad}^{m-n}$ which yields

$$D_{1,d} = 1 - \frac{\mathbb{E}\{X_{1,d}\tilde{X}_{ad}\}^2}{\mathbb{E}\{\tilde{X}_{ad}^2\}} \tag{4.29}$$

where

$$\begin{aligned}\mathbb{E}\{\tilde{X}_{ad}^2\} &= \left(1-2^{-2R_1}\right)\mathbb{E}\{X_{ad}^2\} \\ &= \left(1-2^{-2R_1}\right)\alpha_d^2\end{aligned}$$

and

$$\begin{aligned}\mathbb{E}\{X_{1,d}\tilde{X}_{ad}\} &= \left(1-2^{-2R_1}\right)\mathbb{E}\{X_{1,d}X_{ad}\} \\ &= \left(1-2^{-2R_1}\right)\left(\theta_d+\rho\overline{\theta_d}\right).\end{aligned}$$

For the estimation of $X_{1,h}$ the codeword $S_1^m\left(M_1\right)$ is simply subtracted from the observation V_1^m since it does not contain any information pertaining to that subsource. Hence the distortion for $X_{1,h}$ is

$$D_{1,h} = 1 - \frac{\mathbb{E}\{X_{1,h}\left(V_1-S_1\right)\}^2}{\mathbb{E}\{\left(V_1-S_1\right)^2\}} \tag{4.30}$$

where

$$\begin{aligned}\mathbb{E}\{\,(V_1 - S_1)^2\,\} &= \mathbb{E}\{V_1^2\} - \mathbb{E}\{S_1^2\} \\ &= P + \sigma_{W_1}^2 - \eta\bar{\lambda}P \\ &= (\eta\lambda + \bar{\eta})\,P + \sigma_{W_1}^2\end{aligned}$$

and

$$\begin{aligned}\mathbb{E}\{\,X_{1,h}\,(V_1 - S_1)\,\} &= \frac{\sqrt{\eta\lambda P}}{\alpha_h}\mathbb{E}\{\,X_{1,h}X_{ah}\,\} \\ &= \frac{\sqrt{\eta\lambda P}}{\alpha_h}\left(\theta_h + \rho\overline{\theta_h}\right).\end{aligned}$$

The second receiver makes initial estimations of $X_{2,h}^m$ and $X_{2,d}^{m-n}$ by using the first two layers as follows. As done at the first receiver, the codeword pertaining to the first layer $S_1^m(M_1)$ is subtracted from the observation V_2^m and $V_2^m - S_1^m(M_1)$ is used for initial MMSE estimation of $X_{2,h}^m$. Having decoded the source codeword $\tilde{X}_{ad}^{m-n}$ the receiver uses it for the estimation of $X_{2,h}^m$. The resulting initial distortion expression for $X_{2,h}^m$ is

$$D_{2,h}^{\star} = 1 - \frac{\mathbb{E}\{\,X_{2,h}\,(V_2 - S_1)\,\}^2}{\mathbb{E}\{\,(V_2 - S_1)^2\,\}} \tag{4.31}$$

where

$$\begin{aligned}\mathbb{E}\{\,X_{2,h}\,(V_2 - S_1)\,\} &= \frac{\sqrt{\eta\lambda P}}{\alpha_h}\mathbb{E}\{\,X_{2,h}X_{ah}\,\} \\ &= \frac{\sqrt{\eta\lambda P}}{\alpha_h}\left(\rho\theta_h + \overline{\theta_h}\right)\end{aligned}$$

and

$$\begin{aligned}\mathbb{E}\{\,(V_2 - S_1)^2\,\} &= \mathbb{E}\{V_2^2\} - \mathbb{E}\{S_1^2\} \\ &= (\eta\lambda + \bar{\eta})\,P + \sigma_{W_2}^2\,.\end{aligned}$$

For $X_{2,d}^{m-n}$, the initial distortion becomes

$$D_{2,d}^{\star} = 1 - \frac{\mathbb{E}\{X_{2,d}\tilde{X}_{ad}\}^2}{\mathbb{E}\{\tilde{X}_{ad}^2\}} \tag{4.32}$$

where

$$\begin{aligned}\mathbb{E}\{X_{2,d}\tilde{X}_{ad}\} &= \left(1-2^{-2R_1}\right)\mathbb{E}\{X_{2,d}X_{ad}\} \\ &= \left(1-2^{-2R_1}\right)\left(\rho\theta_d + \overline{\theta_d}\right)\end{aligned}$$

and

$$\begin{aligned}\mathbb{E}\{\tilde{X}_{ad}^2\} &= \left(1-2^{-2R_1}\right)\mathbb{E}\{X_{ad}^2\} \\ &= \left(1-2^{-2R_1}\right)\alpha_d^2 \,.\end{aligned}$$

With the help of the other layers that is used for Wyner-Ziv coding, we obtain

$$D_{2,h} = D_{2,h}^{\star}2^{-2R_2} \tag{4.33}$$

and

$$D_{2,d} = D_{2,d}^{\star}2^{-2R_3} \,. \tag{4.34}$$

Using (4.26)-(4.28) in (4.29) through (4.34) yields the desired result. ■

Corollary 20 *The proposed scheme outperforms both the GT and BAL schemes.*

Proof. First we show that the scheme outperforms GT scheme. Simply by setting $\theta_d = \theta_h = \theta$ and

$$\mu = 1 - \frac{1}{\overline{\eta}\gamma_2}\left[(1+\overline{\eta}\gamma_2)^{1-\kappa} - 1\right] \tag{4.35}$$

$$\lambda = \frac{1}{\eta\gamma_1}\left[(1+\overline{\eta}\gamma_1)^{1-\kappa}(1+\gamma_1)^{\kappa} - 1 - \overline{\eta}\gamma_1\right] \tag{4.36}$$

it can be shown that the distortion region is given by

$$D_1 = 1 - \frac{(\theta + \rho\overline{\theta})^2}{\alpha^2}\left\{1 - \left(\frac{1+\overline{\eta}\gamma_1}{1+\gamma_1}\right)^{\kappa}\right\} \tag{4.37}$$

$$\begin{aligned} D_2 = {} & \kappa\left[1 - \frac{(\rho\theta + \overline{\theta})^2}{\alpha^2}\left\{1 - \left(\frac{1+\gamma_2\bar{\eta}}{1+\gamma_2\left(\eta\lambda+\overline{\eta}\right)}\right)\right\}\right](1+\overline{\eta}\gamma_2)^{-\kappa} \\ & +\overline{\kappa}\left[1 - \frac{(\rho\theta + \overline{\theta})^2}{\alpha^2}\left\{1 - \left(\frac{1+\overline{\eta}\gamma_1}{1+\gamma_1}\right)^{\kappa}\right\}\right](1+\overline{\eta}\gamma_2)^{-\kappa} \ . \end{aligned} \tag{4.38}$$

Note that $0 \leq \mu \leq 1$ and $0 \leq \lambda \leq 1$. Plugging (4.36) into the expression above we have

$$\frac{1+\bar{\eta}\gamma_2}{1+\gamma_2\left(\eta\lambda+\bar{\eta}\right)} \leq \frac{1+\bar{\eta}\gamma_1}{1+\gamma_1\left(\eta\lambda+\bar{\eta}\right)} \tag{4.39}$$

$$= \left(\frac{1+\bar{\eta}\gamma_1}{1+\gamma_1}\right)^{\kappa} . \tag{4.40}$$

Comparing (4.37)-(4.38) with (4.12)-(4.14), it can be seen with the help of (4.39)-(4.40) that the achievable distortion region is larger than that with the GT scheme.

Following the description of the BAL scheme for BC we numerically demonstrated that the second digital layer (information M_2) is redundant. But in the absence of the second digital layer, the BAL scheme for BC is simply subsumed by our scheme where $\theta_d = 1$ and $\mu = 0$. ■

The superiority of our scheme over the others is demonstrated in Fig. 4.10.

As $\kappa \to 1$, both schemes in Sections 4.4 and 4.5 reduce to sending a linear combination of the sources $\theta X_1^n + \bar{\theta} X_2^n$, i.e., an analog layer, with power λP and using the remaining power $(1-\lambda)P$ to send M_3, which is the digital information containing Wyner-Ziv coding index for X_2, by using dirty paper coding. The achievable distortion pair in this case can

be shown to reduce to

$$D_1 = \frac{P\left(1-\frac{\lambda}{\alpha^2}\left(\theta+\rho\bar{\theta}\right)^2\right)+\sigma_{W_1}^2}{P+\sigma_{W_1}^2} \tag{4.41}$$

$$D_2 = \frac{\left(P\left(1-\frac{\lambda}{\alpha^2}\left(\rho\theta+\bar{\theta}\right)^2\right)+\sigma_{W_2}^2\right)\sigma_{W_2}^2}{\left(P+\sigma_{W_2}^2\right)\left(\bar{\lambda}P+\sigma_{W_2}^2\right)}\,. \tag{4.42}$$

We show in Appendix A.3 that (4.41) and (4.42) are equivalent to the original optimal distortion region presented in [41] by finding a one-to-one relation between (θ,λ) and the parameters of the scheme in [41].

This limiting scheme is also subsumed by the classes of schemes introduced in [38, Sections IV-A and IV-B].

4.6 Conclusion

We considered lossy transmission of correlated Gaussian sources over bandwidth mismatched Gaussian broadcast channel where each receiver is interested in only one component of the source. We identified the shortcomings of the BAL scheme, and proposed HDA schemes that outperform, in both BE and BC regimes, the BAL scheme as well as separate source-channel coding (the GT scheme). In some cases, the proposed schemes come close to the genie-aided outer bound. Finally, the proposed schemes collapse to an optimal scheme as the bandwidth expansion ratio approaches one either from above or below.

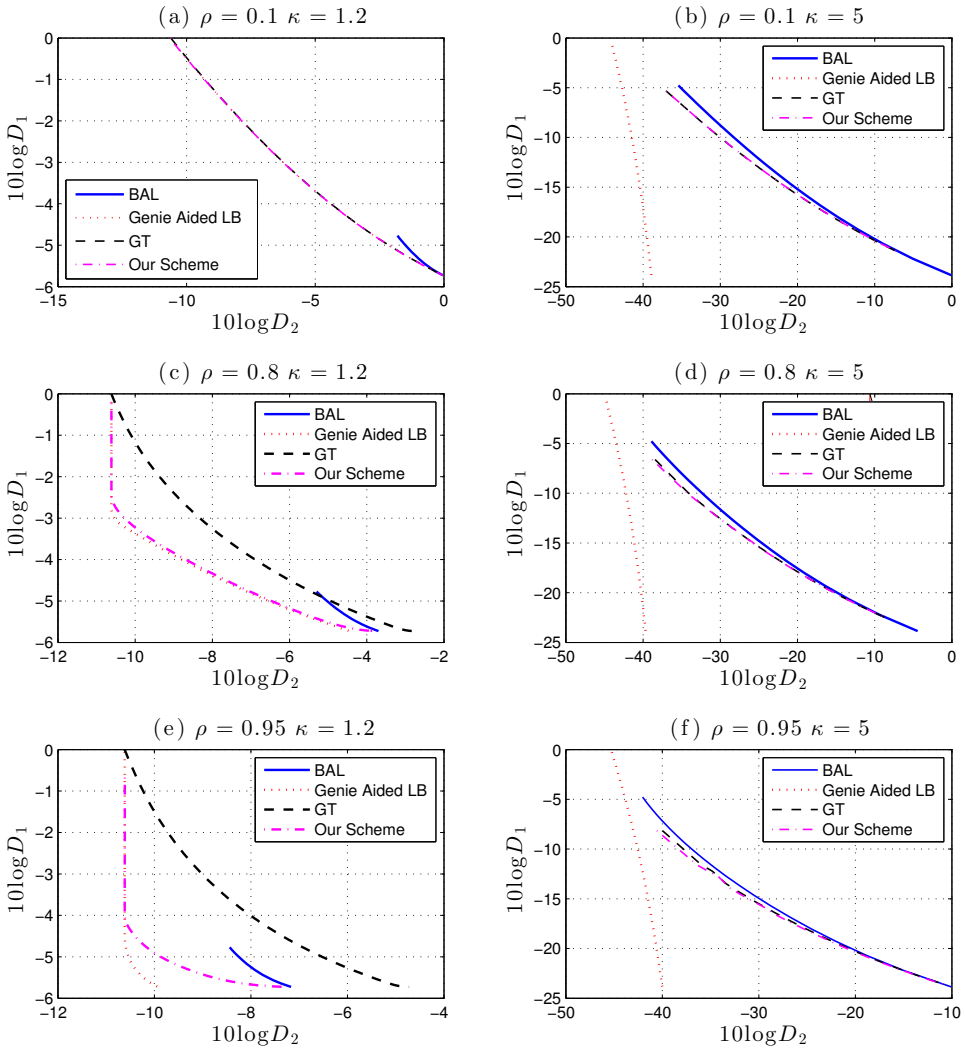

Figure 4.7: The distortion performances of our coding scheme, the BAL scheme and GT scheme are compared with the genie-aided lower bound when $P = 1$, $N_1 = 1$, $N_2 = 0.3$, $\rho = 0.1, 0.8, 0.95$, and $\kappa = 1.2, 5$. The BAL scheme performs poorly especially in (a), (c), and (e), i.e., when κ is close to one. In (e), as ρ and κ are both close to one, uncoded transmission scheme must be almost optimal, and therefore the GT scheme performs poorly compared to the other coding schemes since it is purely digital. When κ is high, as in (b), (d) and (f), the genie-aided outer bound is no longer useful, and the coding schemes seem to perform relatively close to each other.

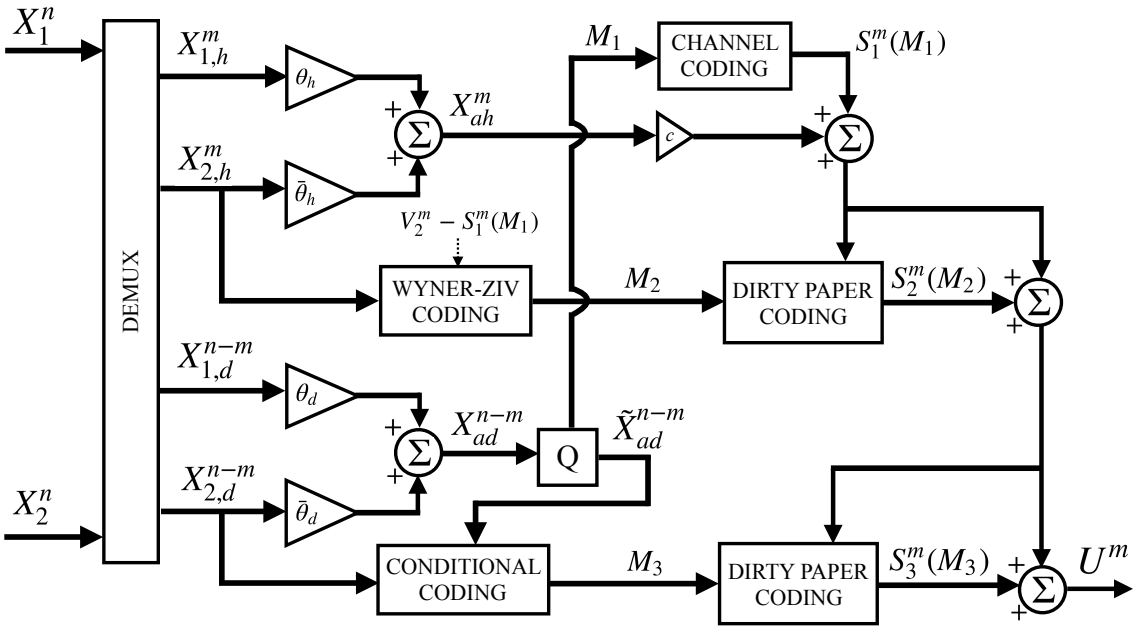

Figure 4.8: The proposed joint source-channel encoder in the bandwidth compression case. The Wyner-Ziv coder exploits the fact that side information $V_2^m - S_1^m(M_1) = cX_{ah}^m + S_2^m(M_2) + S_3^m(M_3) + W_2^m$ is available at the (second) receiver.

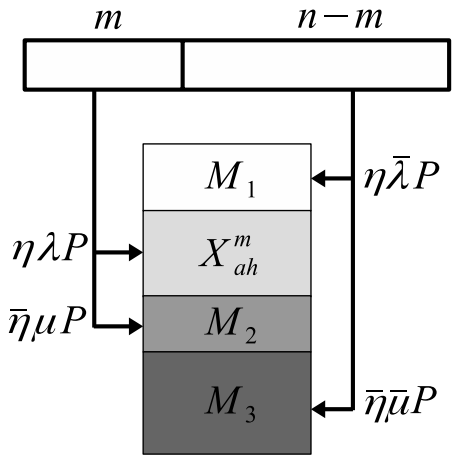

Figure 4.9: The diagram and coding hierarchy of power splitting for bandwidth compression. As in bandwidth expansion case, the upper layers "see" the lower layers as noise, while the lower layers cancel the effect of the upper ones. The lowest two layers are intended for the second receiver only.

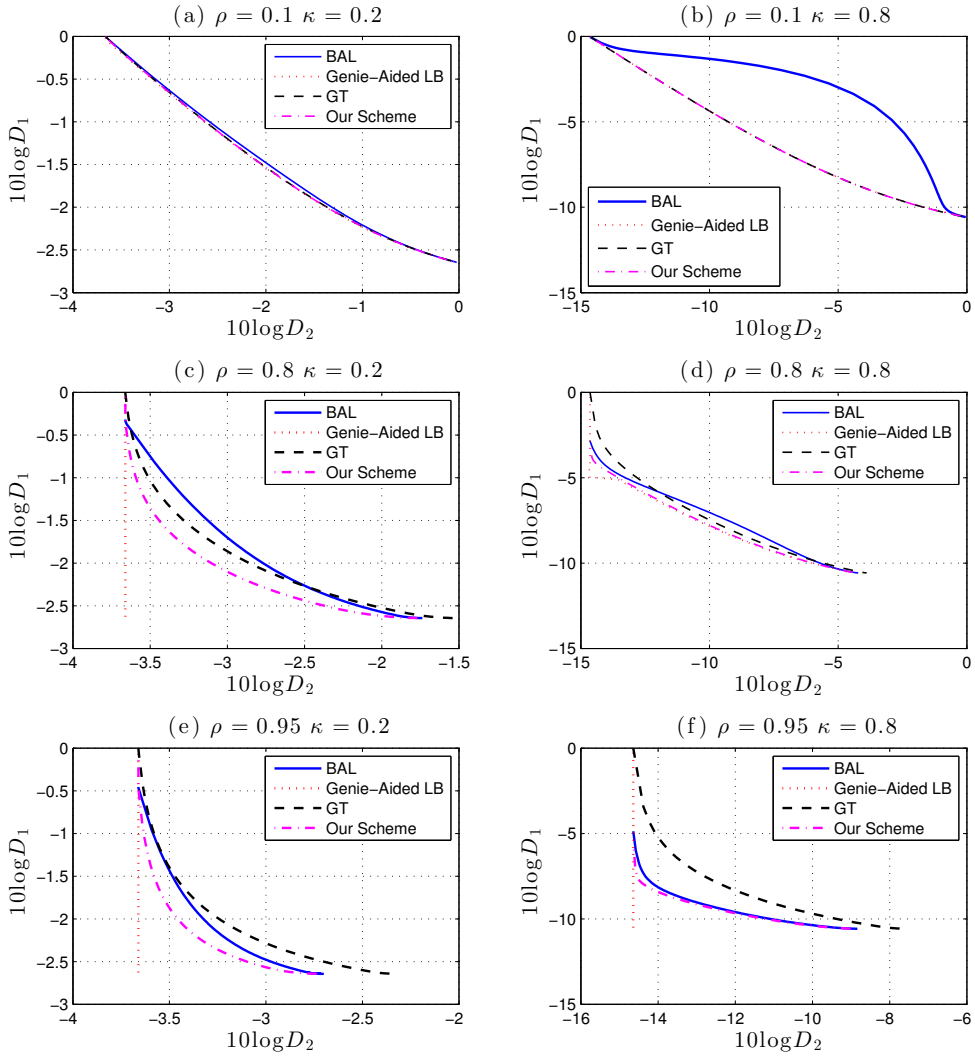

Figure 4.10: The performances of the coding schemes and the genie-aided lower bound are depicted for various (ρ, κ) pairs. Unless ρ is small as in (a) and (b), our scheme clearly outperforms both known schemes. When ρ is close to 1, the lower bound is no longer useful.

Chapter 5

Energy-Distortion Exponents in Lossy Transmission of Gaussian Sources Over Gaussian Channels

5.1 Introduction

In information theory, performance of a communication system is typically analyzed under the average power constraint per unit bandwidth (i.e., Joules/second/Hertz), which automatically translates into infinite energy consumption per source sample when the bandwidth is unlimited. This does not correspond to a meaningful setting for sensor networks which are limited by the total energy available in finite-size batteries, while the relative channel bandwidth per source sample is abundant when the source signal changes slowly over time and each source sample can be transmitted over many uses of the channel.

A more appropriate performance measure for the sensor network scenario is the *energy-distortion tradeoff* [17, 18], which characterizes the minimum average reconstruction distortion that can be achieved under a total energy constraint (per source sample) without any limitation on the channel bandwidth.

In this paper, we introduce the *energy-distortion exponent* as the exponential rate of decay of the square-error distortion as the energy-to-noise ratio (ENR) approaches infinity. Our motivation for defining this measure is the same as in typical high signal-to-noise ratio (SNR) analyses that appear in the literature: in the absence of a completely characterized energy-distortion tradeoff, energy-distortion exponent will provide us with a rough benchmark to strive for when designing practical systems.

Two prominent examples where the energy-distortion characterization is not fully known are (i) the transmission of a single Gaussian source over a Gaussian broadcast channel where each receiver reconstructs its own estimate of the source (see [32] and [35] for inner and outer bounds derived for average power constraint and finite bandwidth), and (ii) the transmission of a pair of correlated Gaussian sources over a Gaussian broadcast channel, where each receiver is interested in reconstructing only one of the sources (similarly, see [6, 8, 14, 19, 38, 39, 41] for existing results). In both cases, the tradeoff is between two distortion levels achieved at each receiver for a given energy budget. Similarly, there will be a tradeoff between energy-distortion exponents at each receiver.

Our first result is a closed-form characterization of the achievable pairs of energy-distortion exponents in the first scenario. More specifically, we show that the achievability and converse results in [35] coincide in the energy-distortion regime for very high ENR.

For the second scenario we prove a similar result. Namely, we show that the converse result in [6], when translated into the energy-distortion tradeoff, yields a pair of energy-distortion exponents that can be achieved using a simple energy splitting scheme.

For both of the broadcast scenarios, as well as the point-to-point channel, we then investigate the energy-distortion exponents in the extreme case of *zero-delay*[1]. Zero-delay transmission is relevant in applications where delay could not be tolerated, such as smart-grid systems where smart-meter measurements are used for monitoring the grid for energy outages. In a typical smart meter scenario, one measurement is taken every 15 minutes and must be transmitted as soon as possible to the central control unit [27]. Our last result is that, in the zero-delay regime, if we allow for a small *outage* event whose probability is vanishingly small, the same energy-distortion exponent(s) can be achieved as in the aforementioned infinite delay scenarios.

The rest of the paper is organized as follows. Section 5.2 is dedicated to preliminaries and notation. In Section 5.3, achievable energy-distortion exponents are derived for both of the broadcast scenarios under the infinite-delay regime. Then, in Section 5.4, we focus on zero-delay transmission for both point-to-point and broadcast channels, and show that the same energy-distortion exponents as in the infinite delay regime can be achieved with distortion outages.

[1]To clarify, in our terminology zero-delay refers to transmission being complete before the next source sample is generated. In other words, zero source delay is incurred.

5.2 Preliminaries and Notation

5.2.1 Point-To-Point Transmission

Let $X^M \sim \mathcal{N}(\mathbf{0}, \mathbf{I}_M)$ be an independent and identically distributed (i.i.d.) Gaussian source sequence to be transmitted over the channel

$$V^N = U^N + W^N \,, \tag{5.1}$$

where U^N and V^N are the channel input and output, respectively, and the channel noise $W^N \sim \mathcal{N}\left(\mathbf{0}, \sigma_W^2 \mathbf{I}_N\right)$ is independent of U^N. The encoder

$$\phi_{M,N} : \mathbb{R}^M \longrightarrow \mathbb{R}^N \tag{5.2}$$

maps X^M into U^N, and the receiver

$$\psi_{M,N} : \mathbb{R}^N \longrightarrow \mathbb{R}^M \tag{5.3}$$

estimates X^M as $\hat{X}^M$. The ratio $\kappa = \frac{N}{M}$ is usually referred to as the bandwidth expansion factor, and it is measured in channel uses per source symbol.

Definition 21 *A pair (D, E) is achievable for point-to-point transmission if for any $\epsilon > 0$, there exists large enough M, N, and a corresponding encoder-decoder pair $(\phi_{M,N}, \psi_{M,N})$, such that*

$$\begin{aligned} \frac{1}{M}\mathbb{E}\left[||U^N||^2\right] &\leq E + \epsilon \\ \frac{1}{M}\mathbb{E}\left[||X^M - \hat{X}^M||^2\right] &\leq D + \epsilon \,. \end{aligned}$$

As usual, we denote by $D(E)$ the minimum possible distortion such that (D, E) is achievable.

Note that in the above definition, the expended energy is measured *per source symbol*. This is in contrast with power-limited transmission where the channel power is measured *per channel symbol*. However, by expressing the energy constraint alternatively as

$$\frac{1}{N}\mathbb{E}\left[||U^N||^2\right] \leq \frac{E}{\kappa} + \epsilon' \,,$$

one can utilize existing power-constrained channel transmission results. For instance, it directly follows from the separation theorem that (D, E) is achievable if and only if

$$R\left(D\right) \leq \sup_{\kappa>0} \kappa C\left(\frac{E}{\kappa}\right) \tag{5.4}$$

where $C\left(P\right)$ is the capacity with power constraint

$$C\left(P\right) = \frac{1}{2}\log_2\left(1 + \frac{P}{\sigma_W^2}\right) \,,$$

and $R\left(D\right)$ is the rate-distortion function given by

$$R\left(D\right) = \frac{1}{2}\log_2\frac{1}{D}.$$

Translating (5.4) then yields

$$D\left(E\right) = \inf_{\kappa>0}\left(1 + \frac{E}{\kappa\sigma_W^2}\right)^{-\kappa} = \lim_{\kappa\to\infty}\left(1 + \frac{E}{\kappa\sigma_W^2}\right)^{-\kappa} = e^{-\frac{E}{\sigma_W^2}}. \tag{5.5}$$

To emphasize the fact that the minimum achievable distortion $D(E)$ depends only on the energy-to-noise ratio (ENR), defined as

$$\gamma = \frac{E}{\sigma_W^2} \,,$$

we write (5.5) in the sequel as

$$D\left(E\right) = e^{-\gamma} \,. \tag{5.6}$$

In all the scenarios we consider in the sequel, we will observe similar energy-distortion behaviors as $E \to \infty$. That motivates us to define

$$\lim_{E\to\infty} -\frac{1}{\gamma} \ln D(E)$$

as the *energy-distortion exponent* for each scenario. Therefore, when we say that a receiver achieves an energy-distortion exponent of β, it is equivalent to stating that the average distortion at that receiver decays to zero as $e^{-\beta\gamma}$ in the high-energy high-bandwidth regime. Thus, though not asymptotic in E, we still observe that the energy-distortion tradeoff $D(E)$ in (5.6) achieves an exponent of 1.

5.2.2 Transmission of a Single Source Over a Broadcast Channel

Let the i.i.d. Gaussian source X^M be transmitted over the Gaussian broadcast channel

$$V_i^N = U^N + W_i^N \tag{5.7}$$

for $i = 1, 2$, where U^N and V_i^N are the channel input and output at the ith receiver, respectively, and the channel noise sequences $W_i^N \sim \mathcal{N}\left(\mathbf{0}, \sigma_{W_i}^2 \mathbf{I}_N\right)$ are independent of U^N and each other.

Let the encoder be the same as given in (5.2). At the ith receiver, the decoder

$$\psi_{M,N}^{(i)} : \mathbb{R}^N \to \mathbb{R}^M \tag{5.8}$$

maps the observation V_i^N into the estimation $\hat{X}_i^M = \psi_{M,N}^{(i)}\left(V_i^N\right)$. We refer the reader to Fig. 5.1 for the block diagram of the system.

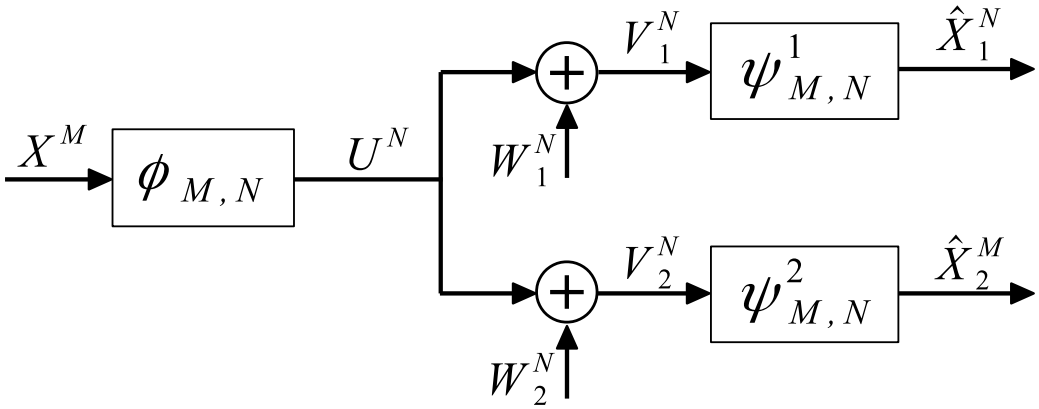

Figure 5.1: The block diagram for transmission of a single Gaussian source sequence X^M over the Gaussian broadcast channel $V_i^N = U^N + W_i^N$, $i = 1, 2$. Each receiver estimates its version $\hat{X}_i^M$ of the source.

Definition 22 *An energy-distortion triplet* (D_1, D_2, E) *is achievable if for any* $\epsilon > 0$*, there exists large enough* M, N *and* $(\phi_{M,N}, \psi^1_{M,N}, \psi^2_{M,N})$ *such that*

$$\begin{aligned} \frac{1}{M}\mathbb{E}\left[||U^N||^2\right] &\leq E + \epsilon \\ \frac{1}{M}\mathbb{E}\left[||X^M - \hat{X}_i^M||^2\right] &\leq D_i + \epsilon \end{aligned}$$

for $i = 1, 2$.

As in the point-to-point case, for a fixed energy budget E, the tradeoff between D_1 and D_2 will depend only on the ENR values $\gamma_i = \frac{E}{\sigma^2_{W_i}}$. Without loss of generality, we assume that the second receiver is the "better" one, i.e., $\sigma^2_{W_1} = g\sigma^2_{W_2}$ for some $g > 1$. This also implies $\gamma_2 = g\gamma_1$ for all E.

Definition 23 *An* energy-distortion exponent pair (β_1, β_2) *is achievable if there exist functions* $D_1(E)$ *and* $D_2(E)$ *such that* $(D_1(E), D_2(E), E)$ *is achievable for all* $E > 0$ *and*

$$\lim_{E\to\infty} -\frac{1}{\gamma_i} \ln D_i(E) = \beta_i$$

for $i = 1, 2$.

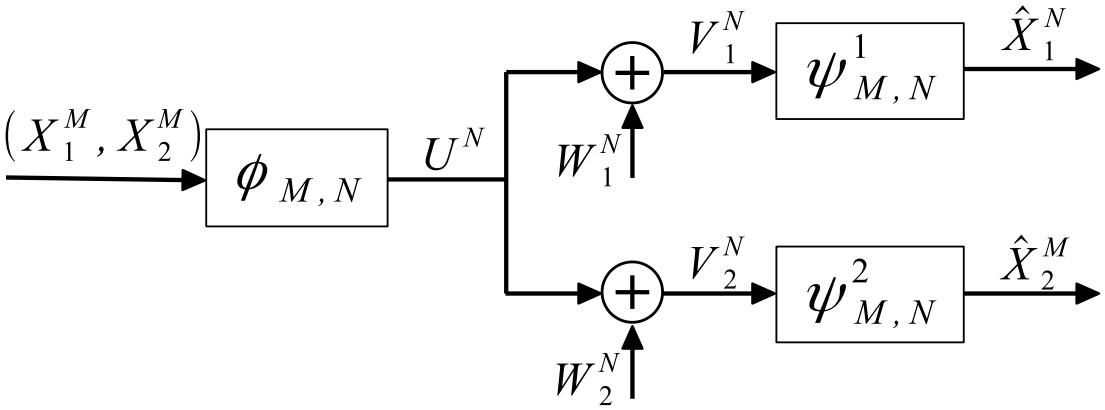

Figure 5.2: The block diagram for transmission of a bivariate Gaussian source sequence (X_1^M, X_2^M) over the Gaussian broadcast channel $V_i^N = U^N + W_i^N$, $i = 1, 2$. Each receiver estimates only one source.

5.2.3 Transmission of a Bivariate Source Over a Broadcast Channel

Consider the transmission of an i.i.d. bivariate zero-mean Gaussian source $\left(X_1^M, X_2^M\right)$ over the same channel given in (5.7), where $(X_{1,m}X_{2,m}) \sim \mathcal{N}(0, \Sigma)$ with covariance matrix

$$\Sigma = \begin{bmatrix} 1 & \rho \\ \rho & 1 \end{bmatrix}$$

and $|\rho| < 1$. The encoder (5.2) is modified as

$$\phi_{M,N} : \mathbb{R}^M \times \mathbb{R}^M \longrightarrow \mathbb{R}^N \tag{5.9}$$

which maps $\left(X_1^M, X_2^M\right)$ into U^N, and at the ith receiver the decoder

$$\psi_{M,N}^{(i)} : \mathbb{R}^N \to \mathbb{R}^M \tag{5.10}$$

estimates the ith source as $\hat{X}_i^M = \psi_{M,N}^{(i)}\left(V_i^N\right)$. See Fig. 5.2 for the pictorial description of the system.

Definition 24 *An energy-distortion triplet (D_1, D_2, E) is achievable if for any $\epsilon > 0$, there exists large enough M, N and $(\phi_{M,N}, \psi^1_{M,N}, \psi^2_{M,N})$ such that*

$$\begin{aligned} \frac{1}{M}\mathbb{E}\left[||U^N||^2\right] &\leq E + \epsilon \\ \frac{1}{M}\mathbb{E}\left[||X_i^M - \hat{X}_i^M||^2\right] &\leq D_i + \epsilon \end{aligned}$$

for $i = 1, 2$.

Definition of achievable energy-distortion exponent pairs for this scenario is exactly as given in Definition 23.

5.3 Achievable Energy-Distortion Exponents

We begin by characterizing the energy-distortion exponent pair for the transmission of a single Gaussian source over a Gaussian broadcast channel. To that end, we utilize the inner and outer bounds on the achievable distortion region given in [35] for a fixed bandwidth expansion factor κ and average channel input power P. In particular, the bounds coincide when translated into the energy-distortion exponent regime. We note in passing that even though the inner bound of [35] was improved in [32], the former suffices for our purposes.

Theorem 25 *The set of achievable energy-distortion exponent pairs for the transmission of a single Gaussian source over a Gaussian broadcast channel is given as*

$$\mathcal{B}_{\text{single}} = \left\{ (\beta_1, \beta_2) \,\middle|\, 0 \leq \beta_1 \leq 1,\, 0 \leq \beta_2 \leq \frac{\beta_1}{g} + (1 - \beta_1) \right\}$$

as shown in Fig. 5.3.

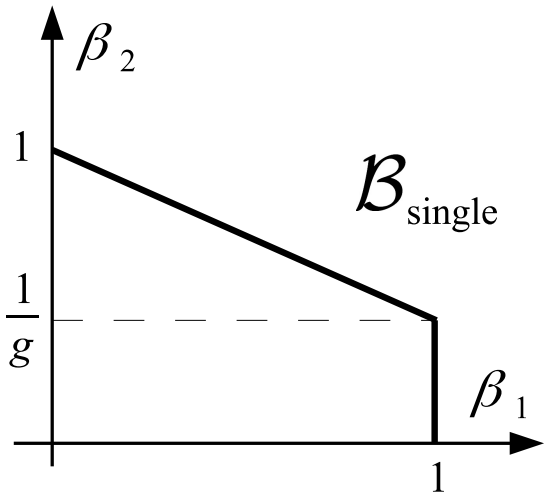

Figure 5.3: The region of all achievable energy-distortion exponent pairs (β_1, β_2) for transmission of a single Gaussian source over a Gaussian broadcast channel.

Proof. We first show that all energy-distortion exponent pairs in $\mathcal{B}_{\text{single}}$ are achievable. For a fixed bandwidth expansion factor κ and an average power budget P per channel use, the scheme in [35] achieves

$$D_1 = \frac{1}{1+\frac{P}{\sigma_{W_1}^2}} \left(1 + \frac{\alpha P}{\sigma_{W_1}^2 + (1-\alpha)\, P}\right)^{1-\kappa} \tag{5.11}$$

$$D_2 = \frac{1}{1+\frac{P}{\sigma_{W_2}^2}} \left(1 + \frac{\alpha P}{\sigma_{W_1}^2 + (1-\alpha)\, P}\right)^{1-\kappa} \left(1 + \frac{(1-\alpha)P}{\sigma_{W_2}^2}\right)^{1-\kappa} \tag{5.12}$$

for all $0 \leq \alpha \leq 1$.

Substituting in (5.11) and (5.12) the identity $P = \frac{E}{\kappa}$, and letting $\kappa \to \infty$, we obtain

$$
\begin{aligned}
D_1 &= \lim_{\kappa\to\infty} \frac{1}{1+\frac{\gamma_1}{\kappa}} \left(1+\frac{\alpha\gamma_1}{\kappa+(1-\alpha)\gamma_1}\right)^{1-\kappa} \\
&= \lim_{\kappa\to\infty} \left(1+\frac{\alpha\gamma_1}{\kappa+(1-\alpha)\gamma_1}\right)^{1-\kappa} \\
&= \lim_{\kappa'\to\infty} \left(1+\frac{1}{\kappa'}\right)^{1+(1-\alpha)\gamma_1-\alpha\gamma_1\kappa'} \\
&= \lim_{\kappa'\to\infty} \left(1+\frac{1}{\kappa'}\right)^{1+(1-\alpha)\gamma_1} \lim_{\kappa'\to\infty} \left(1+\frac{1}{\kappa'}\right)^{-\alpha\gamma_1\kappa'} \\
&= \lim_{\kappa'\to\infty} \left(1+\frac{1}{\kappa'}\right)^{-\alpha\gamma_1\kappa'} \\
&= e^{-\alpha\gamma_1} \qquad (5.13)
\end{aligned}
$$

where $\kappa' = \frac{\kappa+(1-\alpha)\gamma_1}{\alpha\gamma_1}$, and

$$
\begin{aligned}
D_2 &= \lim_{\kappa\to\infty} \frac{1}{1+\frac{\gamma_2}{\kappa}} \left(1+\frac{\alpha\gamma_1}{\kappa+(1-\alpha)\gamma_1}\right)^{1-\kappa} \left(1+(1-\alpha)\frac{\gamma_2}{\kappa}\right)^{1-\kappa} \\
&= \lim_{\kappa\to\infty} \left(1+\frac{\alpha\gamma_1}{\kappa+(1-\alpha)\gamma_1}\right)^{1-\kappa} \lim_{\kappa\to\infty} \left(1+(1-\alpha)\frac{\gamma_2}{\kappa}\right)^{1-\kappa} \\
&= e^{-\alpha\gamma_1} e^{-(1-\alpha)\gamma_2} \\
&= e^{-\gamma_2\left[\frac{\alpha}{g}+1-\alpha\right]}. \qquad (5.14)
\end{aligned}
$$

It follows from (5.13) and (5.14) that all energy-distortion pairs in the set $\mathcal{B}_{\text{single}}$ are indeed achievable.

For the converse, we use the outer bound for the finite bandwidth power-constrained problem given in [35] as follows. For any achievable (D_1, D_2) such that

$$
D_1 = \delta \left(1+\frac{P}{\sigma_{W_1}^2}\right)^{-\kappa},
$$

with $\delta > 1$, D_2 must satisfy

$$
D_2 \geq \sup_{m>0} \frac{m}{\left(\frac{\sigma_{W_1}^2}{\sigma_{W_2}^2}\left[\delta + m\left(\frac{P}{\sigma_{W_1}^2}+1\right)^{\kappa}\right]^{1/\kappa} - \left(\frac{\sigma_{W_1}^2}{\sigma_{W_2}^2}-1\right)(1+m)^{1/\kappa}\right)^{\kappa} - 1}.
$$

In the energy-distortion regime, this bound translates to

$$\begin{aligned} D_1 &= \lim_{\kappa\to\infty} \delta\left(1+\frac{\gamma_1}{\kappa}\right)^{-\kappa} \\ &= \delta e^{-\gamma_1} \end{aligned} \tag{5.15}$$

and

$$\begin{aligned} D_2 &\geq \lim_{\kappa\to\infty}\sup_{m>0} \frac{m}{\left(g\left[\delta+m\left(1+\frac{\gamma_1}{\kappa}\right)^{\kappa}\right]^{1/\kappa}-(g-1)\left(1+m\right)^{1/\kappa}\right)^{\kappa}-1} \\ &= \sup_{m>0}\frac{m}{(1+m)L(m)-1} \end{aligned} \tag{5.16}$$

where

$$\begin{aligned} L\left(m\right) &= \frac{1}{1+m}\lim_{\kappa\to\infty}\left(g\left[\delta+m\left(1+\frac{\gamma_1}{\kappa}\right)^{\kappa}\right]^{1/\kappa}-(g-1)\left(1+m\right)^{1/\kappa}\right)^{\kappa} \\ &= \lim_{\kappa\to\infty}\left(1+g\left[\left(\frac{\delta+m\left(1+\frac{\gamma_1}{\kappa}\right)^{\kappa}}{1+m}\right)^{\frac{1}{\kappa}}-1\right]\right)^{\kappa}. \end{aligned}$$

Now, for $f(\kappa)$ non-decreasing in κ, and $h(\theta,\kappa)$ non-decreasing in θ, we can write

$$h(f(\kappa_-),\kappa)\leq h(f(\kappa),\kappa)\leq h(f(\kappa_+),\kappa) \tag{5.17}$$

for any $\kappa_-\leq\kappa\leq\kappa_+$. Moreover, the inequality chain in (5.17) remains intact if we first let $\kappa_+\to\infty$, then let $\kappa\to\infty$, and finally $\kappa_-\to\infty$, to obtain

$$\lim_{\kappa_-\to\infty}\lim_{\kappa\to\infty}h(f(\kappa_-),\kappa)\leq\lim_{\kappa\to\infty}h(f(\kappa),\kappa)\leq\lim_{\kappa\to\infty}h\big(\lim_{\kappa_+\to\infty}f(\kappa_+),\kappa\big) \tag{5.18}$$

whenever the above limits exist. Setting

$$f(\kappa)=\frac{\delta+m\left(1+\frac{\gamma_1}{\kappa}\right)^{\kappa}}{1+m}$$

and

$$h(\theta,\kappa)=\left(1+g\left[\theta^{\frac{1}{\kappa}}-1\right]\right)^{\kappa},$$

together with the observation that

$$\lim_{\kappa\to\infty} f(\kappa) = \frac{\delta + me^{\gamma_1}}{1+m}$$

and

$$\lim_{\kappa\to\infty} h(\theta,\kappa) = \theta^g$$

for any fixed θ, we notice that the upper and lower bounds in (5.18) collapse and yield

$$L(m) = \left(\frac{\delta + me^{\gamma_1}}{1+m}\right)^g \ .$$

Therefore (5.16) is the same as

$$D_2 \geq \sup_{m>0} \frac{m}{(1+m)\left(\frac{\delta+me^{\gamma_1}}{1+m}\right)^g - 1} \ .$$

The supremum above is difficult to compute. However, substitution of any $m > 0$ obviously results in a (looser) lower bound on the achievable D_2. In particular, it is easy to show after some algebra that the choice

$$m = \frac{\delta}{(g-1)e^{\gamma_1} - \delta g}.$$

results in

$$D_2 \geq \frac{\delta}{(g-1)(e^{\gamma_1}-\delta)\left(\frac{\delta g}{g-1}\right)^g - (g-1)e^{\gamma_1} + \delta g} \tag{5.19}$$

for any fixed $D_1 = \delta e^{-\gamma_1}$.

Note that we are interested in the asymptotic behavior of achievable (D_1, D_2) as $E \to \infty$. To that end, let $D_1(E) = \delta(E)e^{-\gamma_1}$ for some arbitrary $\delta(E) > 1$ such that

$$\lim_{E\to\infty} -\frac{1}{\gamma_1} \ln D_1(E) = \beta_1 \tag{5.20}$$

for some $0 \leq \beta_1 \leq 1$. This implies that for any such $\delta(E)$,

$$\lim_{E\to\infty} -\frac{1}{\gamma_1}\ln\delta(E) = \beta_1 - 1\ ,$$

or in other words, $\delta(E)$ must grow as $e^{\gamma_1(1-\beta_1)}$. For the second energy-distortion exponent, (5.19) then translates to the upper bound

$$\begin{aligned}
\lim_{E\to\infty}\frac{-\ln D_2(E)}{\gamma_2} &\leq \lim_{E\to\infty}\Bigg\{\frac{-\ln\delta(E)}{\gamma_2} \\
&\quad +\frac{1}{\gamma_2}\ln\left[(g-1)(e^{\gamma_1}-\delta(E))\left(\frac{\delta(E)g}{g-1}\right)^g - (g-1)e^{\gamma_1} + g\delta(E)\right]\Bigg\} \\
&= \frac{\beta_1-1}{g} + \lim_{E\to\infty}\frac{1}{\gamma_2}\ln\left[\frac{g^g}{(g-1)^{g-1}}[e^{\gamma_1}-\delta(E)]\delta(E)^g - (g-1)e^{\gamma_1} + g\delta(E)\right] \\
&\overset{(a)}{=} \frac{\beta_1-1}{g} + \frac{1}{g} + 1 - \beta_1 \\
&= \frac{\beta_1}{g} + 1 - \beta_1 \qquad (5.21)
\end{aligned}$$

where (a) follows from the fact that $[e^{\gamma_1}-\delta(E)]\delta(E)^g$ grows as $e^{\gamma_1+\gamma_2(1-\beta_1)}$, which is faster than the other terms e^{γ_1} and $\delta(E)$. The proof is therefore complete because (5.20) and (5.21) implies that $\mathcal{B}_{\text{single}}$ is indeed an outer bound to achievable energy-distortion exponents. ■

In the next theorem, we characterize the achievable energy-distortion exponent pairs for the transmission of bivariate Gaussian sources over the Gaussian broadcast channel. As in the single source case, we utilize an existing outer bound introduced in [6] on achievable (D_1, D_2) pairs for a given channel input power P and bandwidth expansion factor κ. Interestingly, a very simple coding scheme achieves the same energy-distortion exponents as the outer bound.

Theorem 26 *The set of achievable energy-distortion exponent pairs for the transmission of a bivariate Gaussian source over a Gaussian broadcast channel is given as*

$$\mathcal{B}_{\text{bivariate}} = \{(\beta_1,\beta_2)\,|0 \leq \beta_1 \leq 1,\, 0 \leq \beta_2 \leq 1-\beta_1\,\}$$

as shown in Fig. 5.4.

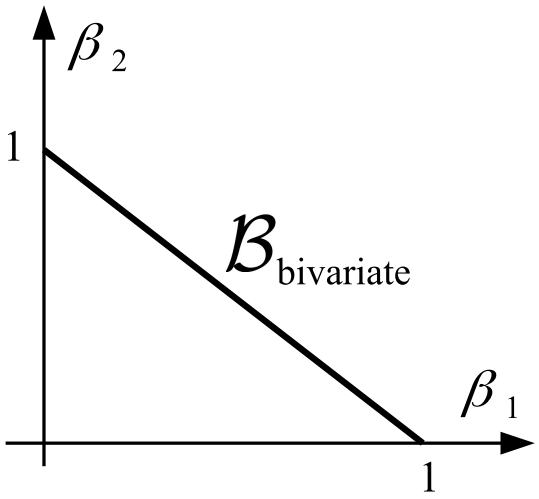

Figure 5.4: The region of all achievable energy-distortion exponent pairs (β_1, β_2) for transmission of a bivariate Gaussian source over a Gaussian broadcast channel.

Proof. We start with the converse. It follows from the outer bound derived in [6] that for fixed channel input power P and bandwidth expansion factor κ, (D_1, D_2) is achievable only if there exists $0 \leq \alpha \leq 1$ such that

$$\begin{aligned} D_1 &\geq \left(1 + \frac{\alpha P}{(1-\alpha)P + \sigma_{W_1}^2}\right)^{-\kappa} \\ D_2 &\geq \left(1-\rho^2\right)\left(1 + \frac{(1-\alpha)P}{\sigma_{W_2}^2}\right)^{-\kappa} \end{aligned}$$

In the energy-distortion framework, this implies that for any fixed energy budget E per source symbol, there must exist $0 \leq \alpha \leq 1$ such that

$$\begin{aligned} D_1 &\geq \lim_{\kappa\to\infty} \left(1 + \frac{\alpha\gamma_1}{(1-\alpha)\,\gamma_1 + \kappa}\right)^{-\kappa} \\ &= e^{-\alpha\gamma_1} \\ D_2 &\geq \lim_{\kappa\to\infty} \left(1-\rho^2\right) \left(1 + \frac{(1-\alpha)\gamma_2}{\kappa}\right)^{-\kappa} \\ &= \left(1-\rho^2\right) e^{-(1-\alpha)\gamma_2}\,. \end{aligned}$$

Thus, for any $D_1(E)$ and $D_2(E)$ such that $(D_1(E), D_2(E), E)$ is achievable, we must have

$$\begin{aligned} \lim_{E\to\infty} -\frac{1}{\gamma_1} \ln D_1(E) &\leq \alpha \\ \lim_{E\to\infty} -\frac{1}{\gamma_2} \ln D_2(E) &\leq 1-\alpha \end{aligned}$$

for some $0 \leq \alpha \leq 1$, proving that $\mathcal{B}_{\text{bivariate}}$ is indeed an outer bound for all achievable exponent pairs (β_1, β_2).

To prove achievability of any $(\beta_1, \beta_2) \in \mathcal{B}_{\text{bivariate}}$, it suffices to simply send the source pair with two rounds of transmission, where in each round $i = 1, 2$, we transmit X_i^M with energy $\beta_i E$ and bandwidth expansion factor κ_i. Note that (i) $\beta_1 E + \beta_2 E \leq E$, and therefore this is a feasible choice, and (ii) the individual κ_i can be arbitrarily taken to infinity, resulting in

$$\begin{aligned} D_1(E) &= e^{-\beta_1\gamma_1} \\ D_2(E) &= e^{-\beta_2\gamma_2} \end{aligned}$$

which follows from (5.6). The proof is therefore complete. ■

5.4 Zero-Delay Communication with Distortion Outage

In this section we focus on the extreme case of zero source delay, i.e., $M = 1$. In other words, a single random variable X is mapped into the channel input U^N where the channel, the encoder, and the decoder(s) are in the same form in each aforementioned scenario. We have $\kappa = N$, and once again, we are interested in the energy-distortion tradeoff when the bandwidth is not limited, i.e., $N \to \infty$. However, we slightly change the achievability definition for distortion by allowing a vanishingly small probability of *distortion outage*, and evaluating the expected distortion conditioned on no distortion outages.

The motivation behind this change is as follows. While one should ultimately search for an analog mapping between X and U^N, that proves a difficult task for even moderate values of N [3, 9, 16, 44], let alone $N \to \infty$. That leaves the alternative of either *digital* coding or hybrid digital/analog coding. On the other hand, any coding scheme that transmits some digital information through the channel is prone to error in decoding of that information. Regardless of how small the probability of incorrect decoding is, the overall expected distortion might still be very adversely affected.

We generalize this "error event" as the *outage region* in the product space of (X, W^N), and formally define the energy-distortion-outage tradeoff. We then show that in each scenario we consider, zero-delay communication with distortion outage achieves the same energy-distortion exponent as in the infinite-delay case discussed in the previous section.

5.4.1 Point-to-Point Transmission

Definition 27 *A triple (D, E, δ) is achievable for zero-delay point-to-point transmission with distortion outage if for any $\epsilon > 0$, there exist a large enough N, an encoder-decoder pair $(\phi_{1,N}, \psi_{1,N})$, and an outage region $\mathcal{O} \in \mathbb{R} \times \mathbb{R}^N$ such that*

$$\begin{aligned} \mathbb{E}\left[||U^N||^2\right] &\leq E + \epsilon \\ \Pr\left[\left(X, W^N\right) \in \mathcal{O}\right] &\leq \delta \\ \mathbb{E}\left[(X - \hat{X})^2 \middle| \mathcal{O}^c\right] &\leq D + \epsilon \, . \end{aligned}$$

Also denote by $D(E, \delta)$ the minimum possible distortion such that (D, E, δ) is achievable.

It should be clear that the region of all achievable $(D, E, 0)$ coincides with the set of achievable (D, E) as in Definition 21, and therefore this is a more general achievability concept.

We modify the definition of energy-distortion exponents accordingly as follows.

Definition 28 *An* energy-distortion exponent β *is achievable for zero-delay point-to-point transmission with distortion outage if*

$$\beta = \lim_{\delta \to 0} \lim_{E \to \infty} -\frac{1}{\gamma} \ln D(E, \delta)$$

where, as before, $\gamma = \frac{E}{\sigma_W^2}$.

In what follows we show that we can achieve $\beta = 1$ just as in the infinite-delay case (5.6).

Theorem 29 *$\beta = 1$ is an achievable energy-distortion exponent for zero-delay point-to-point transmission of a Gaussian source with distortion outage.*

Proof. We quantize the single random variable X with $N \gg 1$ levels and use orthogonal signaling to transmit the quantization index. At the receiver, we use maximum likelihood decoding, and classify incorrect decoding as the distortion outage event.

It is well-known [15] that the optimal high-resolution quantizer has the point density function $\lambda(x)$ given by

$$\lambda(x) = \frac{f_X(x)^{\frac{1}{3}}}{\int_{-\infty}^{\infty} f_X(x')^{\frac{1}{3}}\, dx'} \tag{5.22}$$

which, for $X \sim \mathcal{N}(0,1)$, boils down to a Gaussian with zero mean and variance 3. The resultant distortion can be approximated using the Bennett integral [15] as

$$\begin{aligned} D &\approx \frac{1}{12N^2} \int_{-\infty}^{\infty} \frac{f_X(x)}{\lambda(x)^2} dx \\ &= \frac{1}{12N^2} \left(\int_{-\infty}^{\infty} f_X\left(x'\right)^{\frac{1}{3}} dx' \right)^3 \\ &= \frac{\sqrt{3}\pi}{2N^2}\,. \end{aligned} \tag{5.23}$$

One can formalize this approximation by

$$D \leq \frac{\sqrt{3}\pi}{2N^2} + \epsilon \tag{5.24}$$

for arbitrarily small $\epsilon > 0$ and large enough N.

The quantized indices are mapped into orthogonal channel input vectors U^N such that

$$U_t = \begin{cases} \sqrt{E} & t = k(X) \\ 0 & t \neq k(X) \end{cases}$$

where $1 \leq k(X) \leq N$ is the integer quantization index. Note that $\left\|U^N\right\|^2 = E$ always. At the receiver end, upon receiving $V^N = U^N + W^N$, the decoder simply selects

$$\hat{K} = \arg\max_{1 \leq i \leq N} V_i$$

and then outputs

$$\hat{X} = r_{\hat{K}}$$

where r_k is the kth reconstruction level of the quantizer. Thus, the distortion outage event is given by

$$\mathcal{O} = \left\{ k(X) \neq \hat{K} \right\} .$$

Since the analysis of the probability of decoding error for orthogonal signaling can be found in the literature (for example, see [34, Section 6.6]), we include it only for convenience and defer it to Appendix A.4[2]. The analysis yields

$$\Pr[\mathcal{O}] \leq \begin{cases} 2e^{\left(\ln N - \frac{\gamma}{4}\right)} & \ln N < \frac{\gamma}{8} \\ 2e^{-\frac{1}{2}\left(\sqrt{\gamma} - \sqrt{2\ln N}\right)^2} & \frac{\gamma}{8} \leq \ln N \leq \frac{\gamma}{2} \end{cases} . \tag{5.25}$$

This upper bound is depicted in Fig. 5.5, for a given ENR γ.

Now, for a given $\delta > 0$ and ENR γ, we need to use the maximum possible number of quantization levels $N_{\max}(\gamma, \delta)$ such that $\Pr[\mathcal{O}] \leq \delta$ to minimize the distortion (see Fig. 5.5). It follows from (5.25) that

$$N_{\max}(\gamma, \delta) = \begin{cases} \frac{\delta}{2} e^{\frac{\gamma}{4}} & 4\ln\frac{2}{\delta} < \gamma < 8\ln\frac{2}{\delta} \\ e^{\frac{1}{2}\left(\sqrt{\gamma} - \sqrt{2\ln\frac{2}{\delta}}\right)^2} & \gamma \geq 8\ln\frac{2}{\delta} \end{cases} .$$

It then follows by choosing $N = N_{\max}(\gamma, \delta)$ in (5.24) that for any $\delta > 0$,

$$\mathbb{E}\left[||X - \hat{X}||^2 \middle| \mathcal{O}^c \right] \leq \frac{\sqrt{3}\pi}{2} e^{-\left(\sqrt{\gamma} - \sqrt{2\ln\frac{2}{\delta}}\right)^2} + \epsilon .$$

[2]We also refer the reader to [31] for a similar analysis.

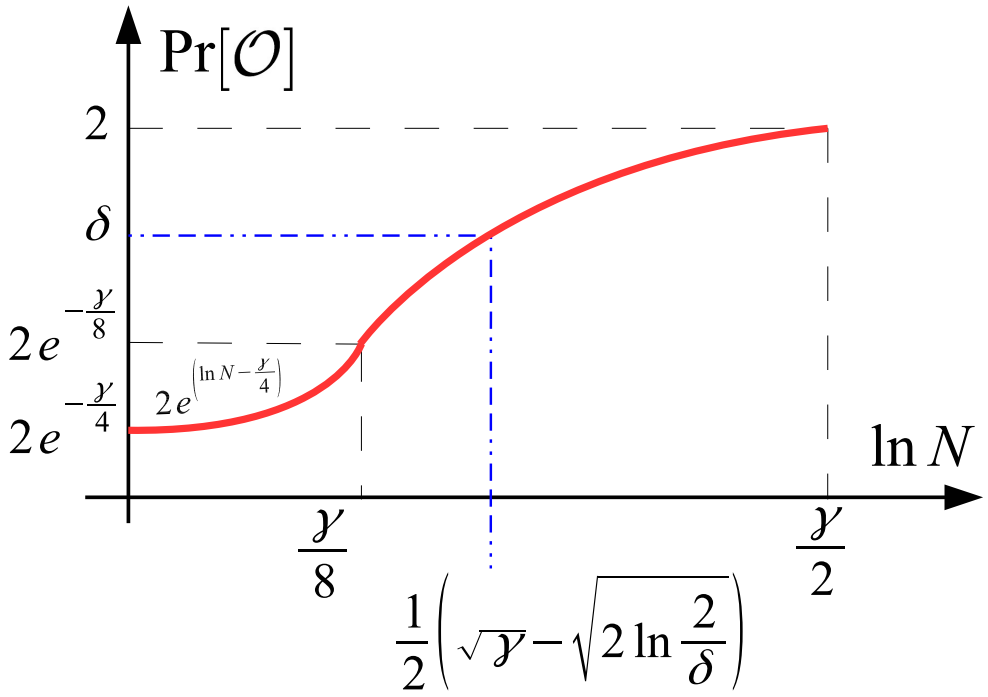

Figure 5.5: The upper bound on the probability of distortion outage as a function of $\ln N$ for a fixed ENR γ. The maximum allowed $\ln N$ to guarantee $\Pr[\mathcal{O}] \leq \delta$ when $\delta \geq 2e^{-\frac{\gamma}{8}}$ is also shown.

for arbitrarily small $\epsilon > 0$ and large enough[3] γ. Thus,

$$D(E,\delta) \leq \frac{\sqrt{3}\pi}{2} e^{-\left(\sqrt{\gamma}-\sqrt{2\ln\frac{2}{\delta}}\right)^2}$$

for any $\delta > 0$ and large enough E, and therefore

$$\lim_{\delta\to 0} \lim_{E\to\infty} -\frac{1}{\gamma} \ln D(E,\delta) \geq 1$$

finishing the proof. ■

[3]Large enough γ is necessary because (i) we need $\gamma \geq 8 \ln \frac{2}{\delta}$, and (ii) $N_{\max}(\gamma,\delta)$ must be large enough for the Bennett approximation (5.24) to be valid.

5.4.2 Broadcasting of a Single Gaussian Source

Definition 30 *A quadruple (D_1, D_2, E, δ) is achievable for zero-delay broadcasting of a single source with distortion outage if for any $\epsilon > 0$, there exist a large enough N, an encoder $\phi_{1,N}$, decoders $\psi_{1,N}^{(i)}$, and outage regions $\mathcal{O}_i \in \mathbb{R} \times \mathbb{R}^N$ for $i = 1, 2$ such that*

$$\begin{aligned} \mathbb{E}\left[||U^N||^2\right] &\leq E + \epsilon \\ \Pr\left[\left(X, W_i^N\right) \in \mathcal{O}_i\right] &\leq \delta \\ \mathbb{E}\left[(X - \hat{X}_i)^2 \middle| \mathcal{O}_i^c\right] &\leq D_i + \epsilon \, . \end{aligned}$$

Definition 31 *An* energy-distortion exponent pair (β_1, β_2) *is achievable for zero-delay broadcasting of a single source with distortion outage if there exist functions $D_1(E, \delta)$ and $D_2(E, \delta)$ such that $(D_1(E, \delta), D_2(E, \delta), E, \delta)$ is achievable for all $E > 0, \delta > 0$ and*

$$\lim_{\delta \to 0} \lim_{E \to \infty} -\frac{1}{\gamma_i} \ln D_i\left(E, \delta\right) = \beta_i$$

for $i = 1, 2$.

We are now ready to state and prove the following theorem.

Theorem 32 *Any pair $(\beta_1, \beta_2) \in \mathcal{B}_{\text{single}}$ is achievable for zero-delay broadcasting of a single Gaussian source with distortion outage.*

Proof. We quantize X with successive refinement with $N_1 \gg 1$ levels in the base layer and $N_2 \gg 1$ levels in the refinement layer. We then use orthogonal signaling and maximum likelihood decoding as in point-to-point transmission, with the modification that the transmission is done in two rounds: In the ith round, $i = 1, 2$, the channel is used N_i times to transmit the ith layer quantization index. Although both receivers have access to both

rounds, only the second receiver attempts to decode the refinement layer. We define $\mathcal{O}_1$ as the event that receiver 1 decodes the base layer index incorrectly, as in point-to-point transmission. On the other hand, we let $\mathcal{O}_2$ indicate that the second receiver incorrectly decodes either of the quantization indices.

It is clear from (5.24) that if the point density function $\lambda(x)$ for the base layer is chosen as in (5.22), there exist large enough N_1 such that

$$\mathbb{E}\left[(X-\hat{X}_1)^2\Big|\mathcal{O}_1^c\right] \leq \frac{\sqrt{3}\pi}{N_1^2}+\epsilon \tag{5.26}$$

for any $\epsilon > 0$. We claim that for large enough N_1 and N_2, one can simultaneously achieve (5.26) and

$$\mathbb{E}\left[(X-\hat{X}_2)^2\Big|\mathcal{O}_2^c\right] = \frac{\sqrt{3}\pi}{N_1^2 N_2^2}+\epsilon \tag{5.27}$$

for any $\epsilon > 0$. To that end, it suffices to recall that high-resolution quantization is equivalent to mapping the sample X onto the interval $[0,1]$ using $G(x) = \int_{-\infty}^{x}\lambda(z)dz$ followed by uniform quantization. Thus, not only does dividing the interval $[0,1]$ into N_1 equal-width intervals (followed by the inverse mapping G^{-1}) yield the optimal quantizer for the base layer, but further dividing each subinterval into N_2 equal-width intervals yield the optimal quantizer for the refinement layer. In other words, X is successively refineable in the high-resolution regime[4].

Let the two rounds of transmission expend energies αE and $(1-\alpha)E$, respectively,

[4]This argument is independent of the PDF of X. The notion of successive refineability here is not to be confused with the notion that appears in the literature. The latter deals with finite rates but infinite blocklengths, whereas we are interested in infinite rates and scalar coding.

for some $0 < \alpha < 1$. Then, as in the proof of Theorem 29, one can upper bound $\Pr[\mathcal{O}_1]$ as

$$\Pr[\mathcal{O}_1] \leq \begin{cases} 2e^{\left(\ln N_1 - \frac{\alpha\gamma_1}{4}\right)} & \ln N_1 < \frac{\alpha\gamma_1}{8} \\ 2e^{-\frac{1}{2}\left(\sqrt{\alpha\gamma_1} - \sqrt{2\ln N_1}\right)^2} & \frac{\alpha\gamma_1}{8} \leq \ln N_1 \leq \frac{\alpha\gamma_1}{2} \end{cases} . \tag{5.28}$$

Then, also as in the proof of Theorem 29, to guarantee $\Pr[\mathcal{O}_1] \leq \delta$, we need to satisfy $N_1 \leq N_{1,\max}(\alpha, \gamma_1, \delta)$, where

$$N_{1,\max}(\alpha, \gamma_1, \delta) = \begin{cases} \frac{\delta}{2} e^{\frac{\alpha\gamma_1}{4}} & 4\ln\frac{2}{\delta} < \alpha\gamma_1 < 8\ln\frac{2}{\delta} \\ e^{\frac{1}{2}\left(\sqrt{\alpha\gamma_1} - \sqrt{2\ln\frac{2}{\delta}}\right)^2} & \alpha\gamma_1 \geq 8\ln\frac{2}{\delta} \end{cases} . \tag{5.29}$$

Combining (5.26) and (5.29) then yields for any $\epsilon > 0$, $\delta > 0$, and large enough E that

$$\mathbb{E}\left[(X - \hat{X}_1)^2 \middle| \mathcal{O}_1^c\right] \leq D_1(E, \delta) + \epsilon$$

with

$$D_1(E, \delta) = \frac{\sqrt{3}\pi}{2} e^{-\left(\sqrt{\alpha\gamma_1} - \sqrt{2\ln\frac{2}{\delta}}\right)^2} . \tag{5.30}$$

At the second receiver, one can use the union bound to write

$$\Pr[\mathcal{O}_2] \leq P_{e,1} + P_{e_2}$$

where $P_{e,1}$ and $P_{e,2}$ are the probabilities of the second receiver incorrectly decoding the base and refinement layer index incorrectly, respectively. Since the second channel is less noisy, it is clear that

$$P_{e,1} < \Pr[\mathcal{O}_1] \leq \delta .$$

We can in fact tighten this upper bound by first translating (5.28) for the second receiver as

$$P_{e,1} \leq \begin{cases} 2e^{\left(\ln N_1 - \frac{\alpha\gamma_2}{4}\right)} & \ln N_1 < \frac{\alpha\gamma_2}{8} \\ 2e^{-\frac{1}{2}\left(\sqrt{\alpha\gamma_2} - \sqrt{2\ln N_1}\right)^2} & \frac{\alpha\gamma_2}{8} \leq \ln N_1 \leq \frac{\alpha\gamma_2}{2} \end{cases} \tag{5.31}$$

and then assuming $\alpha\gamma_1 \geq 8 \ln \frac{2}{\delta}$ without loss of generality (because we will eventually let $E \to \infty$), using (5.29) to show both

$$\begin{aligned} 2e^{\left(\ln N_1 - \frac{\alpha\gamma_2}{4}\right)} &\leq 2e^{\left(\frac{1}{2}\left(\sqrt{\alpha\gamma_1} - \sqrt{2\ln\frac{2}{\delta}}\right)^2 - \frac{g\alpha\gamma_1}{4}\right)} \\ &\leq 2e^{\left(\frac{1}{2}\left(\sqrt{\alpha\gamma_1} - \sqrt{2\ln\frac{2}{\delta}}\right)^2 - 2g\ln\frac{2}{\delta}\right)} \\ &\leq 2e^{-2g\ln\frac{2}{\delta}} \\ &= 2\left(\frac{\delta}{2}\right)^{2g} \end{aligned} \tag{5.32}$$

and

$$\begin{aligned} 2e^{-\frac{1}{2}\left(\sqrt{\alpha\gamma_2} - \sqrt{2\ln N_1}\right)^2} &\leq 2e^{-\frac{1}{2}\left((\sqrt{g}-1)\sqrt{\alpha\gamma_1} + \sqrt{2\ln\frac{2}{\delta}}\right)^2} \\ &\leq 2e^{-\frac{1}{2}\left(2(\sqrt{g}-1)\sqrt{2\ln\frac{2}{\delta}} + \sqrt{2\ln\frac{2}{\delta}}\right)^2} \\ &\leq 2e^{-\left(2\sqrt{g}-1\right)^2\ln\frac{2}{\delta}} \\ &\leq 2\left(\frac{\delta}{2}\right)^{g}. \end{aligned} \tag{5.33}$$

Bringing together (5.31)-(5.33), we obtain

$$P_{e,1} \leq 2\left(\frac{\delta}{2}\right)^{g}. \tag{5.34}$$

Letting $\delta' = \delta - 2\left(\frac{\delta}{2}\right)^g$, we can once again use the analysis in Theorem 29 to conclude that

$$P_{e,2} \leq \begin{cases} 2e^{\left(\ln N_2 - \frac{(1-\alpha)\gamma_2}{4}\right)} & \ln N_2 < \frac{(1-\alpha)\gamma_2}{8} \\ 2e^{-\frac{1}{2}\left(\sqrt{(1-\alpha)\gamma_2} - \sqrt{2\ln N_2}\right)^2} & \frac{(1-\alpha)\gamma_2}{8} \leq \ln N_2 \leq \frac{(1-\alpha)\gamma_2}{2} \end{cases} \tag{5.35}$$

and that to guarantee $\Pr[\mathcal{O}_2] \leq \delta$, it suffices to choose $N_2 \leq N_{2,\max}(g, \alpha, \gamma_1, \delta)$, where

$$N_{2,\max}(g,\alpha,\gamma_1,\delta) = \begin{cases} \frac{\delta'}{2}e^{\frac{g(1-\alpha)\gamma_1}{4}} & 4\ln\frac{2}{\delta'} < g(1-\alpha)\gamma_1 < 8\ln\frac{2}{\delta'} \\ e^{\frac{1}{2}\left(\sqrt{g(1-\alpha)\gamma_1} - \sqrt{2\ln\frac{2}{\delta'}}\right)^2} & g(1-\alpha)\gamma_1 \geq 8\ln\frac{2}{\delta'} \end{cases}. \tag{5.36}$$

Combining (5.27), (5.29), and (5.36) then yields for any $\epsilon > 0$, $\delta > 0$, and large enough E that

$$\mathbb{E}\left[(X - \hat{X})^2 \middle| \mathcal{O}_2^c\right] \leq D_2(E, \delta) + \epsilon$$

with

$$D_2(E,\delta) = \frac{\sqrt{3}\pi}{2} e^{-\left(\sqrt{\alpha\gamma_1} - \sqrt{2\ln\frac{2}{\delta}}\right)^2} e^{-\left(\sqrt{g(1-\alpha)\gamma_1} - \sqrt{2\ln\frac{2}{\delta'}}\right)^2} . \tag{5.37}$$

The proof is complete by observing that for any $\delta > 0$,

$$\lim_{E\to\infty} -\frac{1}{\gamma_1} \ln D_1(E,\delta) = \alpha$$

and

$$\lim_{E\to\infty} -\frac{1}{\gamma_2} \ln D_2(E,\delta) = \frac{\alpha}{g} + 1 - \alpha .$$

■

5.4.3 Broadcasting of a Bivariate Gaussian Source

Definition 33 *A quadruple (D_1, D_2, E, δ) is achievable for zero-delay broadcasting of bivariate sources with distortion outage if for any $\epsilon > 0$, there exist a large enough N, an encoder $\phi_{1,N}$, decoders $\psi_{1,N}^{(i)}$, and outage regions $\mathcal{O}_i \in \mathbb{R} \times \mathbb{R}^N$ for $i = 1, 2$ such that*

$$\begin{aligned} \mathbb{E}\left[||U^N||^2\right] &\leq E + \epsilon \\ \Pr\left[\left(X_1, X_2, W_i^N\right) \in \mathcal{O}_i\right] &\leq \delta \\ \mathbb{E}\left[(X_i - \hat{X}_i)^2 \middle| \mathcal{O}_i^c\right] &\leq D_i + \epsilon . \end{aligned}$$

The definition of achievable energy-distortion exponent pairs is exactly as in Definiton 31.

Just as in the proof of Theorem 26, separately encoding the two sources and splitting the available energy E into αE and $(1-\alpha)E$ to transmit the quantization indices using orthogonal signaling is a sufficient strategy to achieve the same energy-distortion exponents in $\mathcal{B}_{\text{bivariate}}$ as stated in the next theorem.

Theorem 34 *Any pair $(\beta_1, \beta_2) \in \mathcal{B}_{\text{bivariate}}$ is achievable for zero-delay broadcasting of bivariate Gaussian sources with distortion outage.*

Proof. We provide only a sketch of the proof as it is straightforward. Using the same technique as in the proof of Theorem 32, it is possible to show that for any $\epsilon > 0$, $\delta > 0$, and large enough E,

$$\begin{aligned} \mathbb{E}\left[||U^N||^2\right] &\leq E + \epsilon \\ \Pr\left[\left(X_1, X_2, W_i^N\right) \in \mathcal{O}_i\right] &\leq \delta \\ \mathbb{E}\left[(X_i - \hat{X}_i)^2 \middle| \mathcal{O}_i^c\right] &\leq D_i(E,\delta) + \epsilon \end{aligned}$$

for $i = 1, 2$, can be simultaneously satisfied, where

$$\begin{aligned} D_1(E,\delta) &= \frac{\sqrt{3}\pi}{2} e^{-\left(\sqrt{\alpha\gamma_1} - \sqrt{2\ln\frac{2}{\delta}}\right)^2} \\ D_2(E,\delta) &= \frac{\sqrt{3}\pi}{2} e^{-\left(\sqrt{(1-\alpha)\gamma_2} - \sqrt{2\ln\frac{2}{\delta}}\right)^2}. \end{aligned}$$

Therefore for any $\delta > 0$,

$$\lim_{E\to\infty} -\frac{1}{\gamma_1} \ln D_1(E,\delta) = \alpha$$

and

$$\lim_{E\to\infty} -\frac{1}{\gamma_2} \ln D_2(E,\delta) = 1 - \alpha$$

and the proof is complete. ■

Bibliography

[1] A. Abou Saleh, F. Alajaji, W.-Y. Chan, "Source-interference recovery over broadcast channels: asymptotic bounds and analog codes," *IEEE Trans. Commun.*, vol. 64, no. 8, pp. 3406–3418, Aug. 2016.

[2] I. E. Aguerri and D. Gündüz, "Joint Source-Channel Coding with Time-Varying Channel and Side-Information," *arxiv.org*

[3] E. Akyol, K. Rose, K. Viswanatha, and T. Ramstad, "On zero-delay source-channel coding, *IEEE Transactions on Information Theory*, vol. 60, no. 12, pp. 7473–7489, Dec. 2014

[4] H. Behroozi, F. Alajaji, and T. Linder, "Hybrid digital-analog joint source-channel coding for broadcasting correlated Gaussian sources," *presented at the IEEE Int. Symp. Inf. Theory*, Seoul, Korea, Jun. 2009.

[5] H. Behroozi, F. Alajaji, and T. Linder, "Broadcasting correlated Gaussian sources with bandwidth expansion," *presented at the IEEE Inf. Theory Workshop,* Taormina, Italy, Oct. 2009.

[6] H. Behroozi, F. Alajaji, and T. Linder, "On the performance of hybrid digital-analog coding for broadcasting correlated Gaussian sources," *IEEE Trans. Commun.,* vol. 59, no. 12, pp. 3335–3342, Dec. 2011.

[7] S. Bross, A. Lapidoth, and S. Tinguely, "Superimposed coded and uncoded transmissions of a Gaussian source over the Gaussian channel," in *Proc. IEEE Int Symp. Inf. Theory (ISIT 2006)*, Seattle, WA, Jul. 2006.

[8] S. Bross, A. Lapidoth, and S. Tinguely, "Broadcasting correlated Gaussians," *IEEE Trans. Inf. Theory*, vol. 56, no. 7, pp. 3057–3068, Jul. 2010.

[9] X. Chen and E. Tuncel, "Zero-delay joint source-channel coding using hybrid digital-analog schemes in the Wyner-Ziv setting," *IEEE Transactions on Communications*, vol. 62, no. 2, pp. 726–735, Feb. 2014.

[10] M. H. M. Costa, "Writing on dirty paper," *IEEE Trans. Inf. Theory*, vol. 29, no. 3, pp. 439–441, May 1983.

[11] T. M. Cover, "Broadcast channels," *IEEE Trans. Inf. Theory*, vol. 18, no. 1, pp. 2–14, Jan. 1972.

[12] A. El Gamal and Y. H. Kim, *Network Information Theory.* Cambridge University Press, 2011

[13] Y. Gao and E. Tuncel, "New hybrid digital/analog schemes for transmis- sion of a Gaussian source over a Gaussian channel," *IEEE Trans. Inf. Theory*, (56)12:6014–6019, Dec. 2010.

[14] Y. Gao and E. Tuncel, "Separate source–channel coding for transmitting correlated Gaussian sources over degraded broadcast channels," *IEEE Trans. Inf. Theory*, vol. 59, no. 6, pp. 3619–3634, Jun. 2013.

[15] A. Gersho and R. M. Gray, *Vector Quantization and Signal Compression.* Kluwer Academic Publishers, Boston, MA, 1992.

[16] F. Hekland, P. A. Floor, and T. A. Ramstad, "Shannon-Kotel'nikov mappings in joint source-channel coding," *IEEE Transactions on Communications,* vol. 57, no. 1, pp. 94–105, Jan. 2009.

[17] A. Jain, D. Gündüz, S. R. Kulkarni, H. V. Poor, and S. Verdú, "Energy-distortion tradeoffs in Gaussian joint source-channel coding problems," *IEEE Transactions on Information Theory*, vol. 58, no. 5, pp. 3153–3168, May 2012.

[18] N. Jiang, Y. Yang, A. Host-Madsen, and Z. Xiong, "On the minimum energy of sending correlated sources over the Gaussian MAC," *IEEE Transactions on Information Theory*, vol. 60, no. 10, pp. 6254–6275, Aug 2014.

[19] K. Khezeli and J. Chen, "A source-channel separation theorem with application to the source broadcast problem," *IEEE Transactions on Information Theory*, vol. 62, no. 4, pp. 1764–1781, Apr. 2016.

[20] E. Köken and E. Tuncel, "Gaussian HDA coding with bandwidth expansion and side information at the decoder," in *Proc. IEEE Int. Symposium on Information Theory*, 2013

[21] E. Köken and E. Tuncel, "On robustness of hybrid digital/analog source/channel coding with bandwidth mismatch," *Proc. IEEE Int. Symposium on Information Theory*, 2014

[22] E. Köken and E. Tuncel, "On robustness of hybrid digital/analog source/channel coding with bandwidth mismatch," *IEEE Transaction on Information Theory*, vol. 61, no. 9, pp. 4968–4983, Sep. 2015.

[23] E. Köken, E. Tuncel, and D. Gündüz, "On the distortion-energy tradeoff for zero-delay transmission of a Gaussian source over the AWGN channel," *ITW Jerusalem, Israel 2015*

[24] E. Köken, E. Tuncel, and D. Gündüz, "On the asymptotic distortion-energy tradeoff for zero-delay transmission of a Gaussian source over the AWGN channels," *Proc. IEEE Int Symp. Inf. Theory (ISIT 2015)*, Hong Kong, South Korea, Jun. 2015.

[25] N. Merhav and S. Shamai, "On joint source-channel coding for the Wyner-Ziv source and the Gel'fand-Pinsker channel," *IEEE Trans. Inf. Theory*, vol. 49, no.11 pp. 2844-2855, Nov. 2003

[26] U. Mittal and N. Phamdo, "Hybrid digital-analog (HDA) joint source-channel codes for broadcasting and robust communications," *IEEE Tran. Info. Theory*, vol. 48, pp. 1082-1102, May 2002.

[27] R. R. Mohassel, A. S. Fung, F. Mohammadi, and K. Raahemifar, "A survey on advanced metering infrastructure and its application in smart grids," *IEEE 27th Canadian Conference on Electrical and Computer Engineering*, Toronto, ON, May 2014, pp. 1–8.

[28] K. Narayanan, G. Caire, and M. Wilson, "Duality between broadcasting with bandwidth expansion and bandwidth compression", *ISIT 2007 Nice,France*

[29] J. Nayak and E. Tuncel, "Successive coding of correlated sources," *IEEE Trans. Inf. Theory*, vol. 55, no. 9, pp. 4286-4298, Sep. 2009.

[30] J. Nayak, E. Tuncel, and D. Gündüz, " Wyner-Ziv coding over broadcast channels: digital schemes," *IEEE Trans. Inf. Theory*, (56)4:1782-1799, April 2010.

[31] Y. Polyansky, V. Poor, and S. Verdu, "Minimum energy to send k bits through the Gaussian channel with and without feedback," *IEEE Transactions on Information Theory*, vol. 51, no. 8, pp. 4880–4922, Aug. 2011.

[32] V. M. Prabhakaran, R. Puri, and K. Ramchandran, "Hybrid digital-analog codes for source-channel broadcast of Gaussian sources over Gaussian channels," *IEEE Trans. Inf. Theory*, vol. IT-23, no. 1, pp. 60–64, Jan. 2011.

[33] V. M. Prabhakaran, R. Puri, and K. Ramchandran, "Hybrid Digital-Analog strategies for Source-Channel Broadcast" *Allerton Conference on CCC*, 2005

[34] J. G. Proakis, M. Salehi, *Digital communications Wiley 2008*

[35] Z. Reznic, M. Feder, and R. Zamir, "Distortion bounds for broadcasting with bandwidth expansion," *IEEE Transactions on Information Theory*, vol. 52, no. 8, pp. 3778–3788, Aug. 2006.

[36] S. Shamai, S. Verd, and R. Zamir, "Systematic lossy source/channel coding," *IEEE Trans. Inf. Theory*, vol. 52, pp. 564-579, Mar. 1998.

[37] C. Shannon, "A mathematical theory of communication," *Bell Sys. Tech. Journal*, vol. 27, pp. 379–423, 1948.

[38] L. Song, J. Chen, and C. Tian, "Broadcasting correlated vector Gaussians," *IEEE Trans. Inf. Theory*, vol. 61, pp. 2465–2477, May 2015.

[39] R. Soundararajan and S. Vishwanath, "Hybrid coding for Gaussian broadcast channels with Gaussian sources," *Proc. IEEE Int. Symp. Inf. Theory (ISIT 2009)*, Seoul, Korea, June 2009.

[40] C. Tian and S. Shamai, "A unified coding scheme for hybrid transmission of Gaussian source over Gaussian channel," in *Proc. ISIT*, Toronto, Canada, Jul. 2008, pp. 1548-1552.

[41] C. Tian, S. Diggavi, and S. Shamai, "The achievable distortion region of sending a bivariate Gaussian source on the Gaussian broadcast channel," *IEEE Trans. Inf. Theory*, vol. 57, no. 10, pp. 6419–6427, Oct. 2010.

[42] C. Tian, S. Shamai, "Sending Gaussian source on bandwidth-mismatched Gaussian source on bandwidth-bismatched Gaussian channel with improved robustness", *IEEE ICC* 2011

[43] C. Tian, J. Chen, S. Diggavi, and S. Shamai, "Matched multiuser Gaussian source-channel com- munications via uncoded schemes," *in Proc. IEEE 2015 ISIT*, June 2015, pp. 476–480.

[44] N. Wernersson, M. Skoglund, and T. Ramstad, "Polynomial Based Analog Source-Channel Codes," *IEEE Transactions on Communications*, vol. 57, no. 9, pp. 2600–2606, Sep. 2009.

[45] M. Wilson, K. Narayanan, and G. Caire, "Joint source channel coding with side information using hybrid digital analog codes," *IEEE Trans. Information Theory*, vol. 56, no. 10, pp. 4922-4940, Oct. 2010

Appendix A

Proofs

A.1 Proof of Theorem 15

The source codebook of size 2^{nR_1} used to quantize X_a^n is generated in i.i.d. fashion according to the Gaussian random variable $\tilde{X}_a$ where the relation between $\tilde{X}_a$ and X_a is defined by the backward test channel $X_a = \tilde{X}_a + Q$ with $Q \sim \mathcal{N}\left(0, 2^{-2R_1}\mathbb{E}\left\{X_a^2\right\}\right)$, $\tilde{X}_a \perp Q$, and also such that $\tilde{X}_a - X_a - (X_1, X_2)$ forms a Markov chain. Using standard arguments (i.e., Markov lemma), it can be shown that the selected source codeword at the encoder $\tilde{X}_a^n(M_1)$ that is jointly typical with X_a^n will also be jointly typical with (X_1^n, X_2^n, X_a^n). Using

$$\begin{aligned}\mathbb{E}\{X_a^2\} &= \alpha^2 \\ \mathbb{E}\{X_1 X_a\} &= \theta + \rho\bar{\theta} \\ \mathbb{E}\{X_2 X_a\} &= \rho\theta + \bar{\theta}\,,\end{aligned}$$

it follows that

$$\begin{aligned}\mathbb{E}\{\tilde{X}_a^2\} &= \left(1 - 2^{-2R_1}\right)\alpha^2 \\ \mathbb{E}\{X_1 \tilde{X}_a\} &= \left(1 - 2^{-2R_1}\right)\left(\theta + \rho\bar{\theta}\right) \\ \mathbb{E}\{X_2 \tilde{X}_a\} &= \left(1 - 2^{-2R_1}\right)\left(\rho\theta + \bar{\theta}\right)\,.\end{aligned}$$

Since the first receiver uses only the source codeword $\tilde{X}_a^n(M_1)$, it incurs the distortion

$$\begin{aligned}D_1 &= 1 - \frac{\mathbb{E}\{X_1 \tilde{X}_a\}^2}{\mathbb{E}\{\tilde{X}_a^2\}} \\ &= 1 - \frac{\left(\theta + \rho\bar{\theta}\right)^2\left(1 - 2^{-2R_1}\right)}{\alpha^2}. \qquad \text{(A.1)}\end{aligned}$$

If the second receiver used only $\tilde{X}_a^n(M_1)$ to reconstruct X_2^n, it would incur the distortion

$$\begin{aligned}D_2^\star &= 1 - \frac{\mathbb{E}\{X_2 \tilde{X}_a\}^2}{\mathbb{E}\{\tilde{X}_a^2\}} \\ &= 1 - \frac{\left(\rho\theta + \bar{\theta}\right)^2\left(1 - 2^{-2R_1}\right)}{\alpha^2}\,. \qquad \text{(A.2)}\end{aligned}$$

Therefore, using $\tilde{X}_a^n(M_1)$ as side information, the Wyner-Ziv coding of X_2^n with rate R_2 then yields

$$D_2 = D_2^\star 2^{-2R_2}. \tag{A.3}$$

Using superposition coding over the broadcast channel, the messages M_1 and M_2 can be decoded correctly if the source coding rates are at most

$$\begin{aligned} R_1 &= \frac{\kappa}{2}\log\left(\frac{1+\gamma_1}{1+\bar{\eta}\gamma_1}\right) \\ R_2 &= \frac{\kappa}{2}\log\left(1+\eta\gamma_2\right) \end{aligned}$$

with some $0 \le \eta \le 1$. Substituting R_1 and R_2 above into (A.1), (A.2), and (A.3) yields (4.12), (4.14), and (4.13), respectively, thereby finishing the proof.

A.2 Proof of Lemma 16

The source coding region in Lemma 2 of [14] can be rearranged and combined with the capacity region of Gaussian broadcast channels [11] to conclude that (D_1, D_2) is achievable with separate source channel coding (i.e., the GT scheme) if and only if there exist $0 \le \eta \le 1$ and $\nu \in [\rho, \nu^\star]$ with $\nu^\star = \min\left(\frac{1}{\rho}, \frac{\rho}{1-D_1}, \sqrt{\frac{1-D_2}{1-D_1}}\right)$ such that

$$D_1 \ge 1 - \frac{1-\rho^2}{1-\rho^2+(\nu-\rho)^2}\left\{1-\left(\frac{1+\bar{\eta}\gamma_1}{1+\gamma_1}\right)^\kappa\right\} \tag{A.4}$$

$$D_2 \ge \frac{1-\nu^2(1-D_1)}{(1+\bar{\eta}\gamma_2)^\kappa}\,. \tag{A.5}$$

Now, denote by $(D_1(\theta), D_2(\theta))$ the distortion pairs achieved by the alternative separate coding scheme given in (4.12)-(4.14). We show that for each (D_1, D_2) achieved by the GT scheme, an appropriate θ can be chosen such that $D_1(\theta) \le D_1$ and $D_2(\theta) \le D_2$. Towards that end, define

$$g(\nu) = \frac{1-\nu\rho}{(1+\nu)(1-\rho)}$$

and observe that $g(\nu)$ is a decreasing function with $g(\rho) = 1$ and $g(\frac{1}{\rho}) = 0$, implying that $0 \le g(\nu) \le 1$ for all $\nu \in [\rho, \nu^\star]$. Choosing $\theta = g(\nu)$, we immediately obtain

$$\frac{(\theta+\rho\bar{\theta})^2}{1-2\theta\bar{\theta}(1-\rho)} = \frac{1-\rho^2}{1-\rho^2+(\nu-\rho)^2} \tag{A.6}$$

$$\frac{(\rho\theta+\bar{\theta})^2}{1-2\theta\bar{\theta}(1-\rho)} = \frac{\nu^2(1-\rho^2)}{1-\rho^2+(\nu-\rho)^2}\,. \tag{A.7}$$

Using (4.12) and (A.6), (A.4) can then be rewritten as

$$D_1 \ge D_1(\theta)\,.$$

Similarly, using (A.7) together with (4.13), (4.14) and (A.5), we obtain

$$\begin{aligned} D_2 &\geq \frac{1-\nu^2(1-D_1)}{(1+\overline{\eta}\gamma_2)^{\kappa}} \\ &\geq \frac{1-\nu^2(1-D_1(\theta))}{(1+\overline{\eta}\gamma_2)^{\kappa}} \\ &= D_2(\theta)\ . \end{aligned}$$

Thus, the alternative separate source channel coding scheme can achieve a (D_1, D_2) region *at least* as large as the GT scheme. On the other hand, since the GT scheme is optimal, equivalence of the two schemes follow immediately.

A.3 Optimality when $\kappa = 1$

The hybrid coding scheme proposed in Tian *et al.* [41, Eqs. (39) and (45)] achieves, under the regime where it is optimal, i.e., $P(1-\rho) > 2\rho\sigma^2_{W_2}$, the distortion pairs

$$\tilde{D}_1 = \frac{\phi^2\left(1-\rho^2\right)+\sigma^2_{W_1}}{P+\sigma^2_{W_1}} \tag{A.8}$$

$$\tilde{D}_2 = \frac{\left(1-\rho^2\right)\sigma^2_{W_2}}{\left(1-\rho^2\right)\phi^2+\sigma^2_{W_2}} \tag{A.9}$$

for all

$$\frac{\left(1-\rho^2\right)P-2\rho^2\sigma^2_{W_2}-\sqrt{K}}{2\left(1-\rho^2\right)} \leq \phi^2 \leq \frac{\left(1-\rho^2\right)P-2\rho^2\sigma^2_{W_2}+\sqrt{K}}{2\left(1-\rho^2\right)} \tag{A.10}$$

with

$$K = \left(P^2 - \left(P+2\sigma^2_{W_2}\right)^2\rho^2\right)\left(1-\rho^2\right)\ .$$

Essentially we will need to show that there exists a pair of coding parameters (θ, λ) for every ϕ^2 satisfying (A.10) such that $0 \leq \theta, \lambda \leq 1$ and our scheme achieves $D_1 = \tilde{D}_1$ and $D_2 = \tilde{D}_2$ for the same source/channel parameters ρ, P, $\sigma^2_{W_1}$, and $\sigma^2_{W_2}$.

Comparing (4.41) and (A.8), for $D_1 = \tilde{D}_1$ to be satisfied, we need to set (θ, λ) so that

$$P\left[1-\frac{\lambda}{\alpha^2}\left(\theta+\rho\bar{\theta}\right)^2\right] = \phi^2\left(1-\rho^2\right) \tag{A.11}$$

for any ϕ^2 satisfying (A.10). Substituting (A.11) into (A.9) and comparing with (4.42) yields that (θ, λ) must also satisfy

$$\left[P\left(1-\frac{\lambda}{\alpha^2}\left(\rho\theta+\bar{\theta}\right)^2\right)+\sigma^2_{W_2}\right]\left[P\left(1-\frac{\lambda}{\alpha^2}\left(\theta+\rho\bar{\theta}\right)^2\right)+\sigma^2_{W_2}\right] = \left(1-\rho^2\right)\left(P+\sigma^2_{W_2}\right)\left(\bar{\lambda}P+\sigma^2_{W_2}\right)\ . \tag{A.12}$$

After some algebra, it can be seen that (A.12), which is quadratic in λ, has a repeated solution at

$$\lambda = \lambda(\theta) = \frac{\rho\left(P+\sigma^2_{W_2}\right)\alpha^2}{P\left(\rho\theta+\bar{\theta}\right)\left(\theta+\rho\bar{\theta}\right)}\ . \tag{A.13}$$

Substituting (A.13) in (A.11) then yields

$$\theta = \theta(\phi^2) = \frac{P - \phi^2\left(1-\rho^2\right) - \rho^2\left(P+\sigma_{W_2}^2\right)}{(1-\rho)\left(\rho\left(P+\sigma_{W_2}^2\right) + P - \phi^2\left(1-\rho^2\right)\right)} \,. \tag{A.14}$$

It then suffices to show $0 \le \theta(\phi^2) \le 1$ and $0 \le \lambda(\theta(\phi^2)) \le 1$ for all ϕ^2 satisfying (A.10).

Now, observe that $\theta(\phi^2)$ is decreasing in ϕ^2, and therefore substituting the boundary values for ϕ^2 in (A.10), we can write

$$\frac{1}{2} - \frac{1}{2}\sqrt{M} \le \theta(\phi^2) \le \frac{1}{2} + \frac{1}{2}\sqrt{M} \tag{A.15}$$

for all valid ϕ^2, with

$$M = \frac{(1+\rho)\left(P\left(1-\rho\right) - 2\rho\sigma_{W_2}^2\right)}{(1-\rho)\left(P\left(1+\rho\right) + 2\rho\sigma_{W_2}^2\right)} \,.$$

Note that due to $P(1-\rho) > 2\rho\sigma_{W_2}^2$, we have $M > 0$. It is also easy to see $M \le 1$, and therefore we conclude $0 \le \theta(\phi^2) \le 1$.

Finally, rewriting (A.13) as

$$\lambda(\theta) = \frac{\rho\left(P+\sigma_{W_2}^2\right)\left[1 - 2(1-\rho)\theta\bar{\theta}\right]}{P\left(\rho + (1-\rho)^2\theta\bar{\theta}\right)} \tag{A.16}$$

we observe that λ is a decreasing function of $\theta\bar{\theta}$. But, according to (A.15), we also have

$$\begin{aligned} \theta(\phi^2)\bar{\theta}(\phi^2) &\ge \frac{1-M}{4} \\ &= \frac{\rho\sigma_{W_2}^2}{(1-\rho)\left(P\left(1+\rho\right) + 2\rho\sigma_{W_2}^2\right)} \end{aligned}$$

which, using (A.16), yields

$$\lambda(\theta(\phi^2)) \le 1$$

with equality satisfied if and only if ϕ^2 is at either end of the interval in (A.10). Since $\lambda(\theta) \ge 0$ follows immediately from (A.13), this concludes the proof.

A.4 Analysis of the Probability of Decoding Error

Without loss of generality, we assume that the first codeword is sent. Using the normalized noise vector $Z^N = \frac{W^N}{\sigma_W}$, the probability of erroneous decoding for fixed N and E becomes

$$\begin{aligned} \Pr[\mathcal{O}] &= 1 - \int_{-\infty}^{\infty} f_Z\left(z_1\right) \Pr\left[\max_{2\le i\le N}\left\{Z_i\right\} < \sqrt{\gamma} + z_1\right] dz_1 \\ &= 1 - \int_{-\infty}^{\infty} f_Z\left(z_1\right) \prod_{i=2}^{N} \Pr\left[Z_i < \sqrt{\gamma} + z_1\right] dz_1 \\ &= \int_{-\infty}^{\infty} f_Z\left(z_1\right) \left\{1 - \left(1 - Q\left(\sqrt{\gamma} + z_1\right)\right)^{N-1}\right\} dz_1 \,. \end{aligned}$$

Here, we use the standard definition of the Q-function as

$$Q(x) = \frac{1}{\sqrt{2\pi}} \int_x^\infty e^{-\frac{s^2}{2}} ds.$$

It is well-known that the Chernoff bound on the Q-function is given by

$$Q(x) \leq e^{-\frac{x^2}{2}} \tag{A.17}$$

for all $x \geq 0$. Although there are other established bounds that are tighter than (A.17), the Chernoff bound will suffice for our analysis.

From this point on, we will assume that $\gamma \geq 2 \ln N$. Then defining

$$\alpha = \sqrt{2 \ln N} - \sqrt{\gamma} \tag{A.18}$$

which is always non-positive, we write

$$\Pr[\mathcal{O}] = P_{\mathcal{O},1} + P_{\mathcal{O},2}$$

with

$$\begin{aligned} P_{\mathcal{O},1} &= \int_{-\infty}^{\alpha} f_Z(z_1) \left\{ 1 - (1 - Q(\sqrt{\gamma} + z_1))^{N-1} \right\} dz_1 \\ P_{\mathcal{O},2} &= \int_{\alpha}^{\infty} f_Z(z_1) \left\{ 1 - (1 - Q(\sqrt{\gamma} + z_1))^{N-1} \right\} dz_1 . \end{aligned}$$

We then bound $P_{\mathcal{O},1}$ as

$$\begin{aligned} P_{\mathcal{O},1} &\leq \int_{-\infty}^{\alpha} f_Z(z_1) \, dz_1 \\ &= \frac{1}{\sqrt{2\pi}} \int_{-\infty}^{\alpha} e^{-\frac{z_1^2}{2}} dz_1 \\ &= 1 - Q(\alpha) \\ &= Q(-\alpha) \\ &\leq e^{-\frac{\alpha^2}{2}} \end{aligned} \tag{A.19}$$

where the last inequality follows from (A.17) and the fact that $\alpha \leq 0$. Also, since it follows from (A.18) that $\alpha > -\sqrt{\gamma}$, we have for all $z_1 \geq \alpha$ that

$$\begin{aligned} 1 - (1 - Q(\sqrt{\gamma} + z_1))^{N-1} &\leq (N-1) Q(\sqrt{\gamma} + z_1) \\ &\leq N e^{-\frac{(\sqrt{\gamma} + z_1)^2}{2}} \end{aligned}$$

again using (A.17). Therefore,

$$\begin{aligned} P_{\mathcal{O},2} &\leq N\int_{\alpha}^{\infty} f_Z(z_1)\, e^{-\frac{(\sqrt{\gamma}+z_1)^2}{2}} dz \\ &= \frac{N}{\sqrt{2\pi}} e^{-\frac{\gamma}{4}} \int_{\alpha+\sqrt{\frac{\gamma}{4}}}^{\infty} e^{-s^2} ds \\ &= \frac{N}{2\sqrt{\pi}} e^{-\frac{\gamma}{4}} Q\left(\sqrt{2}\left(\alpha+\sqrt{\frac{\gamma}{4}}\right)\right) \\ &= \begin{cases} \frac{N}{2\sqrt{\pi}} e^{-\frac{\gamma}{4}-\left(\alpha+\sqrt{\frac{\gamma}{4}}\right)^2} & \alpha \geq -\sqrt{\frac{\gamma}{4}} \\ \frac{N}{2\sqrt{\pi}} e^{-\frac{\gamma}{4}} & \alpha < -\sqrt{\frac{\gamma}{4}} \end{cases} \end{aligned} \tag{A.20}$$

After some algebraic manipulations, it can be shown using (A.18) that

$$N e^{-\frac{\gamma}{4}-\left(\alpha+\sqrt{\frac{\gamma}{4}}\right)^2} = e^{-\frac{\alpha^2}{2}}. \tag{A.21}$$

Finally, bringing (A.18)-(A.21) together, we find for all $e^{\frac{\gamma}{8}} \leq N \leq e^{\frac{\gamma}{2}}$ that

$$\begin{aligned} \Pr[\mathcal{O}] &\leq \left(1+\frac{1}{2\sqrt{\pi}}\right) e^{-\frac{\alpha^2}{2}} \\ &\leq 2e^{-\frac{1}{2}\left[\sqrt{\gamma}-\sqrt{2\ln N}\right]^2} \end{aligned} \tag{A.22}$$

and similarly for all $N < e^{\frac{\gamma}{8}}$ that

$$\begin{aligned} \Pr[\mathcal{O}] &\leq N e^{-\frac{\gamma}{4}} \left(\frac{1}{2\sqrt{\pi}} + e^{-\left(\sqrt{2\ln N}-\sqrt{\frac{\gamma}{4}}\right)^2}\right) \\ &\leq 2N e^{-\frac{\gamma}{4}}. \end{aligned} \tag{A.23}$$